Chapter 8

Plates and Shells: Asymptotic Expansions and Hierarchic Models

Monique Dauge[1], Erwan Faou[2] and Zohar Yosibash[3]

[1] *IRMAR, Université de Rennes 1, Campus de Beaulieu, Rennes, France*
[2] *INRIA Rennes, Campus de Beaulieu, Rennes, France*
[3] *Ben-Gurion University, Beer Sheva, Israel*

1 INTRODUCTION

1.1 Structures

Plates and shells are characterized by *(i)* their midsurface S, *(ii)* their thickness d. The plate or shell character is that d is *small* compared to the dimensions of S. In this respect, we qualify such structures as *thin domains*. In the case of plates, S is a domain of the plane, whereas in the case of shells, S is a surface embedded in the three-dimensional space. Of course, plates are shells with zero curvature. Nevertheless, considering plates as a particular class of shells in not so obvious: They have always been treated separately, for the reason that plates are simpler. We think, and hopefully demonstrate in this chapter, that eventually, considering plates as shells sheds some light in the shell theory.

Other classes of thin domains do exist, such as rods, where two dimensions are small compared to the third one. We will not address them and quote, for example, (Nazarov, 1999; Irago and Viaño, 1999). Real engineering structures are often the union (or junction) of plates, rods, shells, and so on. See Ciarlet (1988, 1997) and also Kozlov, Maz'ya and Movchan (1999) and Agratov and Nazarov (2000). We restrict our analysis to an isolated plate or shell. We assume moreover that the midsurface S is smooth, orientable, and has a smooth boundary ∂S. The shell character includes the fact that the principal curvatures have the same order of magnitude as the dimensions of S. See Anicic and Léger (1999) for a situation where a region with strong curvature (like $1/d$) is considered. The opposite situation is when the curvatures have the order of d: We are then in the presence of shallow shells according to the terminology of Ciarlet and Paumier (1986).

1.2 Domains and coordinates

In connection with our references, it is easier for us to consider d as the *half-thickness* of the structure. We denote our plate or shell by Ω^d. We keep the reference to the half-thickness in the notation because we are going to perform

Encyclopedia of Computational Mechanics, Edited by Erwin Stein, René de Borst and Thomas J.R. Hughes. Volume 1: *Fundamentals*. © 2004 John Wiley & Sons, Ltd. ISBN: 0-470-84699-2.

REVISED PAGE PROOFS

an *asymptotic analysis* for which we embed our structure in a whole family of structures $(\Omega^\varepsilon)_\varepsilon$, where the parameter ε tends to 0.

We denote the Cartesian coordinates of $\mathbb{R}^3$ by $\boldsymbol{x} = (x_1, x_2, x_3)$, a tangential system of coordinates on S by $\mathbf{x}_\top = (\mathsf{x}_\alpha)_{\alpha=1,2}$, a normal coordinate to S by x_3, with the convention that the midsurface is parametrized by the equation $\mathsf{x}_3 = 0$. In the case of plates (x_α) are Cartesian coordinates in $\mathbb{R}^2$ and the domain Ω^d has the tensor product form

$$\Omega^d = S \times (-d, d)$$

In the case of shells, $\mathbf{x}_\top = (\mathsf{x}_\alpha)_{\alpha=1,2}$ denotes a local coordinate system on S, depending on the choice of a local chart in an atlas, and x_3 is the coordinate along a smooth unit normal field $\mathbf{n}$ to S in $\mathbb{R}^3$. Such a *normal coordinate system* (also called S-coordinate system) $(\mathbf{x}_\top, \mathsf{x}_3)$ yields a smooth diffeomorphism between Ω^d and $S \times (-d, d)$. The *lateral boundary* Γ^d of Ω^d is characterized by $\mathbf{x}_\top \in \partial S$ and $\mathsf{x}_3 \in (-d, d)$ in coordinates $(\mathbf{x}_\top, \mathsf{x}_3)$.

1.3 Displacement, strain, stress, and elastic energy

The displacement of the structure (deformation from the stress-free configuration) is denoted by $\mathbf{u}$, its Cartesian coordinates by (u_1, u_2, u_3), and its surface and transverse parts by $\mathbf{u}_\top = (\mathsf{u}_\alpha)$ and u_3 respectively. The transverse part u_3 is always an intrinsic function and the surface part $\mathbf{u}_\top$ defines a two-dimensional 1-form field on S, depending on x_3. The components (u_α) of $\mathbf{u}_\top$ depend on the choice of the local coordinate system $\mathbf{x}_\top$.

We choose to work in the framework of *small deformations* (see Ciarlet (1997, 2000)) for more general nonlinear models e.g. the von Kármán model). Thus, we use the strain tensor (linearized from the Green–St Venant strain tensor) $e = (e_{ij})$ given in Cartesian coordinates by

$$e_{ij}(\mathbf{u}) = \frac{1}{2}\left(\frac{\partial u_i}{\partial x_j} + \frac{\partial u_j}{\partial x_i}\right)$$

Unless stated otherwise, we assume the simplest possible behavior for the material of our structure, that is, an *isotropic material*. Thus, the elasticity tensor $A = (A^{ijkl})$ takes the form

$$A^{ijkl} = \lambda \delta^{ij}\delta^{kl} + \mu(\delta^{ik}\delta^{jl} + \delta^{il}\delta^{jk})$$

with λ and μ the Lamé constants of the material and δ^{ij} the Kronecker symbol. We use Einstein's summation convention, and sum over double indices if they appear as subscripts and superscripts (which is nothing but the contraction of tensors), for example, $\sigma^{ij}\, e_{ij} \equiv \Sigma_{i,j=1}^3 \sigma^{ij}\, e_{ij}$. The constitutive equation is given by Hooke's law $\boldsymbol{\sigma} = A\boldsymbol{e}(\mathbf{u})$ linking the stress tensor $\boldsymbol{\sigma}$ to the strain tensor $\boldsymbol{e}(\mathbf{u})$. Thus

$$\begin{aligned} \sigma^{ii} &= \lambda(e_{11} + e_{22} + e_{33}) + 2\mu e_{ii}, \quad i = 1, 2, 3 \\ \sigma^{ij} &= 2\mu e_{ij} \quad \text{for} \quad i \neq j \end{aligned} \tag{1}$$

The elastic bilinear form on a domain Ω is given by

$$a(\mathbf{u}, \mathbf{u}') = \int_\Omega \boldsymbol{\sigma}(\mathbf{u}) : \boldsymbol{e}(\mathbf{u}')\, \mathrm{d}\boldsymbol{x} = \int_\Omega \sigma^{ij}(\mathbf{u})\, e_{ij}(\mathbf{u}')\, \mathrm{d}\boldsymbol{x} \tag{2}$$

and the *elastic energy* of a displacement $\mathbf{u}$ is $(1/2)a(\mathbf{u}, \mathbf{u})$. The *strain–energy norm* of $\mathbf{u}$ is denoted by $\|\mathbf{u}\|_{E(\Omega)}$ and defined as $(\sum_{ij} \int_\Omega |e_{ij}(\mathbf{u})|^2\, \mathrm{d}\boldsymbol{x})^{1/2}$.

1.4 Families of problems

We will address two types of problems on our thin domain Ω^d: *(i)* Find the displacement $\mathbf{u}$ solution to the equilibrium equation $\mathbf{div}\,\boldsymbol{\sigma}(\mathbf{u}) = \mathbf{f}$ for a given load $\mathbf{f}$, *(ii)* Find the (smallest) vibration eigen-modes $(\Lambda, \mathbf{u})$ of the structure. For simplicity of exposition, we assume in general that the structure is clamped (this condition is also called 'condition of place') along its lateral boundary Γ^d and will comment on other choices for lateral boundary conditions. On the remaining part of the boundary $\partial\Omega^d \setminus \Gamma^d$ ('top' and 'bottom') traction free condition is assumed.

In order to investigate the influence of the thickness on the solutions and the discretization methods, we consider our (fixed physical) problem in Ω^d as part of a whole family of problems, depending on one parameter $\varepsilon \in (0, \varepsilon_0]$, the thickness. The definition of Ω^ε is obvious by the formulae given in Section 1.2 (in fact, if the curvatures of S are 'small', we may decide that Ω^d fits better in a family of shallow shells, see Section 4.4 later). For problem *(i)*, we choose the same right hand side $\mathbf{f}$ for all values of ε, which precisely means that we fix a smooth field $\mathbf{f}$ on Ω^{ε_0} and take $\mathbf{f}^\varepsilon := \mathbf{f}|_{\Omega^\varepsilon}$ for each ε.

Both problems *(i)* and *(ii)* can be set in variational form (principle of virtual work). Our three-dimensional variational space is the subspace $V(\Omega^\varepsilon)$ of the Sobolev space $H^1(\Omega^\varepsilon)^3$ characterized by the clamping condition $\mathbf{u}|_{\Gamma^\varepsilon} = 0$, and the bilinear form a (2) on $\Omega = \Omega^\varepsilon$, denoted by a^ε. The variational formulations are

REVISED PAGE PROOFS

$$\textit{Find } \mathbf{u}^\varepsilon \in V(\Omega^\varepsilon) \textit{ such that}$$
$$a^\varepsilon(\mathbf{u}^\varepsilon, \mathbf{u}') = \int_{\Omega^\varepsilon} \mathbf{f}^\varepsilon \cdot \mathbf{u}' \, d\boldsymbol{x}, \quad \forall \mathbf{u}' \in V(\Omega^\varepsilon) \tag{3}$$

for the problem with external load, and

$$\textit{Find } \mathbf{u}^\varepsilon \in V(\Omega^\varepsilon)\,,\ \mathbf{u}^\varepsilon \neq 0, \quad \textit{and} \quad \Lambda^\varepsilon \in \mathbb{R} \quad \textit{such that}$$
$$a^\varepsilon(\mathbf{u}^\varepsilon, \mathbf{u}') = \Lambda^\varepsilon \int_{\Omega^\varepsilon} \mathbf{u}^\varepsilon \cdot \mathbf{u}' \, d\boldsymbol{x}, \quad \forall \mathbf{u}' \in V(\Omega^\varepsilon) \tag{4}$$

for the eigen-mode problem. In engineering practice, one is interested in the natural frequencies, $\omega^\varepsilon = \sqrt{\Lambda^\varepsilon}$. Of course, when considering our structure Ω^d, we are eventually only interested in $\varepsilon = d$. Taking the whole family $\varepsilon \in (0, \varepsilon_0]$ into account allows the investigation of the dependency with respect to the small parameter ε, in order to know if valid simplified models are available and how they can be discretized by finite elements.

1.5 Computational obstacles

Our aim is to study the possible discretizations for a reliable and efficient computation of the solutions $\mathbf{u}^d$ of problem (3) or (4) in our thin structure Ω^d. An option could be to consider Ω^d as a three-dimensional body and use 3-D finite elements. In the standard version of finite elements (h-version), individual elements should not be stretched or distorted, which implies that all dimensions should be bounded by d. Even so, several layers of elements through the thickness may be necessary. Moreover the a priori error estimates may suffer from the behavior of the Korn inequality on Ω^d (the factor appearing in the Korn inequality behaves like d^{-1} for plates and partially clamped shells; see Ciarlet, Lods and Miara (1996) and Dauge and Faou (2004)).

An ideal alternative would simply be to get rid of the thickness variable and compute the solution of an 'equivalent' problem on the midsurface S. This is the aim of the *shell theory*. Many investigations were undertaken around 1960–1970, and the main achievement is (still) the Koiter model, which is a multidegree 3×3 elliptic system on S of half-orders (1, 1, 2) with a singular dependence in d. But, as written in Koiter and Simmonds (1973), 'Shell theory attempts the impossible: to provide a two-dimensional representation of an intrinsically three-dimensional phenomenon'. Nevertheless, obtaining converging error estimates between the 3-D solution $\mathbf{u}^d$ and a *reconstructed 3-D displacement* $\mathbf{U}\mathbf{z}^d$ from the *deformation pattern* $\mathbf{z}^d$ solution of the Koiter model seems possible.

However, due to its fourth order part, the Koiter model cannot be discretized by standard $\mathcal{C}^0$ finite elements. The Naghdi model, involving five unknowns on S, seems more suitable. Yet, endless difficulties arise in the form of various locking effects, due to the singularly perturbed character of the problem.

With the twofold aim of improving the precision of the models and their approximability by finite elements, the idea of hierarchical models becomes natural: Roughly, it consists of an Ansatz of polynomial behavior in the thickness variable, with bounds on the degrees of the three components of the 3-D displacement. The introduction of such models in variational form is due to Vogelius and Babuška (1981c) and Szabó and Sahrmann (1988). Earlier beginnings in that direction can be found in Vekua (1955, 1965). The hierarchy (increasing the transverse degrees) of models obtained in that way can be discretized by the p-version of finite elements.

1.6 Plan of the chapter

In order to assess the validity of hierarchical models, we will compare them with asymptotic expansions of solutions $\mathbf{u}^\varepsilon$ when they are available: These expansions exhibit two or three different scales and boundary layer regions, which can or cannot be properly described by hierarchical models.

We first address plates because much more is known for plates than for general shells. In Section 2, we describe the two-scale expansion of the solutions of (3) and (4): This expansion contains *(i)* a *regular part* each term of which is polynomial in the thickness variable x_3, *(ii)* a part mainly supported in a *boundary layer* around the lateral boundary Γ^ε. In Section 3, we introduce the hierarchical models as Galerkin projections on semidiscrete subspaces $V^{\mathbf{q}}(\Omega^\varepsilon)$ of $V(\Omega^\varepsilon)$ defined by assuming a polynomial behavior of degree $\mathbf{q} = (q_1, q_2, q_3)$ in x_3. The model of degree (1, 1, 0) is the Reissner–Mindlin model and needs the introduction of a *reduced energy*. The (1, 1, 2) model is the lowest degree model to use the same elastic energy (2) as the 3-D model.

We address shells in Section 4 (asymptotic expansions and limiting models) and Section 5 (hierarchical models). After a short introduction of the metric and curvature tensors on the midsurface, we first describe the three-scale expansion of the solutions of (3) on clamped elliptic shells: Two of these scales can be captured by hierarchical models. We then present and comment on the famous classification of shells as flexural or membrane. We also mention two distinct notions of shallow shells. We emphasize the universal role played by the Koiter model for the structure Ω^d, independently of any embedding of Ω^d in a family $(\Omega^\varepsilon)_\varepsilon$.

The last section is devoted to the discretization of the 3-D problems and their 2-D hierarchical projections, by p-version finite elements. The 3-D thin elements (one layer of

REVISED PAGE PROOFS

elements through the thickness) constitute a bridge between 3-D and 2-D discretizations. We address the issue of locking effects (shear and membrane locking) and the issue of capturing boundary layer terms. Increasing the degree p of approximation polynomials and using anisotropic meshes is a way toward solving these problems. We end this chapter by presenting a series of eigen-frequency computations on a few different families of shells and draw some 'practical' conclusions.

2 MULTISCALE EXPANSIONS FOR PLATES

The question of an asymptotic expansion for solutions $\mathbf{u}^\varepsilon$ of problems (3) or (4) posed in a family of plates is difficult: One may think it is natural to expand $\mathbf{u}^\varepsilon$ either in polynomial functions in the thickness variable x_3, or in an asymptotic series in powers ε^k with regular coefficients $\mathbf{v}^k$ defined on the stretched plate $\Omega = S \times (-1, 1)$. In fact, for the class of loads considered here or for the eigen-mode problem, both those Ansätze are relevant, but they are unable to provide a correct description of the behavior of $\mathbf{u}^\varepsilon$ in the vicinity of the lateral boundary Γ^ε, where there is a boundary layer of width $\sim \varepsilon$ (except in the particular situation of a rectangular midsurface with symmetry lateral boundary conditions (hard simple support or sliding edge); see Paumier, 1990). And, worse, in the absence of knowledge of the boundary layer behavior, the determination of the terms $\mathbf{v}^k$ is impossible (except for $\mathbf{v}^0$).

The investigation of asymptotics as $\varepsilon \to 0$ was first performed by the construction of infinite *formal expansions*; see Friedrichs and Dressler (1961), Gol'denveizer (1962), and Gregory and Wan (1984). The principle of multiscale asymptotic expansion is applied to thin domains in Maz'ya, Nazarov and Plamenevskii (1991b). A two-term asymptotics is exhibited in Nazarov and Zorin (1989). The whole asymptotic expansion is constructed in Dauge and Gruais (1996, 1998a) and Dauge, Gruais and Rössle (1999/00).

The multiscale expansions that we propose differ from the matching method in Il'in (1992) where the solutions of singularly perturbed problems are fully described in rapid variables inside the boundary layer and slow variables outside the layer, both expansions being 'matched' in an intermediate region. Our approach is closer to that of Vishik and Lyusternik (1962) and Oleinik, Shamaev and Yosifian (1992).

2.1 Coordinates and symmetries

The midsurface S is a smooth domain of the plane $\Pi \simeq \mathbb{R}^2$ (see Fig. 1) and for $\varepsilon \in (0, \varepsilon_0)$ $\Omega^\varepsilon = S \times (-\varepsilon, \varepsilon)$ is the

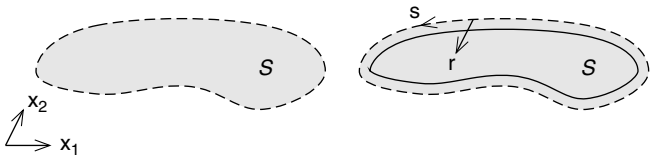

Figure 1. Cartesian and local coordinates on the midsurface.

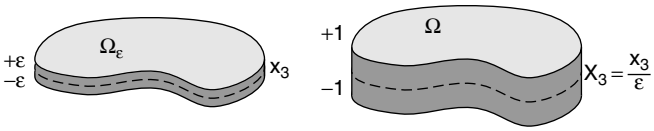

Figure 2. Thin plate and stretched plate.

generic member of the family of plates (see Fig. 2). The plates are symmetric with respect to the plane Π. Since they are assumed to be made of an isotropic material, problems (3) or (4) commute with the symmetry $\mathfrak{S}: \mathbf{u} \mapsto (\mathbf{u}_\top(\cdot, -x_3), -u_3(\cdot, -x_3))$. The eigenspaces of $\mathfrak{S}$ are *membrane* and *bending* displacements (also called stretching and flexural displacements), cf. Friedrichs and Dressler (1961):

$$\begin{aligned} &\mathbf{u} \quad \text{membrane iff} \quad \mathbf{u}_\top(\mathbf{x}_\top, +x_3) = \mathbf{u}_\top(\mathbf{x}_\top, -x_3) \\ &\qquad\qquad \text{and} \quad u_3(\mathbf{x}_\top, +x_3) = -u_3(\mathbf{x}_\top, -x_3) \\ &\mathbf{u} \quad \text{bending iff} \quad \mathbf{u}_\top(\mathbf{x}_\top, +x_3) = -\mathbf{u}_\top(\mathbf{x}_\top, -x_3) \\ &\qquad\qquad \text{and} \quad u_3(\mathbf{x}_\top, +x_3) = u_3(\mathbf{x}_\top, -x_3) \end{aligned} \tag{5}$$

Any general displacement $\mathbf{u}$ is the sum $\mathbf{u}_m + \mathbf{u}_b$ of a membrane and a bending part (according to formulae $\mathbf{u}_m = (1/2)(\mathbf{u} + \mathfrak{S}\mathbf{u})$ and $\mathbf{u}_f = (1/2)(\mathbf{u} - \mathfrak{S}\mathbf{u})$. They are also denoted by $\mathbf{u}^I$ and $\mathbf{u}^{II}$ in the literature).

In addition to the coordinates $\mathbf{x}_\top$ in S, let r be the distance to ∂S in Π and s an arclength function on ∂S (see Fig. 1). In this way, (r, s) defines a smooth coordinate system in a midplane tubular neighborhood $\mathcal{V}$ of ∂S. Let $\chi = \chi(r)$ be a smooth cut-off function with support in $\mathcal{V}$, equal to 1 in a smaller such neighborhood. It is used to substantiate boundary layer terms. The two following stretched (or rapid) variables appear in our expansions:

$$X_3 = \frac{x_3}{\varepsilon} \quad \text{and} \quad R = \frac{r}{\varepsilon}$$

The stretched thickness variable X_3 belongs to $(-1, 1)$ and is present in all parts of our asymptotics, whereas the presence of R characterizes boundary layer terms (see Figure 2).

2.2 Problem with external load

The solutions of the family of problems (3) have a two-scale asymptotic expansion in regular terms $\mathbf{v}^k$ and boundary

REVISED PAGE PROOFS

layer terms $\mathbf{w}^k$, which we state as a theorem (Dauge, Gruais and Rössle, 1999/00; Dauge and Schwab, 2002). Note that in contrast with the most part of those references, we work here with *natural displacements* (i.e. unscaled), which is more realistic from the mechanical and computational point of view, and allows an easier comparison with shells.

Theorem 1. (Dauge, Gruais and Rössle, 1999/00) *For the solutions of problem (3), $\varepsilon \in (0, \varepsilon_0]$, there exist regular terms $\mathbf{v}^k = \mathbf{v}^k(\mathbf{x}_\top, \mathsf{X}_3)$, $k \geq -2$, and boundary layer terms $\mathbf{w}^k = \mathbf{w}^k(\mathsf{R}, \mathsf{s}, \mathsf{X}_3)$, $k \geq 0$, such that*

$$\mathbf{u}^\varepsilon \simeq \varepsilon^{-2}\mathbf{v}^{-2} + \varepsilon^{-1}\mathbf{v}^{-1} + \varepsilon^0(\mathbf{v}^0 + \chi\mathbf{w}^0) + \varepsilon^1(\mathbf{v}^1 + \chi\mathbf{w}^1) + \cdots \tag{6}$$

in the sense of asymptotic expansions: The following estimates hold

$$\left\| \mathbf{u}^\varepsilon - \sum_{k=-2}^{K} \varepsilon^k(\mathbf{v}^k + \chi\mathbf{w}^k) \right\|_{E(\Omega^\varepsilon)} \leq C_K(\mathbf{f})\,\varepsilon^{K+1/2}, \qquad K = 0, 1, \ldots$$

where we have set $\mathbf{w}^{-2} = \mathbf{w}^{-1} = 0$ and the constant $C_K(\mathbf{f})$ is independent of $\varepsilon \in (0, \varepsilon_0]$.

2.2.1 Kirchhoff displacements and their deformation patterns

The first terms in the expansion of $\mathbf{u}^\varepsilon$ are Kirchhoff displacements, that is, displacements of the form (with the surface gradient $\nabla_\top = (\partial_1, \partial_2)$)

$$(\mathbf{x}_\top, \mathsf{x}_3) \longmapsto \mathbf{v}(\mathbf{x}_\top, \mathsf{x}_3) = \big(\boldsymbol{\zeta}_\top(\mathbf{x}_\top) - \mathsf{x}_3\nabla_\top\zeta_3(\mathbf{x}_\top), \zeta_3(\mathbf{x}_\top)\big) \tag{7}$$

Here, $\boldsymbol{\zeta}_\top = (\zeta_\alpha)$ is a surface displacement and ζ_3 is a function on S. We call the three-component field $\boldsymbol{\zeta} := (\boldsymbol{\zeta}_\top, \zeta_3)$, the *deformation pattern* of the KL displacement $\mathbf{v}$. Note that

$$\mathbf{v} \text{ bending iff } \boldsymbol{\zeta} = (\mathbf{0}, \zeta_3) \text{ and } \mathbf{v} \text{ membrane iff } \boldsymbol{\zeta} = (\boldsymbol{\zeta}_\top, 0)$$

In expansion (6) the first terms are Kirchhoff displacements. The next regular terms $\mathbf{v}^k$ are also generated by deformation patterns $\boldsymbol{\zeta}^k$ via higher degree formulae than in (7). We successively describe the $\mathbf{v}^k$, the $\boldsymbol{\zeta}^k$ and, finally, the boundary layer terms $\mathbf{w}^k$.

2.2.2 The four first regular terms

For the regular terms $\mathbf{v}^k$, $k = -2, -1, 0, 1$, there exist bending deformation patterns $\boldsymbol{\zeta}^{-2} = (\mathbf{0}, \zeta_3^{-2})$, $\boldsymbol{\zeta}^{-1} = (\mathbf{0}, \zeta_3^{-1})$, and full deformation patterns $\boldsymbol{\zeta}^0$, $\boldsymbol{\zeta}^1$ such that

$$\begin{aligned}
\mathbf{v}^{-2} &= (\mathbf{0},\ \zeta_3^{-2}) \\
\mathbf{v}^{-1} &= (-\mathsf{X}_3\nabla_\top\zeta_3^{-2},\ \zeta_3^{-1}) \\
\mathbf{v}^0 &= (\boldsymbol{\zeta}_\top^0 - \mathsf{X}_3\nabla_\top\zeta_3^{-1},\ \zeta_3^0) + (\mathbf{0},\ P_\mathsf{b}^2(\mathsf{X}_3)\Delta_\top\zeta_3^{-2}) \\
\mathbf{v}^1 &= (\boldsymbol{\zeta}_\top^1 - \mathsf{X}_3\nabla_\top\zeta_3^0,\ \zeta_3^1) + (P_\mathsf{b}^3(\mathsf{X}_3)\nabla_\top\Delta_\top\zeta_3^{-2}, \\
&\qquad P_\mathsf{m}^1(\mathsf{X}_3)\,\mathrm{div}\,\boldsymbol{\zeta}_\top^0 + P_\mathsf{b}^2(\mathsf{X}_3)\Delta_\top\zeta_3^{-1})
\end{aligned} \tag{8}$$

In the above formulae, $\nabla_\top = (\partial_1, \partial_2)$ is the surface gradient on S, $\Delta_\top = \partial_1^2 + \partial_2^2$ is the surface Laplacian and $\mathrm{div}\,\boldsymbol{\zeta}_\top$ is the surface divergence (i.e. $\mathrm{div}\,\boldsymbol{\zeta}_\top = \partial_1\zeta_1 + \partial_2\zeta_2$). The functions P_b^ℓ and P_m^ℓ are polynomials of degree ℓ, whose coefficients depend on the Lamé constants according to

$$\begin{aligned}
P_\mathsf{m}^1(\mathsf{X}_3) &= -\frac{\lambda}{\lambda + 2\mu}\,\mathsf{X}_3, \\
P_\mathsf{b}^2(\mathsf{X}_3) &= \frac{\lambda}{2\lambda + 4\mu}\left(\mathsf{X}_3^2 - \frac{1}{3}\right), \\
P_\mathsf{b}^3(\mathsf{X}_3) &= \frac{1}{6\lambda + 12\mu}\left((3\lambda + 4\mu)\,\mathsf{X}_3^3 - (11\lambda + 12\mu)\,\mathsf{X}_3\right)
\end{aligned} \tag{9}$$

Note that the first blocks in $\sum_{k\geq -2}\varepsilon^k\mathbf{v}^k$ yield Kirchhoff displacements, whereas the second blocks have zero mean values through the thickness for each $\mathbf{x}_\top \in S$.

2.2.3 All regular terms with the help of formal series

We see from (8) that the formulae describing the successive $\mathbf{v}^k$ are *partly self-similar* and, also, that each $\mathbf{v}^k$ is enriched by a new term. That is why the whole regular term series $\sum_k \varepsilon^k\mathbf{v}^k$ can be efficiently described with the help of the *formal series product*.

A formal series is an infinite sequence $(a^0, a^1, \ldots, a^k, \ldots)$ of coefficients, which can be denoted in a symbolic way by $a[\varepsilon] = \sum_{k\geq 0}\varepsilon^k a^k$, and the product $a[\varepsilon]b[\varepsilon]$ of the two formal series $a[\varepsilon]$ and $b[\varepsilon]$ is the formal series $c[\varepsilon]$ with coefficients $c^\ell = \sum_{0\leq k\leq \ell} a^k b^{\ell-k}$. In other words, the equation $c[\varepsilon] = a[\varepsilon]b[\varepsilon]$ is equivalent to the series of equation $c^\ell = \sum_{0\leq k\leq \ell} a^k b^{\ell-k}$, $\forall\ell$.

With this formalism, we have the following identity, *which extends formulae* (8):

$$\mathbf{v}[\varepsilon] = \mathbf{V}[\varepsilon]\boldsymbol{\zeta}[\varepsilon] + \mathbf{Q}[\varepsilon]\mathbf{f}[\varepsilon] \tag{10}$$

(i) $\boldsymbol{\zeta}[\varepsilon]$ is the formal series of Kirchhoff deformation patterns $\sum_{k\geq -2}\varepsilon^k\boldsymbol{\zeta}^k$ *starting with* $k = -2$.

(ii) $\mathbf{V}[\varepsilon]$ has operator valued coefficients $\mathbf{V}^k$, $k \geq 0$, acting from $\mathcal{C}^\infty(\overline{S})^3$ into $\mathcal{C}^\infty(\overline{\Omega})^3$:

REVISED PAGE PROOFS

$$\begin{aligned}
\mathbf{V}^0\boldsymbol{\zeta} &= (\boldsymbol{\zeta}_\top,\ \zeta_3)\\
\mathbf{V}^1\boldsymbol{\zeta} &= (-\mathsf{X}_3\nabla_\top\zeta_3,\ P^1_{\mathsf{m}}(\mathsf{X}_3)\,\mathrm{div}\,\boldsymbol{\zeta}_\top)\\
\mathbf{V}^2\boldsymbol{\zeta} &= (P^2_{\mathsf{m}}(\mathsf{X}_3)\nabla_\top\,\mathrm{div}\,\boldsymbol{\zeta}_\top,\ P^2_{\mathsf{b}}(\mathsf{X}_3)\Delta_\top\zeta_3)\\
&\dots\\
\mathbf{V}^{2j}\boldsymbol{\zeta} &= (P^{2j}_{\mathsf{m}}(\mathsf{X}_3)\nabla_\top\Delta_\top^{j-1}\,\mathrm{div}\,\boldsymbol{\zeta}_\top,\ P^{2j}_{\mathsf{b}}(\mathsf{X}_3)\Delta_\top^j\zeta_3)\\
\mathbf{V}^{2j+1}\boldsymbol{\zeta} &= (P^{2j+1}_{\mathsf{b}}(\mathsf{X}_3)\nabla_\top\Delta_\top^j\zeta_3,\\
&\qquad P^{2j+1}_{\mathsf{m}}(\mathsf{X}_3)\Delta_\top^j\,\mathrm{div}\,\boldsymbol{\zeta}_\top)
\end{aligned} \tag{11}$$

with P^ℓ_{b} and P^ℓ_{m} polynomials of degree ℓ (the first ones are given in (9)).

(iii) $\mathbf{f}[\varepsilon]$ is the Taylor series of $\mathbf{f}$ around the surface $\mathsf{x}_3 = 0$:

$$\mathbf{f}[\varepsilon] = \sum_{k\geq 0}\varepsilon^k\mathbf{f}^k \text{ with } \mathbf{f}^k(\mathbf{x}_\top,\mathsf{X}_3) = \frac{\mathsf{X}_3^k}{k!}\frac{\partial^k\mathbf{f}}{\partial\mathsf{x}_3^k}\Big|_{\mathsf{x}_3=0}(\mathbf{x}_\top) \tag{12}$$

(iv) $\mathbf{Q}[\varepsilon]$ has operator valued coefficients $\mathbf{Q}^k$ acting from $\mathcal{C}^\infty(\overline{\Omega})^3$ into itself. It starts at $k=2$ (we can see now that the four first equations given by equality (10) are $\mathbf{v}^{-2} = \mathbf{V}^0\boldsymbol{\zeta}^{-2}$, $\mathbf{v}^{-1} = \mathbf{V}^0\boldsymbol{\zeta}^{-1} + \mathbf{V}^1\boldsymbol{\zeta}^{-2}$, $\mathbf{v}^0 = \mathbf{V}^0\boldsymbol{\zeta}^0 + \mathbf{V}^1\boldsymbol{\zeta}^{-1} + \mathbf{V}^2\boldsymbol{\zeta}^{-2}$, $\mathbf{v}^1 = \mathbf{V}^0\boldsymbol{\zeta}^1 + \mathbf{V}^1\boldsymbol{\zeta}^0 + \mathbf{V}^2\boldsymbol{\zeta}^{-1} + \mathbf{V}^3\boldsymbol{\zeta}^{-2}$, which gives back (8))

$$\mathbf{Q}[\varepsilon] = \sum_{k\geq 2}\varepsilon^k\mathbf{Q}^k \tag{13}$$

Each $\mathbf{Q}^k$ is made of compositions of partial derivatives in the surface variables $\mathbf{x}_\top$ with integral operators in the scaled transverse variable. Each of them acts in a particular way between *semipolynomial spaces* $E^q(\Omega)$, $q\geq 0$, in the scaled domain Ω: We define for any integer q, $q\geq 0$

$$E^q(\Omega) = \left\{\mathbf{v}\in\mathcal{C}^\infty(\Omega)^3,\ \exists\mathbf{z}^n\in\mathcal{C}^\infty(\overline{S})^3,\ \mathbf{v}(\mathbf{x}_\top,\mathsf{X}_3) = \sum_{n=0}^q\mathsf{X}_3^n\mathbf{z}^n(\mathbf{x}_\top)\right\} \tag{14}$$

Note that by (12), $\mathbf{f}^k$ belongs to $E^k(\Omega)$.

Besides, for any $k\geq 2$, $\mathbf{Q}^k$ acts from $E^q(\Omega)$ into $E^{q+k}(\Omega)$. The first term of the series $\mathbf{Q}[\varepsilon]\mathbf{f}[\varepsilon]$ is $\mathbf{Q}^2\mathbf{f}^0$ and we have:

$$\mathbf{Q}^2\mathbf{f}^0(\mathbf{x}_\top,\mathsf{X}_3) = \left(\mathbf{0},\ \frac{1-3\mathsf{X}_3^2}{6\lambda+12\mu}\,\mathrm{f}_3^0(\mathbf{x}_\top)\right)$$

As a consequence of formula (10), combined with the structure of each term, we find

Lemma 1. (Dauge and Schwab, 2002) *With the definition* (14) *for the semipolynomial space* $E^q(\Omega)$*, for any* $k\geq -2$ *the regular term* $\mathbf{v}^k$ *belongs to* $E^{k+2}(\Omega)$.

2.2.4 Deformation patterns

From formula (8) extended by (10) we obtain explicit expressions for the regular parts $\mathbf{v}^k$ provided we know the deformation patterns $\boldsymbol{\zeta}^k$. The latter solves boundary value problems on the midsurface S. Our multiscale expansion approach gives back the well-known equations of plates (the Kirchhoff–Love model and the plane stress model) completed by a whole series of boundary value problems.

(i) The first bending generator ζ_3^{-2} solves the Kirchhoff–Love model

$$L_{\mathsf{b}}\zeta_3^{-2}(\mathbf{x}_\top) = \mathrm{f}_3^0(\mathbf{x}_\top),\ \ \mathbf{x}_\top\in S \quad\text{with}\quad \zeta_3^{-2}\big|_{\partial S} = 0,\ \ \partial_{\mathbf{n}}\zeta_3^{-2}\big|_{\partial S} = 0 \tag{15}$$

where L_{b} is the fourth-order operator

$$L_{\mathsf{b}} := \frac{4\mu}{3}\frac{\lambda+\mu}{\lambda+2\mu}\,\Delta_\top^2 = \frac{1}{3}(\widetilde{\lambda}+2\mu)\,\Delta_\top^2 \tag{16}$$

and $\mathbf{n}$ the unit *interior* normal to ∂S. Here $\tilde{\lambda}$ is the 'averaged' Lamé constant

$$\widetilde{\lambda} = \frac{2\lambda\mu}{\lambda+2\mu} \tag{17}$$

(ii) The second bending generator ζ_3^{-1} is the solution of a similar problem

$$L_{\mathsf{b}}\zeta_3^{-1}(\mathbf{x}_\top) = 0,\ \ \mathbf{x}_\top\in S \quad\text{with}\quad \zeta_3^{-1}\big|_{\partial S} = 0,\ \ \partial_{\mathbf{n}}\zeta_3^{-1}\big|_{\partial S} = c^{\mathsf{b}}_{\lambda,\mu}\Delta_\top\zeta_3^{-2} \tag{18}$$

where $c^{\mathsf{b}}_{\lambda,\mu}$ is a positive constant depending on the Lamé coefficients.

(iii) The membrane part $\boldsymbol{\zeta}^0_\top$ of the third deformation pattern solves the plane stress model

$$L_{\mathsf{m}}\boldsymbol{\zeta}^0_\top(\mathbf{x}_\top) = \mathbf{f}^0_\top(\mathbf{x}_\top),\ \ \mathbf{x}_\top\in S \quad\text{and}\quad \boldsymbol{\zeta}^0_\top|_{\partial S} = \mathbf{0} \tag{19}$$

where L_{m} is the second-order 2×2 system

$$\begin{pmatrix}\zeta_1\\ \zeta_2\end{pmatrix}\longmapsto -\begin{pmatrix}(\widetilde{\lambda}+2\mu)\partial_{11}+\mu\partial_{22} & (\widetilde{\lambda}+\mu)\partial_{12}\\ (\widetilde{\lambda}+\mu)\partial_{12} & \mu\partial_{11}+(\widetilde{\lambda}+2\mu)\partial_{22}\end{pmatrix}\times\begin{pmatrix}\zeta_1\\ \zeta_2\end{pmatrix} \tag{20}$$

(iv) Here, again, the whole series of equations over the series of deformation patterns $\sum_{k\geq -2}\varepsilon^k\boldsymbol{\zeta}^k$ can be

REVISED PAGE PROOFS

written in a global way using the formal series product, as *reduced equations on the midsurface*:

$$\mathbf{L}[\varepsilon]\boldsymbol{\zeta}[\varepsilon] = \mathbf{R}[\varepsilon]\mathbf{f}[\varepsilon] \quad \text{in } S \quad \text{with } \mathbf{d}[\varepsilon]\boldsymbol{\zeta}[\varepsilon] = 0 \quad \text{on } \partial S \tag{21}$$

Here, $\mathbf{L}[\varepsilon] = \mathbf{L}^0 + \varepsilon^2\mathbf{L}^2 + \varepsilon^4\mathbf{L}^4 + \cdots$, with

$$\mathbf{L}^0\boldsymbol{\zeta} = \begin{pmatrix} L_{\mathsf{m}} & 0 \\ 0 & 0 \end{pmatrix}\begin{pmatrix} \boldsymbol{\zeta}_\top \\ \zeta_3 \end{pmatrix}$$
$$\mathbf{L}^2\boldsymbol{\zeta} = \begin{pmatrix} L^2_{\mathsf{m}} & 0 \\ 0 & L_{\mathsf{b}} \end{pmatrix}\begin{pmatrix} \boldsymbol{\zeta}_\top \\ \zeta_3 \end{pmatrix}, \ldots \tag{22}$$

where $L^2_{\mathsf{m}}\boldsymbol{\zeta}_\top$ has the form $c\nabla_\top\Delta_\top \operatorname{div}\boldsymbol{\zeta}_\top$. The series of operators $\mathbf{R}[\varepsilon]$ starts at $k = 0$ and acts from $\mathcal{C}^\infty(\overline{\Omega})^3$ into $\mathcal{C}^\infty(\overline{S})^3$. Its first coefficient is the mean-value operator

$$\mathbf{f} \mapsto \mathbf{R}^0\mathbf{f} \quad \text{with} \quad \mathbf{R}^0\mathbf{f}(\mathbf{x}_\top) = \frac{1}{2}\int_{-1}^{1} \mathbf{f}(\mathbf{x}_\top, \mathsf{X}_3)\, d\mathsf{X}_3 \tag{23}$$

Finally, the coefficients of the operator series $\mathbf{d}[\varepsilon]$ are trace operators acting on $\boldsymbol{\zeta}$. The first terms are

$$\mathbf{d}^0\boldsymbol{\zeta} = \begin{pmatrix} \boldsymbol{\zeta}_\top \cdot \mathbf{n} \\ \boldsymbol{\zeta}_\top \times \mathbf{n} \\ 0 \\ 0 \end{pmatrix}, \quad \mathbf{d}^1\boldsymbol{\zeta} = \begin{pmatrix} -c^{\mathsf{m}}_{\lambda,\mu} \operatorname{div}\boldsymbol{\zeta}_\top \\ 0 \\ 0 \\ 0 \end{pmatrix},$$
$$\mathbf{d}^2\boldsymbol{\zeta} = \begin{pmatrix} \bullet \\ \bullet \\ \zeta_3 \\ \partial_{\mathbf{n}}\zeta_3 \end{pmatrix}, \quad \mathbf{d}^3\boldsymbol{\zeta} = \begin{pmatrix} \bullet \\ \bullet \\ 0 \\ -c^{\mathsf{b}}_{\lambda,\mu}\Delta_\top\zeta_3 \end{pmatrix} \tag{24}$$

where $c^{\mathsf{b}}_{\lambda,\mu}$ is the constant in (18), $c^{\mathsf{m}}_{\lambda,\mu}$ is another positive constant and $\bullet$ indicates the presence of higher order operators on $\boldsymbol{\zeta}_\top$.

Note that the first three equations in (21): $\mathbf{L}^0\boldsymbol{\zeta}^{-2} = 0$, $\mathbf{L}^0\boldsymbol{\zeta}^{-1} = 0$, $\mathbf{L}^0\boldsymbol{\zeta}^0 + \mathbf{L}^2\boldsymbol{\zeta}^{-2} = \mathbf{R}^0\mathbf{f}^0$ on S and $\mathbf{d}^0\boldsymbol{\zeta}^{-2} = 0$, $\mathbf{d}^0\boldsymbol{\zeta}^{-1} + \mathbf{d}^1\boldsymbol{\zeta}^{-1} = 0$, $\mathbf{d}^0\boldsymbol{\zeta}^0 + \mathbf{d}^1\boldsymbol{\zeta}^{-1} + \mathbf{d}^2\boldsymbol{\zeta}^{-2} = 0$ on ∂S, give back (15), (18), and (19) together with the fact that $\boldsymbol{\zeta}^{-2}_\top = \boldsymbol{\zeta}^{-1}_\top = 0$.

2.2.5 Boundary layer terms

The terms $\mathbf{w}^k$ have a quite different structure. Their natural variables are $(\mathsf{R}, \mathsf{s}, \mathsf{X}_3)$, see Section 2.1 and Fig. 3, and they are easier to describe in boundary fitted components $(\mathsf{w}_\mathsf{r}, \mathsf{w}_\mathsf{s}, \mathsf{w}_3)$ corresponding to the local coordinates $(\mathsf{r}, \mathsf{s}, \mathsf{x}_3)$. The first boundary layer term, $\mathbf{w}^0$ is a bending displacement in the sense of (5) and has a tensor product form: In boundary fitted components it reads

$$\mathsf{w}^0_\mathsf{s} = 0 \quad \text{and} \quad (\mathsf{w}^0_\mathsf{r}, \mathsf{w}^0_3)(\mathsf{R}, \mathsf{s}, \mathsf{X}_3) = \varphi(\mathsf{s})\,\overline{\mathbf{w}}^0_*(\mathsf{R}, \mathsf{X}_3)$$
$$\text{with} \quad \varphi = \Delta_\top\zeta_3^{-2}\big|_{\partial S}$$

and $\overline{\mathbf{w}}^0_*$ is a two component *exponentially decreasing profile* on the semi-strip $\Sigma_+ := \{(\mathsf{R}, \mathsf{X}_3), \mathsf{R} > 0,\ |\mathsf{X}_3| < 1\}$: There exists $\eta > 0$ such that

$$|e^{\eta\mathsf{R}}\,\overline{\mathbf{w}}^0_*(\mathsf{R}, \mathsf{X}_3)| \quad \text{is bounded as} \quad \mathsf{R} \to \infty$$

The least upper bound of such η is the smallest exponent η_0 arising from the Papkovich–Fadle eigenfunctions; see Gregory and Wan (1984). Both components of $\overline{\mathbf{w}}^0_*$ are nonzero.

The next boundary layer terms $\mathbf{w}^k$ are combinations of products of (smooth) traces on ∂S by profiles $\overline{\mathbf{w}}^{k,\ell}$ in $(\mathsf{R}, \mathsf{X}_3)$. These profiles have singularities at the corners $(0, \pm 1)$ of Σ_+, according to the general theory of Kondrat'ev (1967). Thus, in contrast with the 'regular' terms $\mathbf{v}^k$, which are smooth up to the boundary of Ω, the terms $\mathbf{w}^k$ do have singular parts along the edges $\partial S \times \{\pm 1\}$ of the plate. Finally, the edge singularities of the solution $\mathbf{u}^\varepsilon$ of problem (3) are related with the boundary layer terms only; see Dauge and Gruais (1998a) for further details.

Figure 3. Boundary layer coordinates in $\partial S \times \Sigma_+$.

2.3 Properties of the displacement expansion outside the boundary layer

Let S' be a subset of S such that the distance between $\partial S'$ and ∂S is positive. As a consequence of expansion (6) there holds

$$\mathbf{u}^\varepsilon(\mathbf{x}) = \sum_{k=-2}^{K} \varepsilon^k \mathbf{v}^k(\mathbf{x}_\top, \mathsf{X}_3) + \mathcal{O}(\varepsilon^{K+1})$$
$$\text{uniformly for} \quad \mathbf{x} \in \overline{S'} \times (-\varepsilon, \varepsilon)$$

Coming back to physical variables $(\mathbf{x}_\top, \mathsf{x}_3)$, the expansion terms $\mathbf{v}^k$ being polynomials of degree $k+2$ in X_3 (Lemma 1), we find that

$$\mathbf{u}^\varepsilon(\mathbf{x}) = \sum_{k=-2}^{K} \varepsilon^k\, \widehat{\mathbf{v}}^{K,k}(\mathbf{x}_\top, \mathsf{x}_3) + \mathcal{O}(\varepsilon^{K+1})$$
$$\text{uniformly for} \quad \mathbf{x} \in \overline{S'} \times (-\varepsilon, \varepsilon)$$

REVISED PAGE PROOFS

with fields $\widehat{\mathbf{v}}^{K,k}$ being polynomials in x_3 of degree $K-k$. This means that the expansion (6) can also be seen as a *Taylor expansion* at the midsurface, provided we are at a fixed positive distance from the lateral boundary.

Let us write the first terms in the expansions of the bending and membrane parts $\mathbf{u}^\varepsilon_{\mathsf{b}}$ and $\mathbf{u}^\varepsilon_{\mathsf{m}}$ of $\mathbf{u}^\varepsilon$:

$$\begin{aligned}\mathbf{u}^\varepsilon_{\mathsf{b}} = \varepsilon^{-2}&\left(-\mathsf{x}_3\nabla_\top\zeta_3^{-2},\ \zeta_3^{-2}+\frac{\lambda\mathsf{x}_3^2}{2\lambda+4\mu}\Delta_\top\zeta_3^{-2}\right)\\ &-\left(\mathbf{0},\frac{\lambda}{6\lambda+12\mu}\Delta_\top\zeta_3^{-2}\right)+\varepsilon^{-1}\left(-\mathsf{x}_3\nabla_\top\zeta_3^{-1},\right.\\ &\left.\zeta_3^{-1}+\frac{\lambda\mathsf{x}_3^2}{2\lambda+4\mu}\Delta_\top\zeta_3^{-1}\right)+\cdots\end{aligned}\tag{25}$$

From this formula, we can deduce the following asymptotics for the strain and stress components

$$\begin{aligned}e_{\alpha\beta}(\mathbf{u}^\varepsilon_{\mathsf{b}}) &= -\varepsilon^{-2}\mathsf{x}_3\partial_{\alpha\beta}\big(\zeta_3^{-2}+\varepsilon\zeta_3^{-1}\big)+\mathcal{O}(\varepsilon)\\ e_{33}(\mathbf{u}^\varepsilon_{\mathsf{b}}) &= \varepsilon^{-2}\frac{\lambda\mathsf{x}_3}{\lambda+2\mu}\Delta_\top\big(\zeta_3^{-2}+\varepsilon\zeta_3^{-1}\big)+\mathcal{O}(\varepsilon)\\ \sigma^{33}(\mathbf{u}^\varepsilon_{\mathsf{b}}) &= \mathcal{O}(\varepsilon)\end{aligned}\tag{26}$$

Since $\varepsilon^{-2}\mathsf{x}_3=\mathcal{O}(\varepsilon^{-1})$, we see that $e_{33}=\mathcal{O}(\varepsilon^{-1})$. Thus, σ^{33} is two orders of magnitude less than e_{33}, which means a *plane stress limit*. To compute the shear strain (or stress), we use one further term in the asymptotics of $\mathbf{u}^\varepsilon_{\mathsf{b}}$ and obtain that it is one order of magnitude less than e_{33}:

$$e_{\alpha3}(\mathbf{u}^\varepsilon_{\mathsf{b}})=\frac{2\lambda+2\mu}{\lambda+2\mu}(\varepsilon^{-2}\mathsf{x}_3^2-1)\partial_\alpha\Delta_\top\zeta_3^{-2}+\mathcal{O}(\varepsilon)\tag{27}$$

Computations for the membrane part $\mathbf{u}^\varepsilon_{\mathsf{m}}$ are simpler and yield similar results

$$\begin{aligned}\mathbf{u}^\varepsilon_{\mathsf{m}} &= \left(\boldsymbol{\zeta}^0_\top,\ -\frac{\lambda\mathsf{x}_3}{\lambda+2\mu}\operatorname{div}\boldsymbol{\zeta}^0_\top\right)\\ &\quad+\varepsilon\left(\boldsymbol{\zeta}^1_\top,\ -\frac{\lambda\mathsf{x}_3}{\lambda+2\mu}\operatorname{div}\boldsymbol{\zeta}^1_\top\right)+\cdots\\ e_{\alpha\beta}(\mathbf{u}^\varepsilon_{\mathsf{m}}) &= \frac{1}{2}(\partial_\alpha\zeta^0_\beta+\partial_\beta\zeta^0_\alpha)+\frac{\varepsilon}{2}(\partial_\alpha\zeta^1_\beta+\partial_\beta\zeta^1_\alpha)+\mathcal{O}(\varepsilon^2)\\ e_{33}(\mathbf{u}^\varepsilon_{\mathsf{m}}) &= -\frac{\lambda}{\lambda+2\mu}\operatorname{div}\big(\boldsymbol{\zeta}^0_\top+\varepsilon\boldsymbol{\zeta}^1_\top\big)+\mathcal{O}(\varepsilon^2)\end{aligned}\tag{28}$$

and $\sigma^{33}(\mathbf{u}^\varepsilon_{\mathsf{m}})=\mathcal{O}(\varepsilon^2)$, $e_{\alpha3}(\mathbf{u}^\varepsilon_{\mathsf{m}})=\mathcal{O}(\varepsilon)$.

In (26)–(28) the $\mathcal{O}(\varepsilon)$ and $\mathcal{O}(\varepsilon^2)$ are uniform on any region $\overline{S'}\times(-\varepsilon,\varepsilon)$ where the boundary layer terms have no influence. We postpone global energy estimates to the next section.

2.4 Eigen-mode problem

For each $\varepsilon>0$, the spectrum of problem (4) is discrete and positive. Let Λ^ε_j, $j=1,2,\ldots$ be the increasing sequence of eigenvalues. In Ciarlet and Kesavan (1981) it is proved that $\varepsilon^{-2}\Lambda^\varepsilon_j$ converges to the jth eigenvalue $\Lambda^{\mathsf{KL}}_{\mathsf{b},j}$ of the Dirichlet problem for the Kirchhoff operator L_{b}, cf. (16). In Nazarov and Zorin (1989) and Nazarov (1991c), a two-term asymptotics is constructed for the $\varepsilon^{-2}\Lambda^\varepsilon_j$. Nazarov (2000b) proves that $|\varepsilon^{-2}\Lambda^\varepsilon_j-\Lambda^{\mathsf{KL}}_{\mathsf{b},j}|$ is bounded by an $\mathcal{O}(\sqrt{\varepsilon})$ for a much more general material matrix A.

In Dauge *et al.* (1999), full asymptotic expansions for eigenvalues and eigenvectors are proved: For each j there exist

- bending generators $\zeta_3^{-2}, \zeta_3^{-1},\ldots$ where ζ_3^{-2} is an eigenvector of L_{b} associated with $\Lambda^{\mathsf{KL}}_{\mathsf{b},j}$
- real numbers $\Lambda^1_{\mathsf{b},j}, \Lambda^2_{\mathsf{b},j},\ldots$
- eigenvectors $\mathbf{u}^\varepsilon_{\mathsf{b},j}$ associated with Λ^ε_j for any $\varepsilon\in(0,\varepsilon_0)$

so that for any $K\ge0$

$$\begin{aligned}\Lambda^\varepsilon_j &= \varepsilon^2\Lambda^{\mathsf{KL}}_{\mathsf{b},j}+\varepsilon^3\Lambda^1_{\mathsf{b},j}+\cdots+\varepsilon^{K+2}\Lambda^K_{\mathsf{b},j}+\mathcal{O}(\varepsilon^{K+3})\\ \mathbf{u}^\varepsilon_{\mathsf{b},j} &= \varepsilon^{-2}(-\mathsf{x}_3\nabla_\top\zeta_3^{-2},\zeta_3^{-2})+\varepsilon^{-1}(-\mathsf{x}_3\nabla_\top\zeta_3^{-1},\zeta_3^{-1})\\ &\quad+\cdots+\varepsilon^K(\mathbf{v}^K+\chi\mathbf{w}^K)+\mathcal{O}(\varepsilon^{K+1})\end{aligned}\tag{29}$$

where the terms $\mathbf{v}^k$ and $\mathbf{w}^k$ are generated by the ζ^k_3, $k\ge0$ in a similar way as in Section 2.2, and $\mathcal{O}(\varepsilon^{K+1})$ is uniform over Ω^ε.

The bending and membrane displacements are the eigenvectors of the symmetry operator $\mathfrak{S}$; see (5). Since $\mathfrak{S}$ commutes with the elasticity operator, both have a joint spectrum, which means that there exists a basis of common eigenvectors. In other words, each elasticity eigenvalue can be identified as a bending or a membrane eigenvalue. The expansion (29) is the expansion of *bending* eigen-pairs.

The expansion of membrane eigen-pairs can be done in a similar way. Let us denote by $\Lambda^\varepsilon_{\mathsf{m},j}$ the jth membrane eigenvalue on Ω^ε and by $\Lambda^{\mathsf{KL}}_{\mathsf{m},j}$ the jth eigenvalue of the plane stress operator L_{m}, cf. (20) with Dirichlet boundary conditions. Then we have a similar statement as above, with the distinctive feature that the membrane eigenvalues tend to those of the plane stress model:

$$\Lambda^\varepsilon_{\mathsf{m},j}=\Lambda^{\mathsf{KL}}_{\mathsf{m},j}+\varepsilon^1\Lambda^1_{\mathsf{m},j}+\cdots+\varepsilon^K\Lambda^K_{\mathsf{m},j}+\mathcal{O}(\varepsilon^{K+1})\tag{30}$$

This fact, compared with (29), explains why the smallest eigenvalues are bending. Note that the eigenvalue formal series $\Lambda[\varepsilon]$ satisfy reduced equations $\mathbf{L}[\varepsilon]\boldsymbol{\zeta}[\varepsilon]=\Lambda[\varepsilon]\boldsymbol{\zeta}[\varepsilon]$ like (21) with the same $\mathbf{L}^0$, $\mathbf{L}^1=0$ and $\mathbf{L}^2$ as in (22). In

REVISED PAGE PROOFS

particular, equations

$$\begin{pmatrix} L_{\mathsf{m}} & 0 \\ 0 & \varepsilon^2 L_{\mathsf{b}} \end{pmatrix} \begin{pmatrix} \boldsymbol{\zeta}_\top \\ \zeta_3 \end{pmatrix} = \Lambda \begin{pmatrix} \boldsymbol{\zeta}_\top \\ \zeta_3 \end{pmatrix} \tag{31}$$

give back the 'limiting' eigenvalues $\Lambda_{\mathsf{m}}^{\mathsf{KL}}$ and $\varepsilon^2 \Lambda_{\mathsf{b}}^{\mathsf{KL}}$. Our last remark is that the second terms $\Lambda_{\mathsf{b},j}^{1}$ and $\Lambda_{\mathsf{m},j}^{1}$ are positive; see Dauge and Yosibash (2002) for a discussion of that fact.

2.5 Extensions

2.5.1 Traction on the free parts of the boundary

Instead of a volume load, or in addition to it, tractions $\mathbf{g}^{\pm}$ can be imposed on the faces $S \times \{\pm\varepsilon\}$ of the plate. Let us assume that $\mathbf{g}^{\pm}$ is independent of ε. Then the displacement $\mathbf{u}^{\varepsilon}$ has a similar expansion as in (6), with the following modifications:

- If the bending part of $\mathbf{g}^{\pm}$ is nonzero, then the regular part starts with $\varepsilon^{-3}\mathbf{v}^{-3}$ and the boundary layer part with $\varepsilon^{-1}\chi\mathbf{w}^{-1}$;
- If the membrane part of $\mathbf{g}^{\pm}$ is nonzero, the membrane regular part starts with $\varepsilon^{-1}\mathbf{v}^{-1}$.

2.5.2 Lateral boundary conditions

A similar analysis holds for each of the seven remaining types of 'canonical' boundary conditions: soft clamping, hard simple support, soft simple support, two types of friction, sliding edge, and free boundary. See Dauge, Gruais and Rössle (1999/00) for details. It would also be possible to extend such an analysis to more intimately mixed boundary conditions where only moments through the thickness along the lateral boundary are imposed for displacement or traction components; see Schwab (1996).

If, instead of volume load $\mathbf{f}$ or tractions $\mathbf{g}^{\pm}$, we set $\mathbf{f} \equiv 0$, $\mathbf{g}^{\pm} \equiv 0$, and impose nonzero lateral boundary conditions, $\mathbf{u}^{\varepsilon}$ will have a similar expansion as in (6) with the remarkable feature that the degree of the regular part in the thickness variable is ≤ 3; see Dauge and Schwab (2002), Rem. 5.4. Moreover, in the clamped situation, the expansion starts with $\mathcal{O}(1)$.

2.5.3 Laminated composites

If the material of the plate is homogeneous, but not isotropic, $\mathbf{u}^{\varepsilon}$ will still have a similar expansion; see Dauge and Gruais (1996) and Dauge and Yosibash (2002) for orthotropic plates. If the plate is laminated, that is, formed by the union of several plies made of different homogeneous materials, then $\mathbf{u}^{\varepsilon}$ still expands in regular parts $\mathbf{v}^k$ and boundary layer parts $\mathbf{w}^k$, but the $\mathbf{v}^k$ are no more polynomials in the thickness variable, only *piecewise polynomial* in each ply, and continuous; see Actis, Szabo and Schwab (1999). Nazarov (2000a, 2000b) addresses more general material laws where the matrix A depends on the variables $\mathbf{x}_\top$ and $\mathsf{X}_3 = \mathbf{x}_3/\varepsilon$.

3 HIERARCHICAL MODELS FOR PLATES

3.1 The concepts of hierarchical models

The idea of hierarchical models is a natural and efficient extension to that of limiting models and dimension reduction. In the finite element framework, it has been firstly formulated in Szabó and Sahrmann (1988) for isotropic domains, mathematically investigated in Babuška and Li (1991, 1992a, 1992b), and generalized to laminated composites in Babuška, Szabó and Actis (1992) and Actis, Szabo and Schwab (1999). A hierarchy of models consists of

- a sequence of subspaces $V^{\mathbf{q}}(\Omega^{\varepsilon})$ of $V(\Omega^{\varepsilon})$ with the *orders* $\mathbf{q} = (q_1, q_2, q_3)$ forming a sequence of integer triples, satisfying

$$V^{\mathbf{q}}(\Omega^{\varepsilon}) \subset V^{\mathbf{q}'}(\Omega^{\varepsilon}) \quad \text{if} \quad \mathbf{q} \preceq \mathbf{q}' \tag{32}$$

- a sequence of related Hooke laws $\boldsymbol{\sigma} = A_{\mathbf{q}}\boldsymbol{e}$, corresponding to a sequence of elastic bilinear forms $a^{\varepsilon,\mathbf{q}}(\mathbf{u}, \mathbf{u}') = \int_{\Omega^{\varepsilon}} A_{\mathbf{q}}\boldsymbol{e}(\mathbf{u}) : \boldsymbol{e}(\mathbf{u}')$.

Let $\mathbf{u}^{\varepsilon,\mathbf{q}}$ be the solution of the problem

$$\textit{Find} \ \ \mathbf{u}^{\varepsilon,\mathbf{q}} \in V^{\mathbf{q}}(\Omega^{\varepsilon}) \ \ \textit{such that}$$
$$a^{\varepsilon,\mathbf{q}}(\mathbf{u}^{\varepsilon,\mathbf{q}}, \mathbf{u}') = \int_{\Omega^{\varepsilon}} \mathbf{f}^{\varepsilon} \cdot \mathbf{u}' \, \mathrm{d}\boldsymbol{x}, \quad \forall \mathbf{u}' \in V^{\mathbf{q}}(\Omega^{\varepsilon}) \tag{33}$$

Note that problem (33) is a Galerkin projection of problem (3) if $a^{\varepsilon,\mathbf{q}} = a^{\varepsilon}$.

Any model that belongs to the hierarchical family has to satisfy three requirements; see Szabó and Babuška (1991), Chap. 14.5:

(a) *Approximability.* At any fixed thickness $\varepsilon > 0$:

$$\lim_{\mathbf{q}\to\infty} \|\mathbf{u}^{\varepsilon} - \mathbf{u}^{\varepsilon,\mathbf{q}}\|_{E(\Omega^{\varepsilon})} = 0 \tag{34}$$

(b) *Asymptotic consistency.* For any fixed degree $\mathbf{q}$:

$$\lim_{\varepsilon\to 0} \frac{\|\mathbf{u}^{\varepsilon} - \mathbf{u}^{\varepsilon,\mathbf{q}}\|_{E(\Omega^{\varepsilon})}}{\|\mathbf{u}^{\varepsilon}\|_{E(\Omega^{\varepsilon})}} = 0 \tag{35}$$

REVISED PAGE PROOFS

(c) *Optimality of the convergence rate.* There exists a sequence of positive exponents $\gamma(\mathbf{q})$ with the growth property $\gamma(\mathbf{q}) < \gamma(\mathbf{q}')$ if $\mathbf{q} \prec \mathbf{q}'$, such that 'in the absence of boundary layers and edge singularities':

$$\|\mathbf{u}^\varepsilon - \mathbf{u}^{\varepsilon,\mathbf{q}}\|_{E(\Omega^\varepsilon)} \leq C\varepsilon^{\gamma(\mathbf{q})}\|\mathbf{u}^\varepsilon\|_{E(\Omega^\varepsilon)} \tag{36}$$

The substantiation of hierarchical models for plates, in general, requires the choice of three sequences of finite dimensional nested *director spaces* $\Psi_j^0 \subset \cdots \Psi_j^N \subset \cdots \subset H^1(-1,1)$ for $j = 1, 2, 3$ and the definition of the space $V^{\mathbf{q}}(\Omega^\varepsilon)$ for $\mathbf{q} = (q_1, q_2, q_3)$ as

$$V^{\mathbf{q}}(\Omega^\varepsilon) = \Big\{\mathbf{u} \in V(\Omega^\varepsilon),\ \Big((\mathbf{x}_\top, \mathsf{X}_3) \mapsto \mathsf{u}_j(\mathbf{x}_\top, \varepsilon\mathsf{X}_3)\Big) \in H_0^1(S) \otimes \Psi_j^{q_j},\quad j = 1, 2, 3\Big\} \tag{37}$$

We can reformulate (37) with the help of *director functions*: With $d_j(N)$ being the dimension of Ψ_j^N, let $\Phi_j^n = \Phi_j^n(\mathsf{X}_3)$, $0 \leq n \leq d_j(N)$, be hierarchic bases (the director functions) of Ψ_j^N. There holds

$$V^{\mathbf{q}}(\Omega^\varepsilon) = \Big\{\mathbf{u} \in V(\Omega^\varepsilon),\ \exists \mathsf{z}_j^n \in H_0^1(S),\ 0 \leq n \leq d_j(q_j),\ \mathsf{u}_j(\mathbf{x}_\top, \mathsf{x}_3) = \sum_{n=0}^{d_j(q_j)} \mathsf{z}_j^n(\mathbf{x}_\top)\,\Phi_j^n\Big(\frac{\mathsf{X}_3}{\varepsilon}\Big)\Big\} \tag{38}$$

The choice of the *best* director functions is addressed in Vogelius and Babuška (1981c) in the case of second-order scalar problems with general coefficients (including possible stratifications). For smooth coefficients, the space Ψ_j^N coincides with the space $\mathbb{P}_N$ of polynomial with degree $\leq N$. The director functions can be chosen as the Legendre polynomials $L_n(\mathsf{X}_3)$ or, simply, the monomials X_3^n (and then x_3^n can be used equivalently instead $(\mathsf{x}_3/\varepsilon)^n$ in (38)).

We describe in the sequel in more detail, the convenient hierarchies for plates and discuss the three qualities (34)–(36); see Babuška and Li (1991, 1992a) and Babuška, Szabó and Actis (1992) for early references.

3.2 The limit model (Kirchhoff–Love)

In view of expansion (6), we observe that if the transverse component f_3 of the load is nonzero on the midsurface, $\mathbf{u}^\varepsilon$ is unbounded as $\varepsilon \to 0$. If we multiply by ε^2, we have a convergence to $(0, \zeta_3^{-2})$, which is not kinematically relevant. At that level, a correct notion of limit uses scalings of coordinates: If we define the scaled displacement $\widetilde{\mathbf{u}}^\varepsilon$ by its components on the stretched plate $\Omega = S \times (-1, 1)$ by

$$\widetilde{\mathbf{u}}_\top^\varepsilon := \varepsilon\mathbf{u}_\top^\varepsilon \quad \text{and} \quad \widetilde{\mathsf{u}}_3^\varepsilon := \varepsilon^2\mathsf{u}_3^\varepsilon \tag{39}$$

then $\widetilde{\mathbf{u}}^\varepsilon$ *converges to* $(-\mathsf{X}_3\nabla_\top\zeta_3^{-2},\ \zeta_3^{-2})$ *in* $H^1(\Omega)^3$ *as* $\varepsilon \to 0$. This result, together with the mathematical derivation of the resultant equation (15), is due to Ciarlet and Destuynder (1979a).

The corresponding subspace of $V(\Omega^\varepsilon)$ is that of bending Kirchhoff displacements or, more generally, of Kirchhoff displacements:

$$V^{\mathsf{KL}}(\Omega^\varepsilon) = \{\mathbf{u} \in V(\Omega^\varepsilon),\ \exists\boldsymbol{\zeta} \in H_0^1 \times H_0^1 \times H_0^2(S),\ \mathbf{u} = (\boldsymbol{\zeta}_\top - \mathsf{x}_3\nabla_\top\zeta_3,\ \zeta_3)\} \tag{40}$$

It follows from (40) that $e_{13} = e_{23} = 0$ for which the physical interpretation is that 'normals to S prior to deformation remain straight lines and normals after deformation'. Hooke's law has to be modified with the help of what we call 'the plane stress trick'. It is based on the assumption that the component σ^{33} of the stress is negligible (note that the asymptotics (6) of the three-dimensional solution yields that $\sigma^{33} = \mathcal{O}(\varepsilon)$, whereas $e_{\alpha\beta}$, $e_{33} = \mathcal{O}(\varepsilon^{-1})$ outside the boundary layer, cf. (26), which justifies the plane stress assumption). From standard Hooke's law (1), we extract the relation $\sigma^{33} = \lambda(e_{11} + e_{22}) + (\lambda + 2\mu)e_{33}$, then set σ^{33} to zero, which yields

$$e_{33} = -\frac{\lambda}{\lambda + 2\mu}\,(e_{11} + e_{22}) \tag{41}$$

Then, we modify Hooke's law (1) by substituting e_{33} by its expression (41) in σ^{11} and σ^{22}, to obtain

$$\sigma^{ii} = \frac{2\lambda\mu}{\lambda + 2\mu}(e_{11} + e_{22}) + 2\mu e_{ii},\quad i = 1, 2 \qquad \sigma^{ij} = 2\mu e_{ij} \quad \text{for} \quad i \neq j \tag{42}$$

Thus, $\sigma^{ii} = \widetilde{\lambda}(e_{11} + e_{22}) + 2\mu e_{ii}$, with $\widetilde{\lambda}$ given by (17). Taking into account that $e_{33} = 0$ for the elements of $V^{\mathsf{KL}}(\Omega^\varepsilon)$, we obtain a new Hooke's law given by the same formulae as (1) when replacing the Lamé coefficient λ by $\widetilde{\lambda}$. This corresponds to a modified material matrix $\widetilde{A}^{ijkl}$

$$\widetilde{A}^{ijkl} = \widetilde{\lambda}\delta^{ij}\delta^{kl} + \mu(\delta^{ik}\delta^{jl} + \delta^{il}\delta^{jk}) \tag{43}$$

and a reduced elastic energy $\widetilde{a}(\mathbf{u}, \mathbf{u}) = \int_{\Omega^\varepsilon} \sigma^{ij}(\mathbf{u})e_{ij}(\mathbf{u})$. Note that for $\mathbf{u} = (\boldsymbol{\zeta}_\top - \mathsf{x}_3\nabla_\top\zeta_3,\ \zeta_3)$

$$\widetilde{a}(\mathbf{u}, \mathbf{u}) = 2\varepsilon\int_S \widetilde{A}^{\alpha\beta\sigma\delta}e_{\alpha\beta}(\boldsymbol{\zeta}_\top)e_{\sigma\delta}(\boldsymbol{\zeta}_\top)\,\mathrm{d}\mathbf{x}_\top + \frac{2\varepsilon^3}{3}\int_S \widetilde{A}^{\alpha\beta\sigma\delta}\partial_{\alpha\beta}(\zeta_3)\partial_{\sigma\delta}(\zeta_3)\,\mathrm{d}\mathbf{x}_\top \tag{44}$$

exhibiting a *membrane part* in $\mathcal{O}(\varepsilon)$ and a *bending part* in $\mathcal{O}(\varepsilon^3)$. There hold as a consequence of Theorem 1

REVISED PAGE PROOFS

Theorem 2. *Let* $\mathbf{u}^{\varepsilon,\mathsf{KL}}$ *be the solution of problem (33) with* $V^{\mathbf{q}} = V^{\mathsf{KL}}$ *and* $a^{\mathbf{q}} = \widetilde{a}$. *Then*

(i) *In general* $\mathbf{u}^{\varepsilon,\mathsf{KL}} = \varepsilon^{-2}\big(-\mathsf{x}_3\nabla_\top\zeta_3^{-2},\ \zeta_3^{-2}\big) + \mathcal{O}(1)$ *with* ζ_3^{-2} *the solution of (15);*

(ii) *If* $\mathbf{f}$ *is membrane,* $\mathbf{u}^{\varepsilon,\mathsf{KL}} = \big(\boldsymbol{\zeta}_\top^0, 0\big) + \mathcal{O}(\varepsilon^2)$ *with* $\boldsymbol{\zeta}_\top^0$ *the solution of (19).*

Can we deduce the asymptotic consistency for that model? No! Computing the lower-order terms in the expression (35), we find with the help of (25) that, if $\mathsf{f}_3^0 \not\equiv 0$

$$\|\mathbf{u}^\varepsilon\|_{E(\Omega^\varepsilon)} \simeq \mathcal{O}(\varepsilon^{-1/2})$$

and

$$\|\mathbf{u}^\varepsilon - \mathbf{u}^{\varepsilon,\mathsf{KL}}\|_{E(\Omega^\varepsilon)} \geq \|e_{33}(\mathbf{u}^\varepsilon)\|_{L^2(\Omega^\varepsilon)} \simeq \mathcal{O}(\varepsilon^{-1/2})$$

Another source of difficulty is that, eventually, relation (41) *is not satisfied* by $\mathbf{u}^{\varepsilon,\mathsf{KL}}$. If $\mathsf{f}_3^0 \equiv 0$ and $\mathbf{f}_\top^0 \not\equiv 0$, we have exactly the same difficulties with the membrane part.

A way to overcome these difficulties is to consider a complementing operator $\mathbf{C}$ defined on the elements of V^{KL} by

$$\mathbf{Cu} = \mathbf{u} + \Big(\mathbf{0}, -\frac{\lambda}{\lambda+2\mu}\int_0^{\mathsf{x}_3} \operatorname{div}\mathbf{u}_\top(\cdot,\mathsf{y})\,\mathrm{d}\mathsf{y}\Big) \tag{45}$$

Then (41) is now satisfied by $\mathbf{Cu}$ for any $\mathbf{u} \in V^{\mathsf{KL}}$. Moreover (still assuming $\mathsf{f}_3 \not\equiv 0$), one can show

$$\|\mathbf{u}^\varepsilon - \mathbf{Cu}^{\varepsilon,\mathsf{KL}}\|_{E(\Omega^\varepsilon)} \leq C\sqrt{\varepsilon}\|\mathbf{u}^\varepsilon\|_{E(\Omega^\varepsilon)} \tag{46}$$

The error factor $\sqrt{\varepsilon}$ is due to the first boundary layer term $\mathbf{w}^0$. The presence of $\mathbf{w}^0$ is a direct consequence of the fact that $\mathbf{Cu}^{\varepsilon,\mathsf{KL}}$ does not satisfy the lateral boundary conditions.

Although the Kirchhoff–Love model is not a member of the hierarchical family, it is the limit of all models for $\varepsilon \to 0$.

3.3 The Reissner–Mindlin model

This model is obtained by enriching the space of kinematically admissible displacements, allowing normals to S to rotate after deformation. Instead of (40), we set

$$V^{\mathsf{RM}}(\Omega^\varepsilon) = \{\mathbf{u} \in V(\Omega^\varepsilon),\ \exists\mathbf{z} \in H_0^1(S)^3,\ \exists\boldsymbol{\theta}_\top \in H_0^1(S)^2,\ \mathbf{u} = (\mathbf{z}_\top - \mathsf{x}_3\boldsymbol{\theta}_\top,\ \mathsf{z}_3)\}$$

With the elasticity tensor A corresponding to 3-D elasticity, the displacements and strain–energy limit of the RM model as $d \to 0$ would not coincide with the 3-D limit (or the Kirchhoff–Love limit).

We have again to use instead the reduced elastic bilinear form $\widetilde{a}$ to restore the convergence to the correct limit, by virtue of the same plane stress trick. The corresponding elasticity tensor is $\widetilde{A}$ (43). A further correction can be introduced in the shear components of $\widetilde{A}$ to better represent the fully 3-D shear stresses σ^{13} and σ^{23} (and also the strain energy) for small yet nonzero thickness ε. The material matrix entries A^{1313}, A^{2323} are changed by introducing the so-called *shear correction factor* κ:

$$\widetilde{A}^{1313} = \kappa A^{1313} \quad \widetilde{A}^{2323} = \kappa A^{2323}$$

By properly chosen κ, either the energy of the RM solution, or the deflection u_3 can be optimized with respect to the fully 3-D plate. The smaller the ε, the smaller the influence of κ on the results. For the isotropic case, two possible κ's are (see details in Babuška, d'Harcourt and Schwab (1991a)):

$$\kappa_{\text{Energy}} = \frac{5}{6(1-\nu)} \quad \text{or} \quad \kappa_{\text{Deflection}} = \frac{20}{3(8-3\nu)},$$
$$\text{with} \quad \nu = \frac{\lambda}{2(\lambda+\mu)} \quad \text{(Poisson ratio)}$$

A value of $\kappa = 5/6$ is frequently used in engineering practice, but for modal analysis, no optimal value of κ is available.

Note that, by integrating equations of (33) through the thickness, we find that problem (33) is equivalent to a variational problem for $\mathbf{z}$ and $\boldsymbol{\theta}$ only. For the elastic energy, we have

$$\begin{aligned}\widetilde{a}(\mathbf{u},\mathbf{u}) = {} & 2\varepsilon\int_S \widetilde{A}^{\alpha\beta\sigma\delta}e_{\alpha\beta}(\mathbf{z}_\top)e_{\sigma\delta}(\mathbf{z}_\top)\,\mathrm{d}\mathbf{x}_\top \\ & \qquad \textit{(membrane energy)} \\ & + \varepsilon\int_S \kappa\mu(\partial_\alpha\mathsf{z}_3 - \theta_\alpha)(\partial_\alpha\mathsf{z}_3 - \theta_\alpha)\,\mathrm{d}\mathbf{x}_\top \\ & \qquad \textit{(shear energy)} \\ & + \frac{2\varepsilon^3}{3}\int_S \widetilde{A}^{\alpha\beta\sigma\delta}e_{\alpha\beta}(\boldsymbol{\theta}_\top)e_{\sigma\delta}(\boldsymbol{\theta}_\top)\,\mathrm{d}\mathbf{x}_\top \\ & \qquad \textit{(bending energy)}\end{aligned} \tag{47}$$

Let $\mathbf{u}^{\varepsilon,\mathsf{RM}}$ be the solution of problem (33) with $V^{\mathbf{q}} = V^{\mathsf{RM}}$ and $a^{\mathbf{q}} = \widetilde{a}$. The singular perturbation character appears clearly. In contrast with the Kirchhoff–Love model, the solution admits a boundary layer part. Arnold and Falk (1990b, 1996) have described the two-scale asymptotics of $\mathbf{u}^{\varepsilon,\mathsf{RM}}$. Despite the presence of boundary layer terms, the question of knowing if $\mathbf{u}^{\varepsilon,\mathsf{RM}}$ is closer to $\mathbf{u}^\varepsilon$ than $\mathbf{u}^{\varepsilon,\mathsf{KL}}$ has no clear answer to our knowledge. A careful investigation of the first eigenvalues Λ_1^ε, $\Lambda_1^{\varepsilon,\mathsf{KL}}$, and $\Lambda_1^{\varepsilon,\mathsf{RM}}$ of these three models in the case of lateral Dirichlet conditions shows the following behavior for ε small enough (Dauge and Yosibash, 2002):

REVISED PAGE PROOFS

$$\Lambda_1^{\varepsilon,\mathsf{RM}} < \Lambda_1^{\varepsilon,\mathsf{KL}} < \Lambda_1^{\varepsilon}$$

which tends to prove that RM model is not generically better than KL for (very) thin plates. Nevertheless, an estimate by the same asymptotic bound as in (46) is valid for $\mathbf{u}^\varepsilon - \mathbf{C}\mathbf{u}^{\varepsilon,\mathsf{RM}}$.

3.4 Higher order models

The RM model is a (1, 1, 0) model with reduced elastic energy. For any $\mathbf{q} = (q_\top, q_\top, q_3)$ we define the space $V^{\mathbf{q}}$ by (compare with (38) for monomial director functions)

$$V^{\mathbf{q}}(\Omega^\varepsilon) = \Bigg\{ \mathbf{u} \in V(\Omega^\varepsilon), \quad \exists \mathbf{z}_\top^n \in H_0^1(S)^2,\ 0 \le n \le q_\top,$$
$$\exists z_3^n \in H_0^1(S),\ 0 \le n \le q_3$$
$$\mathbf{u}_\top = \sum_{n=0}^{q_\top} \mathsf{x}_3^n\, \mathbf{z}_\top^n(\mathbf{x}_\top) \quad \text{and} \quad \mathsf{u}_3 = \sum_{n=0}^{q_3} \mathsf{x}_3^n\, z_3^n(\mathbf{x}_\top) \Bigg\} \tag{48}$$

The subspaces $V_{\mathsf{b}}^{\mathbf{q}}$ and $V_{\mathsf{m}}^{\mathbf{q}}$ of bending and membrane displacements in $V^{\mathbf{q}}$ can also be used, according to the nature of the data. The standard 3-D elastic energy (2) is used with $V^{\mathbf{q}}$ and $V_{\mathsf{b}}^{\mathbf{q}}$ for any $\mathbf{q} \succeq (1, 1, 2)$ and with $V_{\mathsf{m}}^{\mathbf{q}}$ for any $\mathbf{q} \succeq (0, 0, 1)$.

Theorem 3.

(i) *If* $\mathbf{f}$ *satisfies* $\mathsf{f}_3\big|_S \not\equiv 0$, *for any* $\mathbf{q} \succeq (1, 1, 2)$ *there exists* $C_{\mathbf{q}} = C_{\mathbf{q}}(\mathbf{f}) > 0$ *such that for all* $\varepsilon \in (0, \varepsilon_0)$

$$\|\mathbf{u}^\varepsilon - \mathbf{u}^{\varepsilon,\mathbf{q}}\|_{E(\Omega^\varepsilon)} \le C_{\mathbf{q}} \sqrt{\varepsilon}\, \|\mathbf{u}^\varepsilon\|_{E(\Omega^\varepsilon)} \tag{49}$$

(ii) *If* $\mathbf{f}$ *is membrane and* $\mathbf{f}_\top\big|_S \not\equiv 0$, *for any* $\mathbf{q} \succeq (0, 0, 1)$ *there exists* $C_{\mathbf{q}} = C_{\mathbf{q}}(\mathbf{f}) > 0$ *such that for all* $\varepsilon \in (0, \varepsilon_0)$ *(49) holds.*

Proof. Since the energy is not altered by the model, $\mathbf{u}^{\varepsilon,\mathbf{q}}$ is a Galerkin projection of $\mathbf{u}^\varepsilon$ on $V^{\mathbf{q}}(\Omega^\varepsilon)$. Since the strain energy is uniformly equivalent to the elastic energy on any Ω^ε, we have by Céa's lemma that there exists $C > 0$

$$\|\mathbf{u}^\varepsilon - \mathbf{u}^{\varepsilon,\mathbf{q}}\|_{E(\Omega^\varepsilon)} \le C \|\mathbf{u}^\varepsilon - \mathbf{v}^{\mathbf{q}}\|_{E(\Omega^\varepsilon)} \qquad \forall \mathbf{v}^{\mathbf{q}} \in V^{\mathbf{q}}(\Omega^\varepsilon)$$

(i) We choose, compare with (25),

$$\mathbf{v}^{\mathbf{q}} = \varepsilon^{-2} \left(-\mathsf{x}_3 \nabla_\top \zeta_3^{-2},\ \zeta_3^{-2} + \frac{\lambda \mathsf{x}_3^2}{2\lambda + 4\mu} \Delta_\top \zeta_3^{-2} \right)$$
$$- \frac{\varepsilon^{-2} \lambda \mathsf{x}_3^2}{2\lambda + 4\mu} \varphi(\mathsf{s}) \left(\mathbf{0}, \xi(\mathsf{R}) \right)$$

with $\varphi = \Delta_\top \zeta_3^{-2}\big|_{\partial S}$ and ξ a smooth cut-off function equal to 1 in a neighborhood of $\mathsf{R} = 0$ and 0 for $\mathsf{R} \ge 1$. Then $\mathbf{v}^{\mathbf{q}}$ satisfies the lateral boundary conditions and we can check (49) by combining Theorem 1 with the use of Céa's lemma.

(ii) We choose, instead

$$\mathbf{v}^{\mathbf{q}} = \left(\boldsymbol{\zeta}_\top^0, -\frac{\lambda \mathsf{x}_3}{\lambda + 2\mu} \operatorname{div} \boldsymbol{\zeta}_\top^0 \right) + \frac{\lambda \mathsf{x}_3}{\lambda + 2\mu} \varphi(\mathsf{s}) \left(\mathbf{0}, \xi(\mathsf{R}) \right)$$
$$\text{with} \quad \varphi = \operatorname{div} \boldsymbol{\zeta}_\top^0\big|_{\partial S}$$

□

It is worthwhile to mention that for the (1, 1, 2) model the shear correction factor (when $\nu \to 0$, $\kappa_{(1,1,2)}$ tends to 5/6, just like for the two shear correction factors of the RM model)

$$\kappa_{(1,1,2)} = \frac{12 - 2\nu}{\nu^2} \left(-1 + \sqrt{1 + \frac{20\nu^2}{(12 - 2\nu)^2}} \right)$$

can be used for optimal results in respect with the error in energy norm and deflection for finite thickness plates; see Babuška, d'Harcourt and Schwab (1991a). For higher plate models, no shear correction factor is furthermore needed.

The result in Schwab and Wright (1995) regarding the approximability of the boundary layers by elements of $V^{\mathbf{q}}$, yields that the constant $C_{\mathbf{q}}$ in (49) should rapidly decrease when $\mathbf{q}$ increases. Nevertheless the factor $\sqrt{\varepsilon}$ is still present, for any $\mathbf{q}$, because of the presence of the boundary layer terms. The numerical experiments in Dauge and Yosibash (2000) demonstrate that the higher the degree of the hierarchical model, the better the boundary layer terms are approximated.

If one wants to have an approximation at a higher order in ε one should

- either consider a problem without boundary layer, as mentioned in requirement (c) (36), that is, a rectangular plate with symmetry boundary conditions: In this case, the convergence rate $\gamma(\mathbf{q})$ in ε is at least $\min_j q_j - 1$,
- or combine a hierarchy of models with a three-dimensional discretization of the boundary layer; see Stein and Ohnimus (1969) and Dauge and Schwab (2002).

The (1, 1, 2) is the lowest order model which is asymptotically consistent for bending. See Paumier and Raoult (1997) and Rössle *et al.* (1999). It is the first model in the bending model hierarchy

$$(1, 1, 2), \quad (3, 3, 2), \quad (3, 3, 4), \ldots$$
$$(2n - 1, 2n - 1, 2n), \quad (2n + 1, 2n + 1, 2n), \ldots$$

REVISED PAGE PROOFS

The exponent $\gamma(\mathbf{q})$ in (36) can be proved to be $2n-1$ if $\mathbf{q}=(2n-1,2n-1,2n)$ and $2n$ if $\mathbf{q}=(2n+1,2n+1,2n)$, thanks to the structure of the operator series $\mathbf{V}[\varepsilon]$ and $\mathbf{Q}[\varepsilon]$ in (11). If the load $\mathbf{f}$ is constant over the whole plate, then the model of degree (3, 3, 4) captures the *whole* regular part of $\mathbf{u}^\varepsilon$, (Dauge and Schwab (2002), Rem. 8.3) and if, moreover, $\mathbf{f}\equiv 0$ (in this case, only a lateral boundary condition is imposed), the degree (3, 3, 2) is sufficient.

3.5 Laminated plates

If the plate is laminated, the material matrix $A=A^\varepsilon$ has a sandwich structure, depending on the thickness variable x_3: We assume that $A^\varepsilon(\mathsf{x}_3)=\mathbb{A}(\mathsf{X}_3)$, where the coefficients of $\mathbb{A}$ are piecewise constant. In Nazarov (2000a) the asymptotic analysis is started, including such a situation. We may presume that a full asymptotic expansion like (6) with a similar internal structure, is still valid.

In the homogeneous case, the director functions in (38) are simply the monomials of increasing degrees; see (48). In the laminated case, the first director functions are still 1 and x_3:

$$\Phi_1^0=\Phi_2^0=\Phi_3^0=1;\quad \Phi_1^1=\Phi_2^1=\mathsf{x}_3$$

In the homogeneous case, we have $\Phi_3^1=\mathsf{x}_3$ and $\Phi_j^2=\mathsf{x}_3^2$, $j=1,2,3$. In Actis, Szabo and Schwab (1999) three more piecewise linear director functions and three piecewise quadratic director functions are exhibited for the laminated case.

How many independent director functions are necessary to increase the convergence rate $\gamma(\mathbf{q})$ (36)? In other words, what is the dimension of the spaces $\Psi_j^{q_j}$ (cf. (37))? In our formalism, see (10)–(11), this question is equivalent to knowing the structure of the operators $\mathbf{V}^j$. Comparing with Nazarov (2000a), we can expect that

$$\begin{aligned}\mathbf{V}^1\boldsymbol{\zeta} &= \Big(-\mathsf{X}_3\nabla_\top\zeta_3,\ P_3^{1,1}(\mathsf{X}_3)\partial_1\zeta_1+P_3^{1,2}(\mathsf{X}_3)(\partial_1\zeta_2+\partial_2\zeta_1)\\ &\quad +P_3^{1,3}(\mathsf{X}_3)\partial_2\zeta_2\Big)\\ \mathbf{V}^2\boldsymbol{\zeta} &= \Big(\sum_{k=1}^{3}P_j^{2,k,1}(\mathsf{X}_3)\partial_1^2\zeta_k+P_j^{2,k,2}(\mathsf{X}_3)\partial_{12}^2\zeta_k\\ &\quad +P_j^{2,k,3}(\mathsf{X}_3)\partial_2^2\zeta_k\Big)_{j=1,2,3}\end{aligned}\tag{50}$$

As soon as the above functions $P_j^{n,*}$ are *independent*, they should be present in the bases of the director space Ψ_j^n. The dimensions of the spaces generated by the $P_j^{n,*}$ have upper bounds depending only on n. But their actual dimensions depend on the number of plies and their nature.

4 MULTISCALE EXPANSIONS AND LIMITING MODELS FOR SHELLS

Up to now, the only available results concerning multiscale expansions for 'true' shells concern the case of clamped elliptic shells investigated in Faou (2001a, 2001b, 2003). For (physical) shallow shells, which are closer to plates than shells, multiscale expansions can also be proved; see Nazarov (2000a) and Andreoiu and Faou (2001).

In this section, we describe the results for clamped elliptic shells, then present the main features of the classification of shells as flexural and membrane. As a matter of fact, multiscale expansions are known for the most extreme representatives of the two types: *(i)* plates for flexural shells, *(ii)* clamped elliptic shells for membrane shells. Nevertheless, multiscale expansions in the general case seem out of reach (or, in certain cases, even irrelevant).

4.1 Curvature of a midsurface and other important tensors

We introduce minimal geometric tools, namely, the *metric* and *curvature tensors* of the midsurface S, the *change of metric tensor* $\gamma_{\alpha\beta}$, and the *change of curvature tensor* $\rho_{\alpha\beta}$. We also address the essential notions of *elliptic*, *hyperbolic*, or *parabolic* point in a surface. We make these notions more explicit for *axisymmetric surfaces*. A general introduction to differential geometry on surfaces can be found in Stoker (1969).

Let us denote by $\langle X,Y\rangle_{\mathbb{R}^3}$ the standard scalar product of two vectors X and Y in $\mathbb{R}^3$. Using the fact that the midsurface S is embedded in $\mathbb{R}^3$, we naturally define the *metric tensor* $(a_{\alpha\beta})$ as the projection on S of the standard scalar product in $\mathbb{R}^3$: Let $\mathbf{p}_\top$ be a point of S and X, Y, two tangent vectors to S in $\mathbf{p}_\top$. In a coordinate system $\mathbf{x}_\top=(\mathsf{x}_\alpha)$ on S, the components of X and Y are (X^α) and (Y^α), respectively. Then the matrix $\big(a_{\alpha\beta}(\mathbf{x}_\top)\big)$ is the only positive definite symmetric 2×2 matrix such that for all such vectors X and Y

$$\big\langle X,Y\big\rangle_{\mathbb{R}^3}=a_{\alpha\beta}(\mathbf{x}_\top)X^\alpha Y^\beta=:\big\langle X,Y\big\rangle_S$$

The inverse of $a_{\alpha\beta}$ is written $a^{\alpha\beta}$ and thus satisfies $a^{\alpha\beta}a_{\beta\sigma}=\delta_\sigma^\alpha$, where δ_σ^α is the Kronecker symbol and where we used the repeated indices convention for the contraction of tensors.

The *covariant derivative* D is associated with the metric $a_{\alpha\beta}$ as follows: It is the unique differential operator such that $\mathsf{D}\langle X,Y\rangle_S=\langle \mathsf{D}X,Y\rangle_S+\langle X,\mathsf{D}Y\rangle_S$ for all vector fields X and Y. In a local coordinate system, we have

$$\mathsf{D}_\alpha=\partial_\alpha+\text{terms of order }0$$

REVISED PAGE PROOFS

where ∂_α is the derivative with respect to the coordinate x_α. The terms of order 0 do depend on the choice of the coordinate system and on the type of the tensor field on which D is applied. They involve the *Christoffel symbols* of S in the coordinate system (x_α).

The *principal curvatures* at a given point $\mathbf{p}_\top \in S$ can be seen as follows: We consider the family $\mathcal{P}$ of planes P containing $\mathbf{p}_\top$ and orthogonal to the tangent plane to S at $\mathbf{p}_\top$. For $P \in \mathcal{P}$, $P \cap S$ defines a curve in P and we denote by κ its signed curvature κ. The sign of κ is determined by the orientation of S. The *principal curvatures* κ_1 and κ_2 are the minimum and maximum of κ when $P \in \mathcal{P}$. The *principal radii of curvature* are $R_i := |\kappa_i|^{-1}$. The *Gaussian curvature* of S in $\mathbf{p}_\top$ is $K(\mathbf{p}_\top) = \kappa_1\kappa_2$.

A point $\mathbf{p}_\top$ is said to be *elliptic* if $K(\mathbf{p}_\top) > 0$, *hyperbolic* if $K(\mathbf{p}_\top) < 0$, *parabolic* if $K(\mathbf{p}_\top) = 0$ but κ_1 or κ_2 is nonzero, and *planar* if $\kappa_1 = \kappa_2 = 0$. An *elliptic shell* is a shell whose midsurface is everywhere elliptic up to the boundary (similar definitions hold for hyperbolic and parabolic shells... and planar shells that are plates).

The curvature tensor is defined as follows: Let $\Psi\colon \mathbf{x}_\top \mapsto \Psi(\mathbf{x}_\top)$ be a parameterization of S in a neighborhood of a given point $\mathbf{p}_\top \in S$ and $\mathbf{n}(\Psi(\mathbf{x}_\top))$ be the normal to S in $\Psi(\mathbf{x}_\top)$. The formula

$$b_{\alpha\beta} := \left\langle \mathbf{n}(\Psi(\mathbf{x}_\top)) \,,\, \frac{\partial \Psi}{\partial \mathsf{x}_\alpha \partial \mathsf{x}_\beta}(\mathbf{x}_\top) \right\rangle_{\mathbb{R}^3}$$

defines, in the coordinate system $\mathbf{x}_\top = (\mathsf{x}_\alpha)$, the components of a covariant tensor field on S, which is called the *curvature tensor*.

The metric tensor yields diffeomorphisms between tensor spaces of different types (covariant and contravariant): We have, for example, $b_\alpha^\beta = a^{\alpha\sigma} b_{\sigma\beta}$. With these notations, we can show that in any coordinate system, the eigenvalues of b_β^α at a point $\mathbf{p}_\top$ are the principal curvatures at $\mathbf{p}_\top$.

In the special case where S is an axisymmetric surface parametrized by

$$\Psi\colon (\mathsf{x}_1, \mathsf{x}_2) \mapsto (\mathsf{x}_1 \cos \mathsf{x}_2, \mathsf{x}_1 \sin \mathsf{x}_2, f(\mathsf{x}_1)) \in \mathbb{R}^3 \qquad (51)$$

where $\mathsf{x}_1 \geq 0$ is the distance to the axis of symmetry, $\mathsf{x}_2 \in [0, 2\pi[$ is the angle around the axis, and $f\colon \mathbb{R} \mapsto \mathbb{R}$ a smooth function, we compute directly that

$$(b_\beta^\alpha) = \frac{1}{\sqrt{1 + f'(\mathsf{x}_1)^2}} \begin{pmatrix} \dfrac{f''(\mathsf{x}_1)}{1 + f'(\mathsf{x}_1)^2} & 0 \\ 0 & \dfrac{f'(\mathsf{x}_1)}{\mathsf{x}_1} \end{pmatrix}$$

whence

$$K = \frac{f'(\mathsf{x}_1) f''(\mathsf{x}_1)}{\mathsf{x}_1 (1 + f'(\mathsf{x}_1)^2)^2}$$

A *deformation pattern* is a three-component field $\boldsymbol{\zeta} = (\zeta_\alpha, \zeta_3)$ where ζ_α is a surface displacement on S, and ζ_3 a function on S. The *change of metric tensor* $\gamma_{\alpha\beta}(\boldsymbol{\zeta})$ associated with the deformation pattern $\boldsymbol{\zeta}$ has the following expression:

$$\gamma_{\alpha\beta}(\boldsymbol{\zeta}) = \tfrac{1}{2}(\mathsf{D}_\alpha \zeta_\beta + \mathsf{D}_\beta \zeta_\alpha) - b_{\alpha\beta}\zeta_3 \qquad (52)$$

The *change of curvature tensor* associated with $\boldsymbol{\zeta}$ writes

$$\rho_{\alpha\beta}(\boldsymbol{\zeta}) = \mathsf{D}_\alpha \mathsf{D}_\beta \zeta_3 - b_\alpha^\sigma b_{\sigma\beta}\zeta_3 + b_\alpha^\sigma \mathsf{D}_\beta \zeta_\sigma + \mathsf{D}_\alpha b_\beta^\sigma \zeta_\sigma \qquad (53)$$

4.2 Clamped elliptic shells

The generic member Ω^ε of our family of shells is defined as

$$S \times (-\varepsilon, \varepsilon) \ni (\mathbf{p}_\top, \mathsf{x}_3) \longrightarrow \mathbf{p}_\top + \mathsf{x}_3 \mathbf{n}(\mathbf{p}_\top) \in \Omega^\varepsilon \subset \mathbb{R}^3 \qquad (54)$$

where $\mathbf{n}(\mathbf{p}_\top)$ is the normal to S at $\mathbf{p}_\top$. Now three stretched variables are required (cf. Section 2.1 for plates):

$$\mathsf{X}_3 = \frac{\mathsf{x}_3}{\varepsilon}, \quad \mathsf{R} = \frac{\mathsf{r}}{\varepsilon} \quad \text{and} \quad \mathsf{T} = \frac{\mathsf{r}}{\sqrt{\varepsilon}}$$

where (r, s) is a system of normal and tangential coordinates to ∂S in S.

4.2.1 Three-dimensional expansion

The solutions of the family of problems (3) have a three-scale asymptotic expansion in powers of $\varepsilon^{1/2}$, with regular terms $\mathbf{v}^{k/2}$, boundary layer terms $\mathbf{w}^{k/2}$ of scale ε like for plates, and new boundary layer terms $\boldsymbol{\varphi}^{k/2}$ of scale $\varepsilon^{1/2}$.

Theorem 4. (Faou, 2003) *For the solutions of problems (3), there exist regular terms* $\mathbf{v}^{k/2}(\mathbf{x}_\top, \mathsf{X}_3)$, $k \geq 0$, *boundary layer terms* $\boldsymbol{\varphi}^{k/2}(\mathsf{T}, \mathsf{s}, \mathsf{X}_3)$, $k \geq 0$ *and* $\mathbf{w}^{k/2}(\mathsf{R}, \mathsf{s}, \mathsf{X}_3)$, $k \geq 2$, *such that*

$$\mathbf{u}^\varepsilon \simeq (\mathbf{v}^0 + \chi\boldsymbol{\varphi}^0) + \varepsilon^{1/2}(\mathbf{v}^{1/2} + \chi\boldsymbol{\varphi}^{1/2}) + \varepsilon(\mathbf{v}^1 + \chi\boldsymbol{\varphi}^1 + \chi\mathbf{w}^1) + \cdots \qquad (55)$$

in the sense of asymptotic expansions: There holds the following estimates

$$\left\| \mathbf{u}^\varepsilon - \sum_{k=0}^{2K} \varepsilon^{k/2}(\mathbf{v}^{k/2} + \chi\boldsymbol{\varphi}^{k/2} + \chi\mathbf{w}^{k/2}) \right\|_{E(\Omega^\varepsilon)} \leq C_K(\mathbf{f})\, \varepsilon^{K+1/2}, \quad K = 0, 1, \ldots$$

REVISED PAGE PROOFS

where we have set $\mathbf{w}^0 = \mathbf{w}^{1/2} = 0$ *and the constant* $C_K(\mathbf{f})$ *is independent of* $\varepsilon \in (0, \varepsilon_0]$.

Like for plates, the terms of the expansion are linked with each other, and are generated by a series of deformation patterns $\boldsymbol{\zeta}^{k/2} = \boldsymbol{\zeta}^{k/2}(\mathbf{x}_\top)$ of the midsurface S. They solve a recursive system of equations, which can be written in a condensed form as an equality between formal series, like for plates. The distinction from plates is that, now, half-integer powers of ε are involved and we write, for example, $\boldsymbol{\zeta}[\varepsilon^{1/2}]$ for the formal series $\sum_k \varepsilon^{k/2}\boldsymbol{\zeta}^{k/2}$.

4.2.2 Regular terms

The regular terms series $\mathbf{v}[\varepsilon^{1/2}] = \sum_k \varepsilon^{k/2}\mathbf{v}^{k/2}$ is determined by an equation similar to (10):

$$\mathbf{v}[\varepsilon^{1/2}] = \mathbf{V}[\varepsilon^{1/2}]\boldsymbol{\zeta}[\varepsilon^{1/2}] + \mathbf{Q}[\varepsilon^{1/2}]\mathbf{f}[\varepsilon^{1/2}]$$

(i) The formal series of deformation patterns $\boldsymbol{\zeta}[\varepsilon^{1/2}]$ starts with $k = 0$ (instead of degree -2 for plates).

(ii) The first terms of the series $\mathbf{V}[\varepsilon]$ are

$$\mathbf{V}^0\boldsymbol{\zeta} = \boldsymbol{\zeta}, \quad \mathbf{V}^{1/2} \equiv 0,$$
$$\mathbf{V}^1\boldsymbol{\zeta} = (-\mathsf{X}_3(\mathsf{D}_\alpha\zeta_3 + 2b_\alpha^\beta\zeta_\beta),\ P_{\mathsf{m}}^1(\mathsf{X}_3)\gamma_\alpha^\alpha(\boldsymbol{\zeta})) \tag{56}$$

where P_{m}^1 is the polynomial defined in (9), and the tensors D (covariant derivative), b (curvature), and γ (change of metric) are introduced in Section 4.1: Even if the displacement $\mathbf{V}^1\boldsymbol{\zeta}$ is given through its components in a local coordinate system, it indeed defines an *intrinsic displacement*, since D_α, b_β^α, and γ_β^α are well-defined independently of the choice of a local parameterization of the surface. Note that $\gamma_\alpha^\alpha(\boldsymbol{\zeta})$ in (56) degenerates to $\operatorname{div}\boldsymbol{\zeta}_\top$ in the case of plates where $b_{\alpha\beta} = 0$. More generally, for all integer $k \geq 0$, all 'odd' terms $\mathbf{V}^{k+1/2}$ are zero and, if $b \equiv 0$, all even terms $\mathbf{V}^k$ degenerate to the operators in (11). In particular, their degrees are the same as in (11).

(iii) The formal series $\mathbf{Q}[\varepsilon^{1/2}]$ appears as a generalization of (13) and $\mathbf{f}[\varepsilon^{1/2}]$ is the formal Taylor expansion of $\mathbf{f}$ around the midsurface $\mathsf{x}_3 = 0$, which means that for all integer $k \geq 0$, $\mathbf{f}^{k+1/2} \equiv 0$ and $\mathbf{f}^k$ is given by (12).

4.2.3 Membrane deformation patterns

The first term $\boldsymbol{\zeta}^0$ solves the membrane equation

$$\boldsymbol{\zeta}^0 \in H_0^1 \times H_0^1 \times L^2(S), \quad \forall\, \boldsymbol{\zeta}' \in H_0^1 \times H_0^1 \times L^2(S),$$
$$a_{S,\mathsf{m}}(\boldsymbol{\zeta}^0, \boldsymbol{\zeta}') = 2\int_S \boldsymbol{\zeta}' \cdot \mathbf{f}^0 \tag{57}$$

where $\mathbf{f}^0 = \mathbf{f}|_S$ and $a_{S,\mathsf{m}}$ is the *membrane form*

$$a_{S,\mathsf{m}}(\boldsymbol{\zeta}, \boldsymbol{\zeta}') = 2\int_S \widetilde{A}^{\alpha\beta\sigma\delta}\gamma_{\alpha\beta}(\boldsymbol{\zeta})\gamma_{\sigma\delta}(\boldsymbol{\zeta}')\,\mathrm{d}S \tag{58}$$

with the reduced energy material tensor on the midsurface (with $\widetilde{\lambda}$ still given by (17)):

$$\widetilde{A}^{\alpha\beta\sigma\delta} = \widetilde{\lambda}a^{\alpha\beta}a^{\sigma\delta} + \mu(a^{\alpha\sigma}a^{\beta\delta} + a^{\alpha\delta}a^{\beta\sigma})$$

Problem (57) can be equivalently formulated as $\mathbf{L}^0\boldsymbol{\zeta}^0 = \mathbf{f}^0$ with Dirichlet boundary conditions $\boldsymbol{\zeta}_\top^0 = 0$ on ∂S and is corresponding to the membrane equations on plates (compare with (19) and (22)). The operator $\mathbf{L}^0$ is called *membrane operator* and, thus, the change of metric $\gamma_{\alpha\beta}(\boldsymbol{\zeta})$ with respect to the deformation pattern $\boldsymbol{\zeta}$ appears to coincide with the *membrane strain tensor*; see Naghdi (1963) and Koiter (1970a). If $b \equiv 0$, the third component of $\mathbf{L}^0\boldsymbol{\zeta}$ vanishes while the surface part degenerates to the membrane operator (20). In the general case, the properties of $\mathbf{L}^0$ depends on the geometry of S: $\mathbf{L}^0$ is elliptic (of multidegree (2, 2, 0) in the sense of Agmon, Douglis and Nirenberg, 1964) in $\mathbf{x}$ if and only if S is elliptic in $\mathbf{x}$; see Ciarlet (2000), Genevey (1996), and Sanchez-Hubert and Sanchez-Palencia (1997).

As in (21), the formal series $\boldsymbol{\zeta}[\varepsilon^{1/2}]$ solves a reduced equation on the midsurface with formal series $\mathbf{L}[\varepsilon^{1/2}]$, $\mathbf{R}[\varepsilon^{1/2}]$, $\mathbf{f}[\varepsilon^{1/2}]$ and $\mathbf{d}[\varepsilon^{1/2}]$, degenerating to the formal series (21) in the case of plates.

4.2.4 Boundary layer terms

Problem (57) cannot solve for the boundary conditions $\zeta_3^0|_{\partial S} = \partial_{\mathbf{n}}\zeta_3^0|_{\partial S} = 0$ (see the first terms in (24)). The two-dimensional boundary layer terms $\boldsymbol{\varphi}^{k/2}$ compensate these nonzero traces: We have for $k = 0$.

$$\boldsymbol{\varphi}^0 = (\mathbf{0}, \varphi_3^0(\mathsf{T}, \mathsf{s})) \quad \text{with} \quad \varphi_3^0(0, \mathsf{s}) = -\zeta_3^0|_{\partial S}$$
$$\text{and} \quad \partial_{\mathbf{n}}\varphi_3^0(0, \mathsf{s}) = 0$$

For $k = 1$, the trace $\partial_{\mathbf{n}}\zeta_3^0|_{\partial S}$ is compensated by $\varphi_3^{1/2}$: The scale $\varepsilon^{1/2}$ arises from these surface boundary layer terms. More generally, the terms $\boldsymbol{\varphi}^{k/2}$ are polynomials of degree $[k/2]$ in X_3 and satisfy

$$|e^{\eta\mathsf{T}}\boldsymbol{\varphi}(\mathsf{T}, \mathsf{s}, \mathsf{X}_3)| \quad \text{bounded as} \quad \mathsf{T} \to \infty$$

for all $\eta < (3\mu(\widetilde{\lambda} + \mu))^{1/4}(\widetilde{\lambda} + 2\mu)^{-1/2}b_{\mathsf{ss}}(0, \mathsf{s})^{1/2}$ where $b_{\mathsf{ss}}(0, \mathsf{s}) > 0$ is the tangential component of the curvature tensor along ∂S.

The three-dimensional boundary layer terms $\mathbf{w}^{k/2}$ have a structure similar to the case of plates. The first nonzero term is $\mathbf{w}^1$.

REVISED PROOFS

4.2.5 The Koiter model

Koiter (1960) proposed the solution $\mathbf{z}^\varepsilon$ of following surface problem

$$\text{Find } \mathbf{z}^\varepsilon \in V_{\mathsf{K}}(S) \text{ such that}$$
$$\varepsilon a_{S,\mathsf{m}}(\mathbf{z}^\varepsilon, \mathbf{z}') + \varepsilon^3 a_{S,\mathsf{b}}(\mathbf{z}^\varepsilon, \mathbf{z}') = 2\varepsilon \int_S \mathbf{z}' \cdot \mathbf{f}^0, \quad \forall\, \mathbf{z}' \in V_{\mathsf{K}}(S) \tag{59}$$

to be a good candidate for approximating the three-dimensional displacement by a two-dimensional one. Here the variational space is

$$V_{\mathsf{K}}(S) := H_0^1 \times H_0^1 \times H_0^2(S) \tag{60}$$

and the bilinear form $a_{S,\mathsf{b}}$ is the *bending form*:

$$a_{S,\mathsf{b}}(\mathbf{z}, \mathbf{z}') = \frac{2}{3} \int_S \widetilde{A}^{\alpha\beta\sigma\delta} \rho_{\alpha\beta}(\mathbf{z}) \rho_{\sigma\delta}(\mathbf{z}')\, \mathrm{d}S \tag{61}$$

Note that the operator underlying problem (59) has the form $\mathbf{K}(\varepsilon) = \varepsilon \mathbf{L}^0 + \varepsilon^3 \mathbf{B}$ where the membrane operator $\mathbf{L}^0$ is the same as in (57) and the *bending* operator $\mathbf{B}$ is associated with $a_{S,\mathsf{b}}$. Thus, the change of curvature tensor $\rho_{\alpha\beta}$ appears to be identified with the *bending strain tensor*. Note that $\mathbf{K}(\varepsilon)$ is associated with the two-dimensional energy (compare with (44))

$$2\varepsilon \int_S \widetilde{A}^{\alpha\beta\sigma\delta} \gamma_{\alpha\beta}(\mathbf{z}) \gamma_{\sigma\delta}(\mathbf{z})\, \mathrm{d}S + \frac{2\varepsilon^3}{3} \int_S \widetilde{A}^{\alpha\beta\sigma\delta} \rho_{\alpha\beta}(\mathbf{z}) \rho_{\sigma\delta}(\mathbf{z})\, \mathrm{d}S \tag{62}$$

For ε small enough, the operator $\mathbf{K}(\varepsilon)$ is elliptic of multidegree (2, 2, 4) and is associated with the Dirichlet conditions $\mathbf{z} = 0$ and $\partial_{\mathbf{n}} z_3 = 0$ on ∂S. The solution $\mathbf{z}^\varepsilon$ of the Koiter model for the clamped case solves equivalently the equations

$$(\mathbf{L}^0 + \varepsilon^2 \mathbf{B})\mathbf{z}^\varepsilon(\mathbf{x}_\top) = \mathbf{f}^0(\mathbf{x}_\top) \text{ on } S \text{ and } \mathbf{z}^\varepsilon|_{\partial S} = \mathbf{0},\ \partial_{\mathbf{n}} z_3^\varepsilon|_{\partial S} = 0 \tag{63}$$

This solution has also a multiscale expansion given by the following theorem.

Theorem 5. (Faou, 2003) *For the solutions of problem (63), $\varepsilon \in (0, \varepsilon_0]$, there exist regular terms $\mathbf{z}^{k/2}(\mathsf{x}_\top)$ and boundary layer terms $\boldsymbol{\psi}^{k/2}(\mathsf{T}, \mathsf{s})$, $k \geq 0$, such that*

$$\mathbf{z}^\varepsilon \simeq \mathbf{z}^0 + \chi \boldsymbol{\psi}^0 + \varepsilon^{1/2}(\mathbf{z}^{1/2} + \chi \boldsymbol{\psi}^{1/2}) + \varepsilon^1(\mathbf{z}^1 + \chi \boldsymbol{\psi}^1) + \cdots \tag{64}$$

in the sense of asymptotic expansions: The following estimates hold

$$\left\| \mathbf{z}^\varepsilon - \sum_{k=0}^{2K} \varepsilon^{k/2}(\mathbf{z}^{k/2} + \chi \boldsymbol{\psi}^{k/2}) \right\|_{\varepsilon,S} \leq C_K(\mathbf{f})\, \varepsilon^{K+1/4}, \quad K = 0, 1, \ldots$$

where $\|\mathbf{z}\|_{\varepsilon,S}^2 = \|\boldsymbol{\gamma}(\mathbf{z})\|_{L^2(S)}^2 + \varepsilon^2 \|\boldsymbol{\rho}(\mathbf{z})\|_{L^2(S)}^2$ and $C_K(\mathbf{f})$ is independent of $\varepsilon \in (0, \varepsilon_0]$.

The precise comparison between the terms in the expansions (55) and (64) shows that [1] $\boldsymbol{\zeta}^0 = \mathbf{z}^0$, $\boldsymbol{\zeta}^{1/2} = \mathbf{z}^{1/2}$, $\boldsymbol{\varphi}^0 = \boldsymbol{\psi}^0$, $\boldsymbol{\varphi}_\top^{1/2} = \boldsymbol{\psi}_\top^{1/2}$, while $\boldsymbol{\zeta}^1$ and $\mathbf{z}^1$, $\varphi_3^{1/2}$ and $\psi_3^{1/2}$ are generically different, respectively. This allows obtaining optimal estimates in various norms: Considering the scaled domain $\Omega \simeq S \times (-1, 1)$, we have

$$\|\mathbf{u}^\varepsilon - \mathbf{z}^\varepsilon\|_{H^1 \times H^1 \times L^2(\Omega)} \leq \|\mathbf{u}^\varepsilon - \boldsymbol{\zeta}^0\|_{H^1 \times H^1 \times L^2(\Omega)} + \|\mathbf{z}^\varepsilon - \boldsymbol{\zeta}^0\|_{H^1 \times H^1 \times L^2(\Omega)} \leq C\varepsilon^{1/4} \tag{65}$$

This estimate implies the convergence result of Ciarlet and Lods (1996a) and improves the estimate in Mardare (1998a). To obtain an estimate in the energy norm, we need to reconstruct a 3-D displacement from $\mathbf{z}^\varepsilon$: First, the Kirchhoff-like [2] displacement associated with $\mathbf{z}^\varepsilon$ writes, cf. (56)

$$\mathbf{U}_{\mathsf{KL}}^{1,1,0}\mathbf{z}^\varepsilon = \left(z_\alpha^\varepsilon - \mathsf{x}_3(\mathsf{D}_\alpha z_3^\varepsilon + 2b_\alpha^\sigma z_\sigma^\varepsilon),\, z_3^\varepsilon\right) \tag{66}$$

and next, according to Koiter (1970a), we define the reconstructed quadratic displacement [3]

$$\mathbf{U}_{\mathsf{K}}^{1,1,2}\mathbf{z}^\varepsilon = \mathbf{U}_{\mathsf{KL}}^{1,1,0}\mathbf{z}^\varepsilon + \frac{\lambda}{\lambda + 2\mu}\left(\mathbf{0}, -\mathsf{x}_3 \gamma_\alpha^\alpha(\mathbf{z}^\varepsilon) + \frac{\mathsf{x}_3^2}{2}\rho_\alpha^\alpha(\mathbf{z}^\varepsilon)\right) \tag{67}$$

Then there holds (compare with (46) for plates):

$$\|\mathbf{u}^\varepsilon - \mathbf{U}_{\mathsf{K}}^{1,1,2}\mathbf{z}^\varepsilon\|_{E(\Omega^\varepsilon)} \leq C\sqrt{\varepsilon}\|\mathbf{u}^\varepsilon\|_{E(\Omega^\varepsilon)} \tag{68}$$

and similar to plates, the error factor $\sqrt{\varepsilon}$ is optimal and is due to the first boundary layer term $\mathbf{w}^1$. Moreover, expansion (64) allows proving that the classical models discussed in Budiansky and Sanders (1967), Naghdi (1963), Novozhilov (1959), and Koiter (1970a) have all the same convergence rate (68).

4.3 Convergence results for general shells

We still embed Ω^d in the family (54) with S the mid-surface of Ω^d. The fact that all the classical models are equivalent for clamped elliptic shells may not be true in more general cases, when the shell becomes sensitive (e.g. for a partially clamped elliptic shell with a free portion in its lateral surface) or produces bending effects (case of parabolic or hyperbolic shells with adequate lateral boundary conditions).

REVISED PAGE PROOFS

4.3.1 Surface membrane and bending energy

Nevertheless, the Koiter model seems to keep good approximation properties with respect to the 3-D model. The variational space V_{K} of the Koiter model is, in the totally clamped case given by the space $V_{\mathsf{K}}(S)$ (60) (if the shell Ω^ε is clamped only on the part $\gamma_0 \times (-\varepsilon, \varepsilon)$ of its boundary (with $\gamma_0 \subset \partial S$), the Dirichlet boundary conditions in the space V_{K} have to be imposed only on γ_0). As already mentioned (62), the Koiter model is associated with the bilinear form $\varepsilon a_{S,\mathsf{m}} + \varepsilon^3 a_{S,\mathsf{b}}$ with $a_{S,\mathsf{m}}$ and $a_{S,\mathsf{b}}$ the membrane and bending forms defined for $\mathbf{z}$, $\mathbf{z}' \in V_{\mathsf{K}}(S)$ by (58) and (61) respectively.

From the historical point of view, such a decomposition into a membrane (or stretching) energy and a bending energy on the midsurface was first derived by Love (1944) in *principal curvature coordinate systems*, that is, for which the curvature tensor (b_β^α) is diagonalized. The expression of the membrane energy proposed by Love is the same as (61), in contrast with the bending part for which the discussion was very controversial; see Budiansky and Sanders (1967), Novozhilov (1959), Koiter (1960), and Naghdi (1963) and the reference therein. Koiter (1960) gave the most natural expression using intrinsic tensor representations: The Koiter bending energy only depends on the change of curvature tensor $\rho_{\alpha\beta}$, in accordance with Bonnet theorem characterizing a surface by its metric and curvature tensors $a_{\alpha\beta}$ and $b_{\alpha\beta}$; see Stoker (1969).

For any geometry of the midsurface S, the Koiter model in its variational form (59) has a unique solution; see Bernadou and Ciarlet (1976).

4.3.2 Classification of shells

According to this principle each shell, in the zero thickness limit, concentrates its energy either in the bending surface energy $a_{S,\mathsf{b}}$ (*flexural* shells) or in the membrane surface energy $a_{S,\mathsf{m}}$ (*membrane* shells).

The behavior of the shell depends on the *'inextensional displacement' space*

$$V_{\mathsf{F}}(S) := \left\{ \boldsymbol{\zeta} \in V_{\mathsf{K}}(S) \,|\, \gamma_{\alpha\beta}(\boldsymbol{\zeta}) = 0 \right\} \tag{69}$$

The key role played by this space is illustrated by the following fundamental result:

Theorem 6.

(i) (Sanchez-Hubert and Sanchez-Palencia, 1997; Ciarlet, Lods and Miara, 1996) *Let* $\mathbf{u}^\varepsilon$ *be the solution of problem (3). In the scaled domain* $\Omega \simeq S \times (-1, 1)$, *the displacement* $\varepsilon^2 \mathbf{u}^\varepsilon(\mathbf{x}_\top, \mathsf{X}_3)$ *converges in* $H^1(\Omega)^3$ *as* $\varepsilon \to 0$. *Its limit is given by the solution* $\boldsymbol{\zeta}^{-2} \in V_{\mathsf{F}}(S)$ *of the bending problem*

$$\forall\, \boldsymbol{\zeta}' \in V_{\mathsf{F}}(S) \quad a_{S,\mathsf{b}}(\boldsymbol{\zeta}^{-2}, \boldsymbol{\zeta}') = 2 \int_S \boldsymbol{\zeta}' \cdot \mathbf{f}^0 \tag{70}$$

(ii) (Ciarlet and Lods, 1996b) *Let* $\mathbf{z}^\varepsilon$ *be the solution of problem (59). Then* $\varepsilon^2 \mathbf{z}^\varepsilon$ *converges to* $\boldsymbol{\zeta}^{-2}$ *in* $V_{\mathsf{K}}(S)$ *as* $\varepsilon \to 0$.

A shell is said *flexural* (or *noninhibited*) when $V_{\mathsf{F}}(S)$ is not reduced to $\{\mathbf{0}\}$. Examples are provided by cylindrical shells (or portions of cones) clamped along their generatrices and free elsewhere. Of course, plates are flexural shells according to the above definition since in that case, $V_{\mathsf{F}}(S)$ is given by $\{\boldsymbol{\zeta} = (\mathbf{0}, \zeta_3) \,|\, \zeta_3 \in H_0^2(S)\}$ and the bending operator (70) coincides with the operator (16).

In the case of clamped elliptic shells, we have $V_{\mathsf{F}}(S) = \{\mathbf{0}\}$. For these shells, $\mathbf{u}^\varepsilon$ and $\mathbf{z}^\varepsilon$ converge in $H^1 \times H^1 \times L^2$ to the solution $\boldsymbol{\zeta}^0$ of the membrane equation (57); see Ciarlet and Lods (1996a) and (65): Such shells are called *membrane shells*. The other shells for which $V_{\mathsf{F}}(S)$ reduces to $\{\mathbf{0}\}$ are called *generalized membrane shells* (or *inhibited shells*) and for these also, a delicate functional analysis provides convergence results to a membrane solution in spaces with special norms depending on the geometry of the midsurface; see Ciarlet and Lods (1996a) and Ciarlet (2000), Ch. 5. It is also proved that the Koiter model converges in the same sense to the same limits; see Ciarlet (2000), Ch. 7.

Thus, plates and elliptic shells represent extreme situations: Plates are a pure bending structures with an inextensional displacement space as large as possible, while clamped elliptic shells represent a pure membrane situation where $V_{\mathsf{F}}(S)$ reduces to $\{\mathbf{0}\}$ and where the membrane operator is elliptic.

4.4 Shallow shells

We make a distinction between 'physical' shallow shells in the sense of Ciarlet and Paumier (1986) and 'mathematical' shallow shells in the sense of Pitkäranta, Matache and Schwab (2001). The former involves shells with a curvature tensor of the same order as the thickness, whereas the latter addresses a boundary value problem obtained by freezing coefficients of the Koiter problem at one point of a standard shell.

4.4.1 Physical shallow shells

Let R denote the smallest principal radius of curvature of the midsurface S and let D denote the diameter of S. As proved in Andreoiu and Faou (2001) if there holds

$$R \geq 2\text{-}D \tag{71}$$

REVISED PAGE PROOFS

then there exists a point $\mathbf{p}_\top \in S$ such that the orthogonal projection of S on its tangent plan in $\mathbf{p}_\top$ allows the representation of S as a $\mathcal{C}^\infty$ graph in $\mathbb{R}^3$:

$$\omega \ni (x_1, x_2) \mapsto \big(x_1, x_2, \Theta(x_1, x_2)\big) := \mathbf{x}_\top \in S \subset \mathbb{R}^3 \quad (72)$$

where ω is an immersed (in particular, ω may have self-intersection) domain of the tangent plane in $\mathbf{p}_\top$, and where Θ is a function on this surface. Moreover, we have

$$|\Theta| \le CR^{-1} \quad \text{and} \quad \|\nabla\Theta\| \le CR^{-1} \quad (73)$$

with constants C depending only on D.

We say that Ω^d is a *shallow shell* if S satisfies a condition of the type

$$R^{-1} \le Cd \quad (74)$$

where C does not depend on d. Thus, if S is a surface satisfying (74), for d sufficiently small S satisfies (71) whence representation (72). Moreover, (73) yields that Θ and $\nabla\Theta$ are $\lesssim d$. In these conditions, we can choose to embed Ω^d into another family of thin domains than (54): We set $\theta = d^{-1}\Theta$ and define for any $\varepsilon \in (0, d]$ the surface S^ε by its parameterization (cf. (72))

$$\omega \ni (x_1, x_2) \mapsto \big(x_1, x_2, \varepsilon\theta(x_1, x_2)\big) := \mathbf{x}_\top \in S^\varepsilon$$

It is natural to consider Ω^d as an element of the family Ω^ε given as the image of the application

$$\omega \times (-\varepsilon, \varepsilon) \ni (x_1, x_2, \mathsf{x}_3) \mapsto \big(x_1, x_2, \varepsilon\,\theta(x_1, x_2)\big) + \mathsf{x}_3\,\mathbf{n}^\varepsilon(\mathbf{x}_\top) \quad (75)$$

where $\mathbf{n}^\varepsilon(\mathbf{x}_\top)$ denotes the unit normal vector to the midsurface S^ε. We are now in the framework of Ciarlet and Paumier (1986).

A multiscale expansion for the solution of (3) is given in Andreoiu and Faou (2001). The expansion is close to that of plates, except that the membrane and bending operators yielding the deformation patterns are linked by lower-order terms: The associated membrane and bending strain components $\tilde\gamma_{\alpha\beta}$ and $\tilde\rho_{\alpha\beta}$ are respectively given by

$$\tilde\gamma_{\alpha\beta} := \tfrac{1}{2}(\partial_\alpha \mathsf{z}_\beta + \partial_\beta \mathsf{z}_\alpha) - \varepsilon\partial_{\alpha\beta}\theta\,\mathsf{z}_3 \quad \text{and} \quad \tilde\rho_{\alpha\beta} := \partial_{\alpha\beta}\mathsf{z}_3 \quad (76)$$

It is worth noticing that the above strains are asymptotic approximations of the Koiter membrane and bending strains associated with the midsurface $S = S^\varepsilon$. As a consequence, the Koiter model and the three-dimensional equations converge to the same Kirchhoff–Love limit.

4.4.2 Mathematical shallow shells

These models consist in freezing coefficients of standard two-dimensional models at a given point $\mathbf{p}_\top \in S$ in a principal curvature coordinate system. That procedure yields, with $b_i := \kappa_i(\mathbf{p}_\top)$:

$$\gamma_{11} = \partial_1\mathsf{z}_1 - b_1\mathsf{z}_3, \quad \gamma_{22} = \partial_2\mathsf{z}_2 - b_2\mathsf{z}_3, \quad \gamma_{12} = \tfrac{1}{2}(\partial_1\mathsf{z}_2 + \partial_2\mathsf{z}_1) \quad (77)$$

for the membrane strain tensor, and

$$\kappa_{11} = \partial_1^2\mathsf{z}_3 + b_1\partial_1\mathsf{z}_1, \quad \kappa_{22} = \partial_2^2\mathsf{z}_3 + b_2\partial_2\mathsf{z}_2, \quad \kappa_{12} = \partial_1\partial_2\mathsf{z}_3 + b_1\partial_2\mathsf{z}_1 + b_2\partial_1\mathsf{z}_2 \quad (78)$$

as a simplified version of the bending strain tensor. Such a localization procedure is considered as valid if the diameter D is small compared to R

$$R \gg D \quad (79)$$

and for the case of cylindrical shells where the strains have already the form (77)–(78) in cylindrical coordinates (see equation (80) below). In contrast with the previous one, this notion of shallowness does not refer to the thickness. Here R is not small, but D is. Such objects are definitively shells and are not plate-like.

These simplified models are valuable so to develop numerical approximation methods, (Havu and Pitkäranta, 2002, 2003) and to find possible boundary layer length scales, (Pitkäranta, Matache and Schwab, 2001): These length scales (width of transition regions from the boundary into the interior) at a point $\mathbf{p}_\top \in \partial S$ are $\varepsilon^{1/2}$ in the nondegenerate case ($b_{\mathsf{ss}}(\mathbf{p}_\top) \neq 0$), $\varepsilon^{1/3}$ for hyperbolic degeneration ($\mathbf{p}_\top$ hyperbolic and $b_{\mathsf{ss}}(\mathbf{p}_\top) = 0$) and $\varepsilon^{1/4}$ for parabolic degeneration ($\mathbf{p}_\top$ parabolic and $b_{\mathsf{ss}}(\mathbf{p}_\top) = 0$).

To compare with the standard shell equations, note that in the case of an axisymmetric shell whose midsurface is represented by

$$\Psi\colon (\mathsf{x}_1, \mathsf{x}_2) \mapsto (f(\mathsf{x}_1)\cos\mathsf{x}_2,\, f(\mathsf{x}_1)\sin\mathsf{x}_2,\, \mathsf{x}_1)$$

where $\mathsf{x}_1 \in \mathbb{R}$, $\mathsf{x}_2 \in [0, 2\pi[$ and $f(\mathsf{x}_1) > 0$ is a smooth function, we have

$$\begin{aligned}
\gamma_{11}(\mathbf{z}) &= \partial_1\mathsf{z}_1 - \frac{f'(\mathsf{x}_1)f''(\mathsf{x}_1)}{1+f'(\mathsf{x}_1)^2}\,\mathsf{z}_1 + \frac{f''(\mathsf{x}_1)}{\sqrt{1+f'(\mathsf{x}_1)^2}}\,\mathsf{z}_3\\
\gamma_{22}(\mathbf{z}) &= \partial_2\mathsf{z}_2 + \frac{f(\mathsf{x}_1)f'(\mathsf{x}_1)}{1+f'(\mathsf{x}_1)^2}\,\mathsf{z}_1 - \frac{f(\mathsf{x}_1)}{\sqrt{1+f'(\mathsf{x}_1)^2}}\,\mathsf{z}_3\\
\gamma_{12}(\mathbf{z}) &= \frac{1}{2}(\partial_1\mathsf{z}_2 + \partial_2\mathsf{z}_1) - \frac{f'(\mathsf{x}_1)}{f(\mathsf{x}_1)}\,\mathsf{z}_2
\end{aligned} \quad (80)$$

REVISED PAGE PROOFS

Hence the equation (77) is exact for the case of cylindrical shells, where $f(\mathsf{x}_1) \equiv R > 0$, and we can show that the same holds for (78).

4.5 Versatility of Koiter model

On any midsurface S, the deformation pattern $\mathbf{z}^\varepsilon$ solution of the Koiter model (59) exists. In general, the mean value of the displacement $\mathbf{u}^\varepsilon$ through the thickness converges to the same limit as $\mathbf{z}^\varepsilon$ when $\epsilon \to 0$ in a weak sense depending on the type of the midsurface and the boundary conditions; see Ciarlet (2000). Nevertheless, actual convergence results hold in energy norm when considering reconstructed displacement from the deformation pattern $\mathbf{z}^\varepsilon$.

4.5.1 Convergence of the Koiter reconstructed displacement

On any midsurface S, the three-dimensional Koiter reconstructed displacement $\mathbf{U}_\mathsf{K}^{1,1,2}\mathbf{z}^\varepsilon$ is well-defined by (66)–(67). Let us set

$$\mathbf{e}(S, \varepsilon, \mathbf{z}^\varepsilon, \mathbf{u}^\varepsilon) := \frac{\|\mathbf{u}^\varepsilon - \mathbf{U}_\mathsf{K}^{1,1,2}\mathbf{z}^\varepsilon\|_{E(\Omega^\varepsilon)}}{\|\mathbf{z}^\varepsilon\|_{E^\varepsilon(S)}} \tag{81}$$

with $\|\mathbf{z}\|_{E^\varepsilon(S)}$, the square root of the Koiter energy (62).

In Koiter (1970a, 1970b), an estimate is given: $\mathbf{e}(S, \varepsilon, \mathbf{z}^\varepsilon, \mathbf{u}^\varepsilon)^2$ would be bounded by $\varepsilon R^{-1} + \varepsilon^2 L^{-2}$, with R the smallest principal radius of curvature of S, and L the smallest wavelength of $\mathbf{z}^\varepsilon$. It turns out that in the case of plates, we have $L = \mathcal{O}(1)$, $R^{-1} = 0$ and, since (46) is optimal, the estimate fails. In contrast, in the case of clamped elliptic shells, we have $L = \mathcal{O}(\sqrt{\varepsilon})$, $R^{-1} = \mathcal{O}(1)$ and the estimate gives back (68).

Two years after the publications of Koiter (1970a, 1970b), it was already known that the above estimate does not hold as $\varepsilon \to 0$ for plates. We read in Koiter and Simmonds (1973) 'The somewhat depressing conclusion for most shell problems is, similar to the earlier conclusions of Gol'denweizer, that no better accuracy of the solutions can be expected than of order $\varepsilon L^{-1} + \varepsilon R^{-1}$, even if the equations of first-approximation shell theory would permit, in principle, an accuracy of order $\varepsilon^2 L^{-2} + \varepsilon R^{-1}$.'

The reason for this is also explained by John (1971) in these terms: 'Concentrating on the interior we sidestep all kinds of delicate questions, with an attendant gain in certainty and generality. The information about the interior behavior can be obtained much more cheaply (in the mathematical sense) than that required for the discussion of boundary value problems, which form a more 'transcendental' stage'.

Koiter's tentative estimate comes from formal computations also investigated by John (1971). The analysis by operator formal series introduced in Faou (2002) is in the same spirit: For any geometry of the midsurface, there exist formal series $\mathbf{V}[\varepsilon]$, $\mathbf{R}[\varepsilon]$, $\mathbf{Q}[\varepsilon]$, and $\mathbf{L}[\varepsilon]$ reducing the three-dimensional formal series problem to a two-dimensional problem of the form (21) with $\mathbf{L}[\varepsilon] = \mathbf{L}^0 + \varepsilon^2\mathbf{L}^2 + \cdots$ where $\mathbf{L}^0$ is the membrane operator associated with the form (58). The bending operator $\mathbf{B}$ associated with $a_{S,\mathsf{b}}$ can be compared to the operator $\mathbf{L}^2$ appearing in the formal series $\mathbf{L}[\varepsilon]$: We have

$$\forall\, \boldsymbol{\zeta}, \boldsymbol{\zeta}' \in V_\mathsf{F}(S) \quad \langle \mathbf{L}^2\boldsymbol{\zeta}, \boldsymbol{\zeta}' \rangle_{L^2(S)^3} = \langle \mathbf{B}\boldsymbol{\zeta}, \boldsymbol{\zeta}' \rangle_{L^2(S)^3} \tag{82}$$

Using this formal series analysis, the first two authors are working on the derivation of a sharp expression of $\mathbf{e}(S, \varepsilon, \mathbf{z}^\varepsilon, \mathbf{u}^\varepsilon)$ including boundary layers effects, and optimal in the case of plates and clamped elliptic shells; see Dauge and Faou (2004).

In this direction also, Lods and Mardare (2002) prove the following estimate for totally clamped shells

$$\|\mathbf{u}^\varepsilon - (\mathbf{U}_\mathsf{K}^{1,1,2}\mathbf{z}^\varepsilon + \mathbf{w}^\sharp)\|_{E(\Omega^\varepsilon)} \le C\varepsilon^{1/4}\|\mathbf{u}^\varepsilon\|_{E(\Omega^\varepsilon)} \tag{83}$$

with $\mathbf{w}^\sharp$ an explicit boundary corrector of $\mathbf{U}_\mathsf{K}^{1,1,2}\mathbf{z}^\varepsilon$.

4.5.2 Convergence of Koiter eigenvalues

The operator $\varepsilon^{-1}\mathbf{K}(\varepsilon)$ has a compact inverse, therefore its spectrum is discrete with only an accumulation point at $+\infty$. We agree to call Koiter eigenvalues the eigenvalues of the former operator, that is, the solutions μ^ε of

$$\exists\, \mathbf{z}^\varepsilon \in V_\mathsf{K}(S) \setminus \{0\} \text{ such that}$$
$$a_{S,\mathsf{m}}(\mathbf{z}^\varepsilon, \mathbf{z}') + \varepsilon^2 a_{S,\mathsf{b}}(\mathbf{z}^\varepsilon, \mathbf{z}') = 2\mu^\varepsilon \int_S \mathbf{z}^\varepsilon \cdot \mathbf{z}', \quad \forall\, \mathbf{z}' \in V_\mathsf{K}(S) \tag{84}$$

As already mentioned in Section 2.4, cf. (31), this spectrum provides the limiting behavior of three-dimensional eigenvalues for plates. Apparently, very little is known for general shells.

Concerning Koiter eigenvalues, interesting results are provided by Sanchez-Hubert and Sanchez-Palencia (1997), Ch. X: The μ^ε are attracted by the spectrum of the membrane operator $\mathfrak{S}(\mathbf{M})$ where $\mathbf{M}$ is the self-adjoint unbounded operator associated with the symmetric bilinear form $a_{S,\mathsf{m}}$ defined on the space $H^1 \times H^1 \times L^2(S)$. There holds (we still assume that S is smooth up to its boundary):

Theorem 7. *The operator* $\mathbf{M} + \mu\,\mathsf{Id}$ *is elliptic of multidegree* $(2, 2, 0)$ *for* $\mu > 0$ *large enough. Moreover its essential spectrum* $\mathfrak{S}_{\mathsf{es}}(\mathbf{M})$ *satisfies:*

REVISED PAGE PROOFS

(i) *If S is elliptic and clamped on its whole boundary, $\mathfrak{S}_{es}(\mathbf{M})$ is a closed interval $[a, b]$, with $a > 0$,*
(ii) *If S is elliptic and not clamped on its whole boundary, $\mathfrak{S}_{es}(\mathbf{M}) = \{0\} \cup [a, b]$ with $a > 0$,*
(iii) *For any other type of shell (i.e. there exists at least one point where the Gaussian curvature is ≤ 0) $\mathfrak{S}_{es}(\mathbf{M})$ is a closed interval of the form $[0, b]$, with $b \geq 0$.*

If the shell is of flexural type, the lowest eigenvalues μ_ε tend to 0 like $\mathcal{O}(\varepsilon^2)$, same as for plates; see (29). If the shell is clamped elliptic, the μ_ε are bounded from below by a positive constant independent of ε. In any other situation, we expect that the lowest μ_ε still tends to 0 as $\varepsilon \to 0$.

5 HIERARCHICAL MODELS FOR SHELLS

The idea of deriving hierarchical models for shells goes back to Vekua (1955, 1965, 1985) and corresponds to classical techniques in mechanics: Try to find asymptotic expansions in x_3 by use of Taylor expansion around the midsurface S. An alternative approach consists in choosing the coefficients z_j^n in (38) as moments through the thickness against Legendre polynomials $L_n(\mathsf{x}_3/\varepsilon)$.

Vogelius and Babuška (1981a, 1981b, 1981c) laid the foundations of hierarchical models in view of their applications to numerical analysis (for scalar problems).

5.1 Hierarchies of semidiscrete subspaces

The concepts mentioned in Section 3 can be adapted to the case of shells. In contrast with plates for which there exist convenient *Cartesian* system of coordinates fitting with the tangential and normal directions to the midsurface, more nonequivalent options are left open for shells. They are; for example;

The *direction of semidiscretization*: The intrinsic choice is of course the normal direction to the midsurface (variable x_3), nevertheless for shells represented by a single local chart like in (72), any transverse direction could be chosen. In the sequel, we only consider semidiscretizations in the normal direction.

The presence or absence of privileged components for the displacement field in the Ansatz (38). If one privileged component is chosen, it is of course the normal one u_3 and the two other ones are $(\mathsf{u}_\alpha) = \mathbf{u}_\top$. Then the sequence of orders $\mathbf{q}$ is of the form $\mathbf{q} = (q_\top, q_\top, q_3)$, and the space $V^{\mathbf{q}}(\Omega^\varepsilon)$ has the form (48). Note that this space is independent of the choice of local coordinates on S.

If there is no privileged component, $\mathbf{q}$ has to be of the form (q, q, q) and the space $V^{\mathbf{q}}(\Omega^\varepsilon)$ can be written

$$V^{\mathbf{q}}(\Omega^\varepsilon) = \Big\{ \mathbf{u} = (u_1, u_2, u_3) \in V(\Omega^\varepsilon), \quad \exists \mathbf{z}^n = (z_1^n, z_2^n, z_3^n) \in H_0^1(S)^3, \ 0 \leq n \leq q, \quad u_j = \sum_{n=0}^{q} \mathsf{x}_3^n \, z_j^n(\mathbf{x}_\top), \quad j = 1, 2, 3 \Big\} \tag{85}$$

Here, for ease of use, we take Cartesian coordinates, but the above definition is independent of any choice of coordinates in $\Omega^\varepsilon \subset \mathbb{R}^3$. In particular, it coincides with the space (48) for $q_\top = q_3$.

Then the requirements of approximability (34), asymptotic consistency (35), and optimality of the convergence rate (36) make sense.

5.2 Approximability

For any fixed thickness ε, the approximability issue is as in the case of plates. By Céa's lemma, there exists an adimensional constant $C > 0$ depending only on the Poisson ratio ν, such that

$$\|\mathbf{u}^\varepsilon - \mathbf{u}^{\varepsilon,\mathbf{q}}\|_{E(\Omega^\varepsilon)} \leq C \|\mathbf{u}^\varepsilon - \mathbf{v}^{\mathbf{q}}\|_{E(\Omega^\varepsilon)} \quad \forall \mathbf{v}^{\mathbf{q}} \in V^{\mathbf{q}}(\Omega^\varepsilon)$$

and the determination of approximability properties relies on the construction of a best approximation of $\mathbf{u}^\varepsilon$ by functions in $V^{\mathbf{q}}(\Omega^\varepsilon)$.

In Avalishvili and Gordeziani (2003), approximability is proved using the density of the sequence of spaces $V^{\mathbf{q}}(\Omega^\varepsilon)$ in $H^1(\Omega^\varepsilon)^3$. But the problem of finding a rate for the convergence in (33) is more difficult, since the solution $\mathbf{u}^\varepsilon$ has singularities near the edges and, consequently, does not belong to $H^2(\Omega^\varepsilon)$ in general. For scalar problems, Vogelius and Babuška (1981a, 1981b, 1981c) prove best approximation results using weighted Sobolev norms [4]. Up to now, for elasticity systems, there are no such results taking the actual regularity of $\mathbf{u}^\varepsilon$ into account.

It is worth noticing that, in order to obtain an equality of the form (36), we must use Korn inequality, since most approximation results are based on Sobolev norms. But due to blow up of the Korn constant when $\varepsilon \to 0$, it seems hard to obtain sharp estimates in the general case. (Let us recall that it behaves as ε^{-1} in the case of partially clamped shells.)

5.3 Asymptotic consistency

Like for plates, the presence of the nonpolynomial three-dimensional boundary layers $\mathbf{w}^k$ generically produces a

REVISED PAGE PROOFS

limitation in the convergence rate in (35). As previously mentioned, the only case where a sharp estimate is available, is the case of clamped elliptic shells. Using (68), we indeed obtain the following result (compare with Theorem 3):

Theorem 8. *If the midsurface S is elliptic, if the shell is clamped along its whole lateral boundary, and if* $\mathbf{f}\big|_S \not\equiv 0$, *then for any* $\mathbf{q} \succeq (1,1,2)$ *with definition (48), and for any* $\mathbf{q} \succeq (2,2,2)$ *with (85), and with the use of the standard 3-D elastic energy (2), there exists* $C_{\mathbf{q}} = C_{\mathbf{q}}(\mathbf{f}) > 0$ *such that for all* $\varepsilon \in (0, \varepsilon_0)$

$$\|\mathbf{u}^\varepsilon - \mathbf{u}^{\varepsilon,\mathbf{q}}\|_{E(\Omega^\varepsilon)} \le C_{\mathbf{q}} \sqrt{\varepsilon}\, \|\mathbf{u}^\varepsilon\|_{E(\Omega^\varepsilon)} \tag{86}$$

Note that in this case, the two-dimensional boundary layers are polynomial in x_3, Therefore they can be captured by the semidiscrete hierarchy of spaces $V^{\mathbf{q}}$.

Using estimate (83) of Lods and Mardare (2002), together with the fact that the corrector term $\mathbf{w}^\sharp$ is polynomial in x_3 of degree $(0,0,2)$, we obtain a proof for the asymptotic consistency for *any (smooth) clamped shell* without assuming that the midsurface is elliptic:

Theorem 9. *If the shell is clamped along its whole lateral boundary, and if* $\mathbf{f}\big|_S \not\equiv 0$, *then for* $\mathbf{q}$ *as in Theorem 8 and the standard energy (2), there exists* $C_{\mathbf{q}} = C_{\mathbf{q}}(\mathbf{f}) > 0$ *such that for all* $\varepsilon \in (0, \varepsilon_0)$

$$\|\mathbf{u}^\varepsilon - \mathbf{u}^{\varepsilon,\mathbf{q}}\|_{E(\Omega^\varepsilon)} \le C_{\mathbf{q}}\, \varepsilon^{1/4}\, \|\mathbf{u}^\varepsilon\|_{E(\Omega^\varepsilon)} \tag{87}$$

5.4 Examples of hierarchical models

Various models of degree $(1,1,0)$, $(1,1,2)$, and $(2,2,2)$ are introduced and investigated in the literature. Note that the model $(1,1,1)$ is *strictly forbidden* for shells because it cannot be associated with any correct energy; see Chapelle, Ferent and Bathe (2004).

5.4.1 (1, 1, 0) models

One of the counterparts of Reissner–Mindlin model for plates is given by the Naghdi model: see Naghdi (1963, 1972). The space of admissible displacements is

$$V^{\mathsf{N}}(\Omega^\varepsilon) = \{\mathbf{u} \in V(\Omega^\varepsilon),\ \exists \mathbf{z} \in H_0^1(S)^3,\ \exists \theta_\alpha \in H_0^1(S)^2,\ \mathbf{u} = (\mathsf{z}_\alpha - \mathsf{x}_3(\theta_\alpha + b_\alpha^\beta \mathsf{z}_\beta),\ \mathsf{z}_3)\} \tag{88}$$

As in (47) the energy splits into three parts (with the shear correction factor κ):

$$\begin{aligned} \widetilde{a}(\mathbf{u},\mathbf{u}) = {} & 2\varepsilon \int_S \widetilde{A}^{\alpha\beta\sigma\delta} \gamma_{\alpha\beta}(\mathbf{z}_\top)\gamma_{\sigma\delta}(\mathbf{z}_\top)\, \mathrm{d}S \\ & \text{(membrane energy)} \\ & + \varepsilon\kappa \int_S \mu a^{\alpha\sigma} (\mathsf{D}_\alpha \mathsf{z}_3 + b_\alpha^\delta \mathsf{z}_\delta - \theta_\alpha) \\ & \times (\mathsf{D}_\sigma \mathsf{z}_3 + b_\sigma^\beta \mathsf{z}_\beta - \theta_\sigma)\, \mathrm{d}S \\ & \text{(shear energy)} \\ & + \frac{2\varepsilon^3}{3} \int_S \widetilde{A}^{\alpha\beta\sigma\delta} \overline{\rho}_{\alpha\beta}(\mathbf{z},\boldsymbol{\theta}) \overline{\rho}_{\sigma\delta}(\mathbf{z},\boldsymbol{\theta})\, \mathrm{d}S \\ & \text{(bending energy)} \end{aligned} \tag{89}$$

where

$$\overline{\rho}_{\alpha\beta}(\mathbf{z},\boldsymbol{\theta}) = \tfrac{1}{2}(\mathsf{D}_\alpha \theta_\beta + \mathsf{D}_\beta \theta_\alpha) - c_{\alpha\beta}\mathsf{z}_3 + \tfrac{1}{2} b_\alpha^\sigma \mathsf{D}_\beta z_\sigma + \tfrac{1}{2} b_\beta^\sigma \mathsf{D}_\alpha z_\sigma$$

Note that when the penalization term in the shear energy goes to zero, we get $\theta_\sigma = \mathsf{D}_\sigma \mathsf{z}_3 + b_\sigma^\beta \mathsf{z}_\beta$ and the displacement $\mathbf{u}$ in (88) coincides with (66). In Lods and Mardare (2002), an estimate of the error between the solution of the Naghdi model and the solution of the 3-D model is provided in a subenergetic norm.

A more recent $(1,1,0)$ model (called *general shell element*; see Chapelle and Bathe, 2000) consists of the reduced energy projection on the space $V^{(1,1,0)}(\Omega^\varepsilon)$. Indeed, it does not coincide with the Naghdi model but both models possess similar asymptotic properties and they are preferred to Koiter's for discretization.

5.4.2 Quadratic kinematics

In accordance with Theorems 8 and 9, it is relevant to use the standard 3-D elastic energy (2) for such kinematics. Quadratic models based on the $(1,1,2)$ model are investigated in Bischoff and Ramm (2000). The enrichment of the general shell element by the introduction of quadratic terms – model $(2,2,2)$ – is thoroughly studied from both asymptotic and numerical point views in Chapelle, Ferent and Bathe (2004) and Chapelle, Ferent and Le Tallec (2003).

6 FINITE ELEMENT METHODS IN THIN DOMAINS

We herein address some of the characteristics of finite element methods (FEM), mainly the *p*-version of the FEM, when applied to the primal weak formulations (3) and (33) for the solution of plate and shell models. We only address isotropic materials, although our analysis could be extended to laminated composites.

As illustrative examples, we present the results of some computations performed with the *p*-version FE computer program StressCheck. (StressCheck is a trade mark of Engineering Software Research and Development, Inc., 10845 Olive Blvd., Suite 170, St. Louis, MO 63141, USA.)

REVISED PAGE PROOFS

6.1 FEM discretizations

Let us recall that, when conformal, the FEM is a Galerkin projection into finite dimensional subspaces V_N of the variational space associated with the models under consideration. In the p-version of the FEM, subspaces are based on *one partition* of the domain into a finite number of subdomains $K \in \mathcal{T}$ (the *mesh*) in which the unknown displacement is discretized by mapped polynomial functions of increasing degree p. The subdomains K are mapped from reference element(s) $\widehat{K}$.

6.1.1 Meshes

All finite element discretizations we consider here are based on a mesh $\mathcal{T}_S$ of the midsurface S: We mean that the 3-D mesh of Ω^ε has in normal coordinates $(\mathbf{x}_\top, \mathsf{x}_3)$ the tensor product form [5] $\mathcal{T}_S \otimes \mathcal{I}_\varepsilon$ where $\mathcal{I}_\varepsilon$ represents a partition of the interval $(-\varepsilon, \varepsilon)$ in layers, for example, the two halves $(-\varepsilon, 0)$ and $(0, \varepsilon)$, or – this case is important in the sequel – , the trivial partition by only *one element through the thickness*. We agree to call that latter mesh a *thin element mesh*.

The 3-D elements K are thus images by maps ψ_K from reference elements $\widehat{K}$, which are either pentahedral (triangle × interval) or hexahedral:

$$\psi_K : \widehat{K} = \widehat{T} \times [0, 1] \ni (\hat{x}_1, \hat{x}_2, \hat{x}_3) \mapsto \mathbf{x} \in K$$

with $\widehat{T}$ the reference triangle or the reference square. For the 2-D FEM, we denote by T the elements in $\mathcal{T}_S$: They are the image of $\widehat{T}$ by maps ψ_T

$$\psi_T : \widehat{T} \ni (\hat{x}_1, \hat{x}_2) \mapsto \mathbf{x}_\top \in T$$

If Ω_ε is a plate, the midsurface S is plane but its boundary ∂S is not straight. For some lateral boundary conditions, for example, the hard, simple supported plate, the approximation of ∂S by a polygonal lines produces, in general, *wrong results*. This effect is known as the *Babuška paradox* (Babuška and Pitkäranta, 1990). If Ω_ε is a shell, the geometric approximation of S by 'plane' elements is also an issue: If the mappings are affine, the shell is approximated by a faceted surface which has quite different rigidity properties than the smooth surface; see Akian and Sanchez-Palencia (1992) and Chapelle and Bathe (2003), Section 6.2.

As a conclusion, good mappings have to be used for the design of the elements K (high degree polynomials or other analytic functions).

6.1.2 Polynomial spaces for hierarchical models

For hierarchical models (33), the discretization is indeed two-dimensional: The degree $\mathbf{q}$ of the hierarchy being fixed, the unknowns of (33) are the functions z_j^n defined on S and representing the displacement according to (38), where the director functions Φ_j^n form adequate bases of polynomials in one variable, for example, Legendre polynomials L_n.

We have already mentioned in Section 5 that the only *intrinsic* option for the choice of components is taking $j = (\alpha, 3)$, which results into the Ansatz (written here with Legendre polynomials)

$$\mathsf{u}_\top = \sum_{n=0}^{q_\top} \mathsf{z}_\top^n(\mathbf{x}_\top)\, L_n\Big(\frac{\mathsf{x}_3}{\varepsilon}\Big)$$

and

$$\mathsf{u}_3 = \sum_{n=0}^{q_3} \mathsf{z}_3^n(\mathbf{x}_\top)\, L_n\Big(\frac{\mathsf{x}_3}{\varepsilon}\Big)$$

Now the discretization consists in requiring that $\mathsf{z}_\alpha^n|_T \circ \psi_T$, $\alpha = 1, 2$, and $\mathsf{z}_3^n|_T \circ \psi_T$ belong to the space $\mathbb{P}_p(\widehat{T})$ for some p where $\mathbb{P}_p(\widehat{T})$ is the space of polynomials in two variables

- of degree $\leq p$ if $\widehat{T}$ is the reference triangle,
- of partial degree $\leq p$ if $\widehat{T}$ is the reference square $[0, 1] \times [0, 1]$.

It makes sense to fix different degrees p_j in relation with $j = \alpha, 3$, and we set $\mathbf{p} = (p_1, p_2, p_3)$. When plugged back into formula (38), this discretization of the z_j^n, $j = \alpha, 3$, yields a finite dimensional subspace $V_{\mathbf{p}}^{\mathbf{q}}(\Omega^\varepsilon)$ of $V^{\mathbf{q}}(\Omega^\varepsilon)$. As already mentioned for the transverse degrees $\mathbf{q}$, cf. (48) and Section 5, we have to assume for coherence that $p_1 = p_2$ for shells. In the situation of plates, if T is affinely mapped from the reference square, the $\mathsf{z}_j^n|_T$ are simply given by

$$\mathsf{z}_1^n(\mathbf{x}_\top) = \sum_{i,k=0}^{p_1} z_{1,ik}^n P_i(x_1) P_k(x_2)$$

$$\mathsf{z}_2^n(\mathbf{x}_\top) = \sum_{i,k=0}^{p_2} z_{2,ik}^n P_i(x_1) P_k(x_2)$$

$$\mathsf{z}_3^n(\mathbf{x}_\top) = \sum_{i,k=0}^{p_3} z_{3,ik}^n P_i(x_1) P_k(x_2)$$

where the $z_{j,ik}^n$ are real coefficients and P_i denotes a polynomial of degree i which is obtained from Legendre polynomials; see for example Szabó and Babuška (1991).

The discretization of hierarchical models (33) can also be done through the h-version or the h-p versions of FEM.

REVISED PAGE PROOFS

6.1.3 Polynomial spaces for 3-D discretization. Case of thin elements

In 3-D, on the reference element $\widehat{K} = \widehat{T} \times [0, 1]$, we can consider any of the polynomial spaces $\mathbb{P}_{p,q}(\widehat{K}) = \mathbb{P}_p(\widehat{T}) \otimes \mathbb{P}_q([0, 1])$, $p, q \in \mathbb{N}$, For the discretization of (3), each Cartesian component u_i of the displacement is sought for in the space of functions $v \in H^1(\Omega^\varepsilon)$ such that for any K in the mesh, $v|_K \circ \psi_K$ belongs to $\mathbb{P}_{p,q}(\widehat{K})$. We denote by $V_{p,q}(\Omega^\varepsilon)$ the corresponding space of admissible displacements over Ω^ε.

In the situation where we have only one layer of elements over Ω^ε in the thickness (thin element mesh) with a (p, q) discretization, let us set $\mathbf{q} = (q, q, q)$ and $\mathbf{p} = (p, p, p)$. Then it is easy to see that, *in the framework of semidiscrete spaces* (85), we have the equality between discrete spaces:

$$V_{p,q}(\Omega^\varepsilon) = V_{\mathbf{p}}^{\mathbf{q}}(\Omega^\varepsilon) \tag{90}$$

In other words, thin elements are equivalent to the discretization of underlying hierarchical models. Let us insist on the following fact: For a true shell, the correspondence between the Cartesian components u_j and the tangential and transverse components $(\mathbf{u}_\top, \mathsf{u}_3)$ is nonaffine. As a consequence, equality (90) holds only if the space $V_{\mathbf{p}}^{\mathbf{q}}(\Omega^\varepsilon)$ corresponds to the discretization of a hierarchical model in *Cartesian coordinates*.

Conversely, hierarchical models of the type $\mathbf{q} = (q, q, q)$ with the 'Cartesian' unknowns z_j^n, $n = 0, \ldots, q$, $j = 1, 2, 3$ can be discretized directly on S, or inherit a 3-D discretization; see Chapelle, Ferent and Bathe (2004). Numerical evidence that the p-version with anisotropic Ansatz spaces allows the analysis of three-dimensional shells with high accuracy was firstly presented in Düster, Bröker and Rank (2001).

6.1.4 FEM variational formulations

Let us fix the transverse degree $\mathbf{q}$ of the hierarchical model. Its solution $\mathbf{u}^{\varepsilon,\mathbf{q}}$ solves problem (33). For each $\varepsilon > 0$ and each polynomial degree $\mathbf{p}$, (33) is discretized by its finite dimensional subspace $V_{\mathbf{p}}^{\mathbf{q}}(\Omega^\varepsilon)$. Let $\mathbf{u}_{\mathbf{p}}^{\varepsilon,\mathbf{q}}$ be the solution of

$$\begin{aligned} &\textit{Find } \mathbf{u}_{\mathbf{p}}^{\varepsilon,\mathbf{q}} \in V_{\mathbf{p}}^{\mathbf{q}}(\Omega^\varepsilon) \quad \textit{such that} \\ &a^{\varepsilon,\mathbf{q}}(\mathbf{u}_{\mathbf{p}}^{\varepsilon,\mathbf{q}}, \mathbf{u}') = \int_{\Omega^\varepsilon} \mathbf{f}^\varepsilon \cdot \mathbf{u}' \, \mathrm{d}\boldsymbol{x}, \quad \forall \mathbf{u}' \in V_{\mathbf{p}}^{\mathbf{q}}(\Omega^\varepsilon) \end{aligned} \tag{91}$$

We can say that (91) is a sort of 3-D discretization of (33). But, indeed, the actual unknowns of (91) are the $\mathbf{z}_\alpha^n$, $n = 0, \ldots, q_\top$, and z_3^n, $n = 0, \ldots, q_3$, or the z_j^n for $n = 0, \ldots, q$ and $j = 1, 2, 3$. Thus, (91) can be alternatively formulated as a 2-D problem involving spaces $Z_{\mathbf{p}}^{\mathbf{q}}(S)$ independent of ε, and a coercive bilinear form $a_S^{\mathbf{q}}(\varepsilon)$ polynomial in ε. Examples are provided by the Reissner–Mindlin model, cf. (47), the Koiter model (84), and the Naghdi model, cf. (89). The variational formulation now takes the form

$$\begin{aligned} &\textit{Find } \mathbf{Z} =: (\mathbf{z}^n)_{0 \le n \le q} \in Z_{\mathbf{p}}^{\mathbf{q}}(S) \quad \textit{such that} \\ &a_S^{\mathbf{q}}(\varepsilon)(\mathbf{Z}, \mathbf{Z}') = F(\varepsilon)(\mathbf{f}, \mathbf{Z}'), \quad \forall \mathbf{Z}' \in Z_{\mathbf{p}}^{\mathbf{q}}(S) \end{aligned} \tag{92}$$

where $F(\varepsilon)(\mathbf{f}, \mathbf{Z}')$ is the suitable bilinear form coupling loadings and test functions. Let us denote by $\mathbf{Z}_{\mathbf{p}}^{\varepsilon,\mathbf{q}}$ the solution of (92).

6.2 Locking issues

In the framework of the family of discretizations considered above, the *locking* effect is said to appear when a *deterioration* in the resulting approximation of $\mathbf{u}^{\varepsilon,\mathbf{q}}$ by $\mathbf{u}_{\mathbf{p}}^{\varepsilon,\mathbf{q}}$, $\mathbf{p} \to \infty$ tends to ∞, occurs as $\varepsilon \to 0$. Of course, a similar effect is reported in the h-version of FEM: The deterioration of the h-approximation also occurs when the thickness ε approaches zero.

Precise definition of locking may be found in Babuška and Suri (1992): It involves the locking parameter (the thickness ε in the case of plates), the sequence of finite element spaces $V_{\mathbf{p}}^{\mathbf{q}}$ that comprise the extension procedure (the p-version in our case, but h and h-p versions can also be considered), and the norm in which error is to be measured. Of course, in different error measures different locking phenomena are expected.

6.2.1 Introduction to membrane locking

A locking-free approximation scheme is said to be *robust*. For a bilinear form $a_S(\varepsilon)$ of the form $a_0 + \varepsilon^2 a_1$ like Koiter's, a necessary condition for the robustness of the approximation is that the intersections of the discrete spaces with the kernel of a_0 are a sequence of dense subspaces for the whole kernel of a_0; see Sanchez-Hubert and Sanchez-Palencia (1997), Ch. XI. In the case of the Koiter model, this means that the whole inextensional space $V_{\mathsf{F}}(S)$ (69) can be approximated by the subspaces of the inextensional elements belonging to FE spaces. For hyperbolic shells, the only inextensional elements belonging to FE spaces are zero; see Sanchez-Hubert and Sanchez-Palencia (1997) and Chapelle and Bathe (2003), Section 7.3, which prevents all approximation property of $V_{\mathsf{F}}(S)$ if it is not reduced to $\{0\}$.

This fact is an extreme and general manifestation of the *membrane locking* of shells, also addressed in Pitkaranta (1992) and Gerdes, Matache and Schwab (1998) for cylindrical shells, which are a prototype of shells having a nonzero inextensional space. Plates do not present membrane locking since all elements $\mathbf{z} = (\mathbf{0}, \mathsf{z}_3)$ are inextensional, thus can be approximated easily by finite element

REVISED PAGE PROOFS

subspaces. Nevertheless, as soon as the RM model is used, as can be seen from the structure of the energy (47), a shear locking may appear.

6.2.2 *Shear locking of the RM and hierarchical plate models*

Shear locking occurs because the FE approximation using $\mathcal{C}^0$ polynomials for the RM family of plates at the limit when $\varepsilon \to 0$ has to converge to the KL model in energy norm Suri, 2001, requiring $\mathcal{C}^1$ continuity. Let us consider the three-field RM model on the subspace of $V^{\mathrm{RM}}(\Omega^\varepsilon)$, cf. Section 3.3, of displacements with bending parity: $\{\mathbf{u} \in V(\Omega^\varepsilon),\ \mathbf{u} = (-\mathsf{x}_3\boldsymbol{\theta}_\top,\ \mathsf{z}_3)\}$. According to Suri, Babuška and Schwab (1995) we have the following:

Theorem 10. *The p-version of the FEM for the RM plate model without boundary layers, on a mesh of triangles and parallelograms, with polynomial degrees of* $p_\top \geq 1$ *for rotations* $\boldsymbol{\theta}_\top$ *and* $p_3 \geq p_\top$ *for* z_3 *is free of locking in the energy norm.*

For the h-version over a uniform mesh consisting either of triangles or rectangles, to avoid locking the tangential degree $p_\top$ has to be taken equal to four or larger, with the transverse degree p_3 being chosen equal to $p+1$. A similar phenomenon was earlier found in connection with 'Poisson Ratio' locking for the equations of elasticity. (i.e. conforming elements of degree four or higher encounter no locking); see Scott and Vogelius (1985). In Suri, Babuška and Schwab (1995), it is proven that locking effects (and results) for the $(1, 1, 2)$ plate model are similar to the RM model because no additional constraints arise as the thickness $\varepsilon \to 0$. Furthermore, it is stated that locking effects carry over to all hierarchical plate models.

Here we have discussed locking in energy norm. However, if shear stresses are of interest, then locking is significantly worse because these involve an extra power ε^{-1}.

For illustration purposes, consider a *clamped* plate with ellipsoidal midsurface of radii 10 and 5, Young modulus (we recall that the Young modulus is given by $E = \mu(3\lambda + 2\mu)/2(\lambda + \mu)$ and the Poisson ratio by $\nu = \lambda/2(\lambda + \mu)$) $E = 1$ and Poisson ratio $\nu = 0.3$; see Figure 4. The plate is loaded by a constant pressure of value $(2\varepsilon)^2$.

The discretization is done over a 32 p-element mesh (see Figure 4(a) and (b) for $2\varepsilon = 1$ and 0.1) using two layers, each of dimension ε in the vicinity of the boundary. The FE space is defined with $p_3 = p_\top$ ranging from 1 to 8. We show in Figure 5 the locking effects for the RM model with κ_{Energy}.

The error plotted in ordinates is the estimated relative *discretization error* in energy norm between the numerical and exact solution of the RM plate model for each fixed thickness ε (it is not the error between the RM numerical solution and the exact 3-D plate model). A similar behavior can be observed with the model $\mathbf{q} = (1, 1, 2)$.

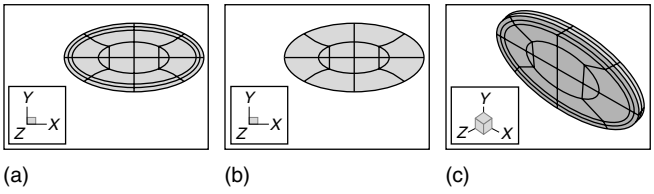

Figure 4. p-FE mesh for $2\varepsilon = 1$, 0.1 for RM model and $2\varepsilon = 1$ for 3-D model. A color version of this image is available at http://www.mrw.interscience.wiley.com/ecm

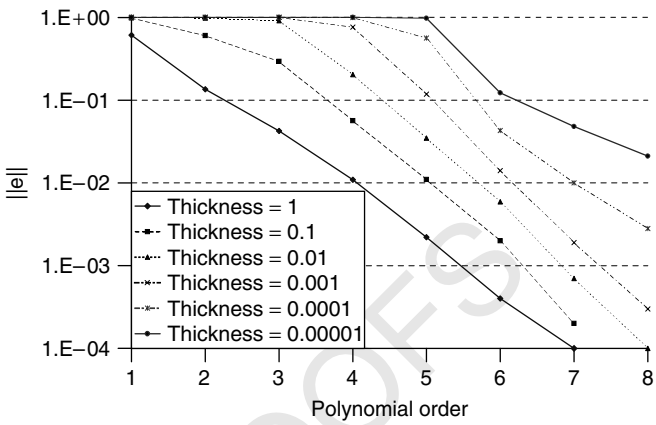

Figure 5. Discretization error versus polynomial degree p for RM plates of various thicknesses ε. A color version of this image is available at http://www.mrw.interscience.wiley.com/ecm

To illustrate both the locking effects for the hierarchical family of plates and the modeling errors between the plate models and their 3-D counterpart, we have computed for two thicknesses of plates ($2\varepsilon = 1$ or $2\varepsilon = 0.01$), the solution for the first four plate models (see Table 1 [6]), and for the fully 3-D plate with the degrees $p_\top = p_3 = 1, 2, \ldots, 8$ with the model represented in Figure 4(c) for $2\varepsilon = 1$.

The relative errors between energy norms of the hierarchical models and the 3D plate model versus the polynomial degree p is shown in Figure 6. As predicted, increasing the order of the plate model does not improve the locking ratio, and as the hierarchical model number is increased the relative error decreases. We note that when

Table 1. Hierarchical plate-model definitions for bending symmetry.

Model #	1 (RM)	2	3	4
Degrees $\mathbf{q} = (q_1, q_2, q_3)$	(1,1,0)	(1,1,2)	(3,3,2)	(3,3,4)
# independent fields $\mathbf{d} = (d_1, d_2, d_3)$	(1,1,1)	(1,1,2)	(2,2,2)	(2,2,3)

REVISED PAGE PROOFS

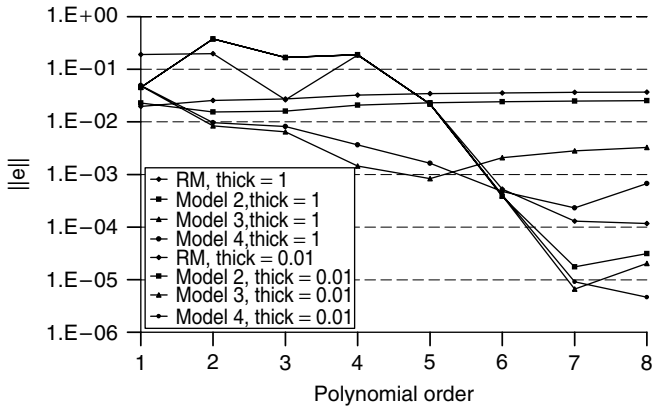

Figure 6. Relative error versus polynomial degree for $2\varepsilon = 1$ and 0.01 for the first 4 hierarchical models. A color version of this image is available at http://www.mrw.interscience.wiley.com/ecm

$2\varepsilon = 1$ the relative error of the four models converges to the modeling error, which is still quite big since ε is not small, whereas when $2\varepsilon = 0.01$, the error stays larger that 15% for all models when $p \leq 4$, and starts converging for $p \geq 5$.

6.3 Optimal mesh layout for hierarchical models with boundary layers

All hierarchical plate models (besides KL model) exhibit boundary layers. These are rapidly varying components, which decay exponentially with respect to the stretched distance $\mathsf{R} = \mathsf{r}/\varepsilon$ from the edge, so that at a distance $\mathcal{O}(2\varepsilon)$ these are negligible. Finite element solutions should be able to capture these rapid changes. Using the p-version of the finite element method, one may realize exponential convergence rates if a proper design of meshes and selection of polynomial degrees is applied in the presence of boundary layers.

In a 1-D problem with boundary layers, it has been proven in Schwab and Suri (1996) that the p-version over a refined mesh can achieve exponential convergence for the boundary layers, uniformly in ε. The mesh has to be designed so to consist of one $\mathcal{O}(p(2\varepsilon))$ boundary layer element at each boundary point. More precisely, the optimal size of the element is $\alpha p(2\varepsilon)$, where, $0 < \alpha < 4/e$ (see Fig. 7).

This result carries over to the heat transfer problem on 2-D domains as shown in Schwab, Suri and Xenophontos (1998), and to the RM plate model, as demonstrated by numerical examples. Typical boundary layer meshes are shown in Figure 4 for $2\varepsilon = 1$ and 0.1: In practice, for ease of computations, two elements in the boundary layer zone are being used, each having the size in the normal direction of ε, independent of the polynomial degree used. This,

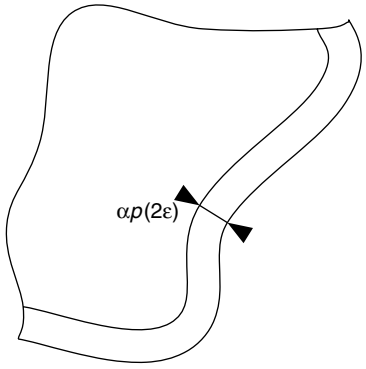

Figure 7. A typical design of the mesh near the boundary for the p-version of the FEM.

although not optimal, still captures well the rapid changes in the boundary layer.

In order to realize the influence of the mesh design over the capture of boundary layer effects, we have again solved numerically the RM plate model for a thickness of $2\varepsilon = 0.01$ (and $\kappa_{\text{Deflection}}$ as shear correction factor). Three different mesh layouts have been considered, with two layers of elements in the vicinity of the edge of dimension 0.5, 0.05, and 0.005 (the first two ones are represented in Figure 4). For comparison purposes, we have computed the 3-D solution over a domain having two layers in the thickness direction and two elements in the boundary layer zone of dimension 0.005. We have extracted the vertical displacement u_3 and the shear strain e_{23} along the line starting at $(x_1, x_2) = (9.95, 0)$ and ending at the boundary $(x_1, x_2) = (10, 0)$, that is, in the boundary layer region. Computations use the degrees $p_\top = p_3 = 8$. It turns out that the vertical displacement u_3 is rather insensitive to the mesh, whereas the shear strain e_{23} is inadequately computed if the mesh is not properly designed: With the mesh containing fine layers of thickness 0.005, the average relative error is 10%, but this error reaches 100% with mesh layer thickness 0.05 and 400% for the mesh layer thickness 0.5.

Concerning *shells*, we have seen in Section 4.2 that the Koiter model for clamped elliptic shells admits boundary layers of length scale $\sqrt{\varepsilon}$, and in Section 4.4 that other length scales may appear for different geometries ($\varepsilon^{1/3}$ and $\varepsilon^{1/4}$). Moreover, for Naghdi model, the short length scale ε is also present; see Pitkäranta, Matache and Schwab (2001). Nevertheless, the "long" length scales $\varepsilon^{1/3}$ and $\varepsilon^{1/4}$ appear to be less frequent. We may expect a similar situation for other hierarchical models. As a conclusion the mesh design for shell of small thicknesses should (at least) take into account both length scales ε and $\sqrt{\varepsilon}$. Another phenomenon should also be considered: Hyperbolic and parabolic shells submitted to a concentrated load or a singular data are expected to propagate singularities along

REVISED PAGE PROOFS

their zero curvature lines, with the scale width $\varepsilon^{1/3}$; see Pitkäranta, Matache and Schwab (2001).

6.4 Eigen-frequency computations

Eigen-frequency computations are, in our opinion, a very good indicator of *(i)* the quality of computations, *(ii)* the nature of the shell (or plate) response. In particular, the bottom of the spectrum indicates the maximal possible stress–strain energy to be expected under a load of given potential energy. From Theorem 7, we may expect that, except in the case of clamped elliptic shells, the ratio between the energy of the response and the energy of the excitation will behave almost as $\mathcal{O}(\varepsilon^{-2})$.

6.4.1 Eigen-frequency of RM versus 3-D for plates

Eigen-frequencies obtained by the *p*-version finite element method for clamped RM plates and their counterpart 3-D eigen-frequencies have been compared in Dauge and Yosibash (2002), where rectangular plates of dimensions $1 \times 2 \times 2\varepsilon$ have been considered. For isotropic materials with Poisson coefficient $\nu = 0.3$, the relative error for the first three eigen-frequencies was found negligible (less than 0.12%), for thin plates with slender ratio of less than 1%, and still small (0.2%) for moderately thick plates (slander ratio about 5%).

For some orthotropic materials, much larger relative errors between the RM eigen-frequencies and their 3-D counterparts have been observed even for relatively thin plates. In one of the orthotropic rectangular plate examples in Dauge and Yosibash (2002), for which the boundary layer effect on the eigen-frequencies should be the most pronounced, a very large relative error of 25% has been reported for the first eigen-frequency at $\varepsilon = 0.1$. This is a significant deviation, whereas the RM model underestimates the 'true' 3-D by 25%, and is attributed to the boundary layer effect.

6.4.2 3-D eigen-frequency computations for shells

We present computations on three families of shells, see Figure 8: (a) clamped spherical shells, (b) sensitive spherical shells, (c) flexural cylindrical shells, all with material

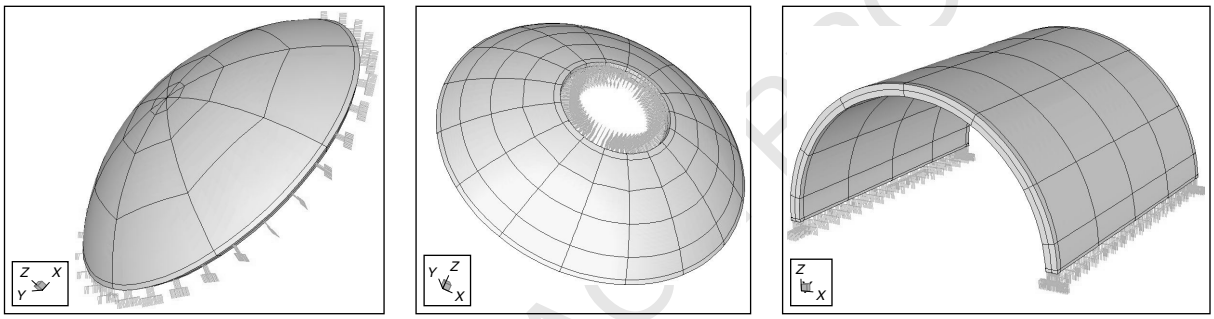

Figure 8. Shell models (a), (b) and (c) for $\varepsilon = 0.04$. A color version of this image is available at http://www.mrw.interscience.wiley.com/ecm

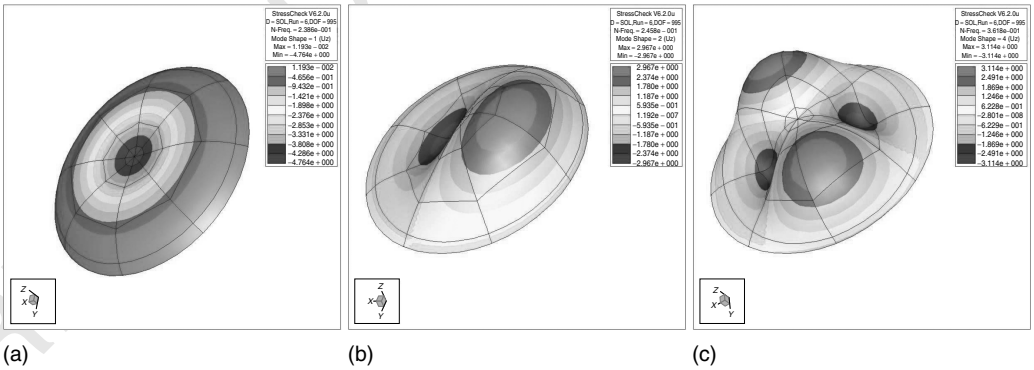

Figure 9. Model (a). vertical components of eigen-modes 1, 2 and 4 for $\varepsilon = 0.08$. A color version of this image is available at http://www.mrw.interscience.wiley.com/ecm

PROOFS

parameters $\nu = 0.3$ and $E = 1$. These three families illustrate the three cases *(i)*, *(ii)* and *(iii)* in Theorem 7: The shells (a) are elliptic clamped on their whole boundary, (b) are elliptic, but clamped only on a part of their boundaries, and (c) are parabolic. *Note that Theorem 7 states results relating to Koiter eigenvalues and not for 3-D eigenvalues. Nevertheless, a similar behavior can be expected for 3-D eigenvalues.*

Family (a). The midsurface S is the portion of the unit sphere described in spherical coordinates by $\varphi \in [0, 2\pi)$ and $\theta \in (\pi/4, \pi/2]$. Thus S a spherical cap containing the north pole. The family of shells Ω^ε has its upper and lower surfaces characterized by the same angular conditions, and the radii $\rho = 1 + \varepsilon$ and $\rho = 1 - \varepsilon$, respectively. We clamp Ω^ε along its lateral boundary $\theta = \pi/4$.

We have computed the first five eigen-frequencies of the 3-D operator (4) by a FE p-discretization based on two layers of elements in the transverse direction and 8×5 elements in the midsurface, including one thin layer of elements in the boundary layer. The *vertical* (i.e. normal to the tangent plane at the north pole, not transverse to the midsurface!) component u_3 for three modes are represented in Figure 9 for the (half)-thickness $\varepsilon = 0.08$. Mode 3 is rotated from mode 2, and mode 5 from mode 4 (double eigen-frequencies). The shapes of the eigen-modes for smaller values of the thickness are similar. Figure 10 provides the three first distinct eigen-frequencies as a function of the thickness in natural scales. In accordance with

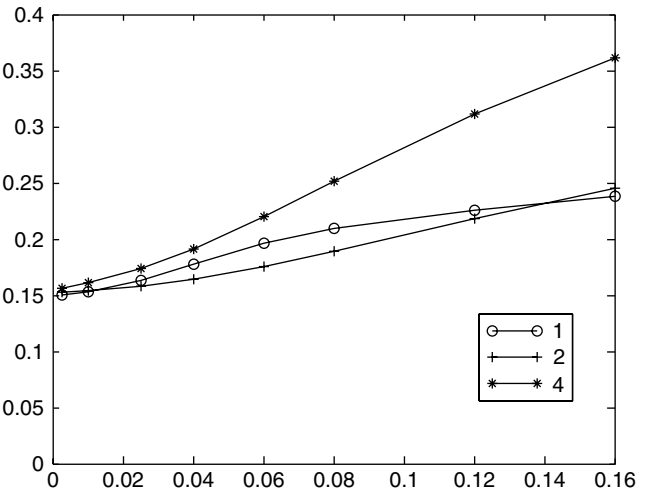

Figure 10. Model (a). Eigen-frequencies versus thickness (2ε). A color version of this image is available at http://www.mrw.interscience.wiley.com/ecm

Theorem 7 *(i)*, the smallest eigen-frequencies all tend to the same nonzero limit, which should be the (square root of the) bottom of the membrane spectrum.

Family (b). The midsurface S is the portion of the unit sphere described in spherical coordinates by $\varphi \in [0, 2\pi)$ and $\theta \in (\pi/4, 5\pi/12]$. The family of shells Ω^ε has its upper and lower surfaces characterized by the same angular conditions, and the radii $\rho = 1 + \varepsilon$ and $\rho = 1 - \varepsilon$, respectively.

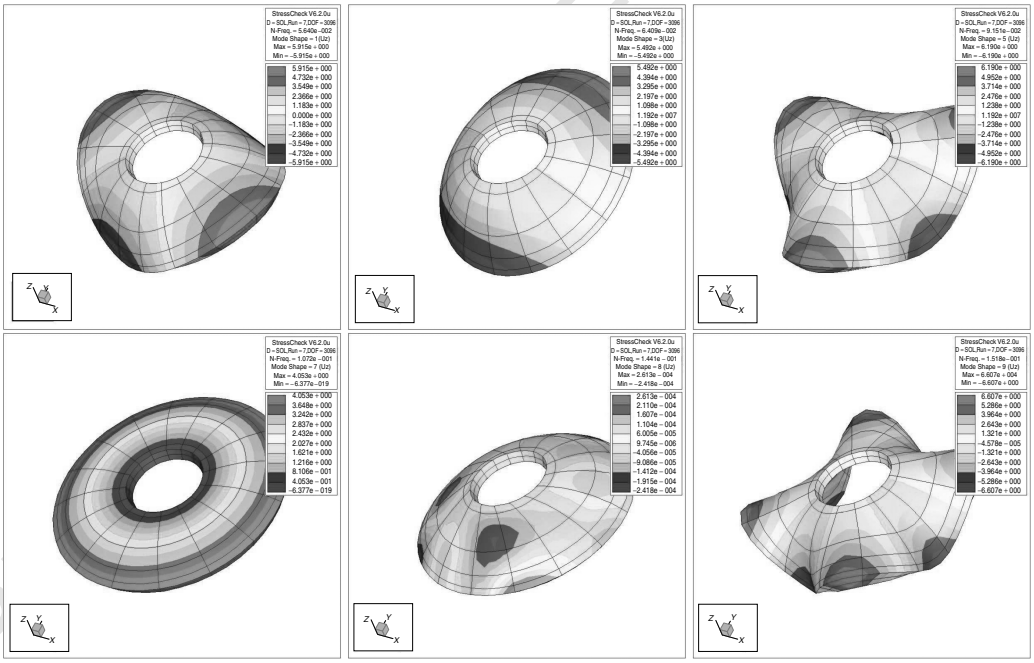

Figure 11. Model (b). Vertical components of modes 1, 3, 5, 7, 8, 9 for $\varepsilon = 0.04$. A color version of this image is available at http://www.mrw.interscience.wiley.com/ecm

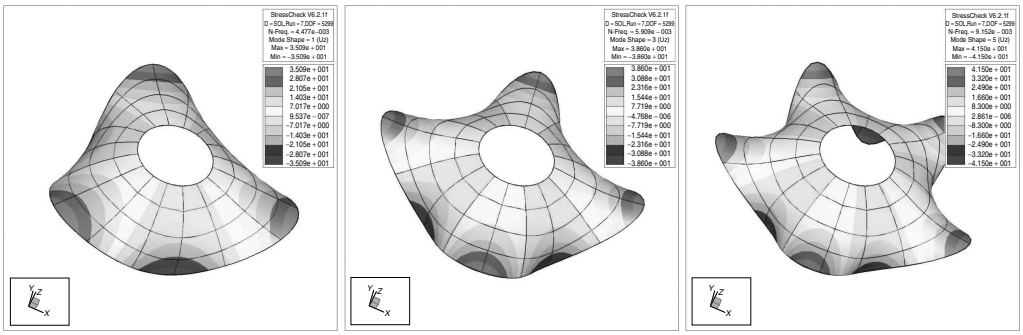

Figure 12. Model (b). Vertical components of modes 1, 3, 5 for $\varepsilon = 0.00125$. A color version of this image is available at http://www.mrw.interscience.wiley.com/ecm

We clamp Ω^ε along its lateral boundary $\theta = 5\pi/12$ and let it free along the other lateral boundary $\theta = \pi/4$. This shell is a sensitive one in the sense of Pitkäranta and Sanchez-Palencia (1997), which means that it is sensitive to the thickness and answers differently according to the value of ε.

We have computed the first five (or first ten) eigen-frequencies of the 3-D operator (4) by a FE p-discretization similar to that of (a) (two layers in the transverse direction and 8×4 elements in the surface direction – for the 'small' thickness, a globally refined mesh of 16×6 elements has been used). In Figure 11, we plot the vertical components of modes number 1, 3, 5, 7, 8, and 9 for $\varepsilon = 0.04$ and in Figure 12, modes number 1, 3, 5 for $\varepsilon = 0.00125$. In both cases, modes 2, 4, and 6 are similar to modes 1, 3, and 5 respectively and associated with the same (double) eigen-frequencies.

For $\varepsilon = 0.04$, we notice the axisymmetric mode at position 7 (it is at position 5 when $\varepsilon = 0.08$, and 9 for $\varepsilon = 0.02$). Mode 8 looks odd. Indeed, it is very small (less than 10^{-4}) for normalized eigenvectors in $\mathcal{O}(1)$. This means that this mode is mainly supported in its tangential components (we have checked they have a reasonable size). Mode 8 is in fact a *torsion mode*, which means a dominant stretching effect, whereas the other ones have a more pronounced bending character.

Figure 13 provides the first distinct eigen-frequencies classified by the nature of the eigenvector (namely the number of nodal regions of u_3) as a function of the thickness in natural scales. The organization of these eigen-frequencies along affine lines converging to positive limits as $\varepsilon \to 0$ is remarkable. We may expect a convergence as $\varepsilon \to 0$ of the solution $\mathbf{u}^\varepsilon$ of problem (3) *provided the loading has a finite number of angular frequencies in* φ (the displacement will converge to the highest angular frequency of the load). Nevertheless, such a phenomenon is specific to the axisymmetric nature of the shell (b) and could not be generalized to other sensitive shells. Computations with a concentrated load (which, of course, has an infinite number of angular frequencies) display a clearly nonconverging behavior (Chapelle and Bathe (2003), Section 4.5.3).

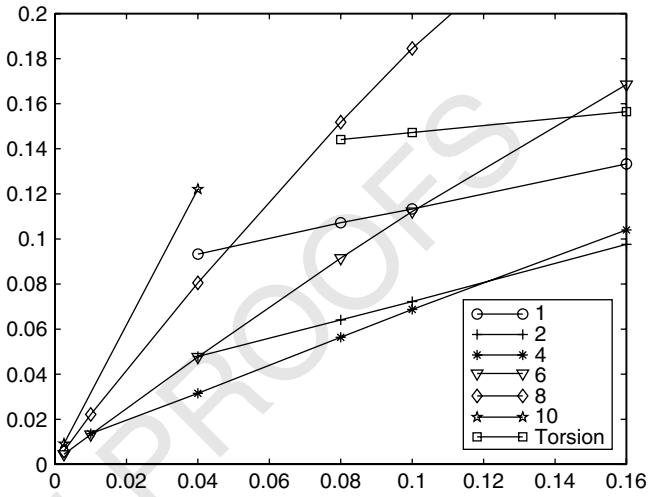

Figure 13. Model (b). Eigen-frequencies versus thickness (2ε). A color version of this image is available at http://www.mrw.interscience.wiley.com/ecm

Family (c). The midsurface S is a half-cylinder described in cylindrical coordinates (r, θ, y) by $\theta \in (0, \pi)$, $r = 1$ and $y \in (-1, 1)$. The family of shells Ω^ε has its upper and lower surfaces characterized by the same angular and axial condition, and the radii $r = 1 + \varepsilon$ and $r = 1 - \varepsilon$, respectively. We clamp Ω^ε along its lateral boundaries $\theta = 0$ and $\theta = \pi$ and leave it free everywhere else. This is a well-known example of flexural shell, where the space of inextensional displacements contains the space, cf. (80) (note that, below, $\mathsf{z}_r = \mathsf{z}_3$)

$$V_{\mathrm{F},0} := \big\{\mathbf{z} = (\mathsf{z}_r, \mathsf{z}_\theta, \mathsf{z}_y);\ \mathsf{z}_y = 0,\ \mathsf{z}_r = \mathsf{z}_r(\theta),\ \mathsf{z}_\theta = \mathsf{z}_\theta(\theta) \text{ with } \partial_\theta \mathsf{z}_\theta = \mathsf{z}_r \quad \text{and} \quad \mathsf{z}_\theta = \mathsf{z}_r = \partial_\theta \mathsf{z}_r = 0 \text{ in } \theta = 0, \pi\big\} \tag{93}$$

REVISED PAGE PROOFS

Besides these patterns independent of the axial variable y, there is another subspace $V_{\mathsf{F},1}$ of inextensional displacements, where z_y is independent on y and z_r, z_θ are linear in y:

$$V_{\mathsf{F},1} := \Big\{ \mathbf{z} = (\mathsf{z}_r, \mathsf{z}_\theta, \mathsf{z}_y);\ \ \mathsf{z}_y = \mathsf{z}_y(\theta),$$
$$\mathsf{z}_\theta = -y\partial_\theta \mathsf{z}_y(\theta),\ \ \mathsf{z}_r = -y\partial_\theta^2 \mathsf{z}_y(\theta)$$
$$\text{with} \qquad \mathsf{z}_y = \mathsf{z}_\theta = \mathsf{z}_r = \partial_\theta \mathsf{z}_r = 0 \ \text{ in } \ \theta = 0, \pi \Big\} \tag{94}$$

and $V_{\mathsf{F}} = V_{\mathsf{F},0} \oplus V_{\mathsf{F},1}$. We agree to call 'constant' the displacements associated with $V_{\mathsf{F},0}$ and 'linear' those associated with $V_{\mathsf{F},1}$.

We have computed the first ten eigen-frequencies (4) by a FE p-discretization based on two layers of elements in the transverse direction and a midsurface mesh of 8×6 curved quadrangles. For the half-thickness $\varepsilon = 0.0025$, we plot the *vertical* component $u_z = \mathsf{u}_r \sin\theta + \mathsf{u}_\theta \cos\theta$ of the eigenmodes $\mathbf{u}$: In Figure 14, the first six constant flexural eigenmodes and in Figure 15, the first three linear flexural eigen-modes (their components u_y clearly display a nonzero constant behavior in y). The shapes of the eigen-modes for larger values of the thickness are similar. In Figure 16, we have plotted in logarithmic scale these eigen-frequencies, classified according to the behavior of the flexural eigen-modes ('constant' and 'linear'). The black line has the equation $\varepsilon \mapsto \varepsilon/4$: Thus we can see that the slopes of the eigen-frequency lines are close to 1, as expected by the theory (at least for Koiter model). In Figure 17, we represent the first nonflexural modes (with rank 10 for $\varepsilon = 0.01$ and rank 8, 9 for $\varepsilon = 0.04$).

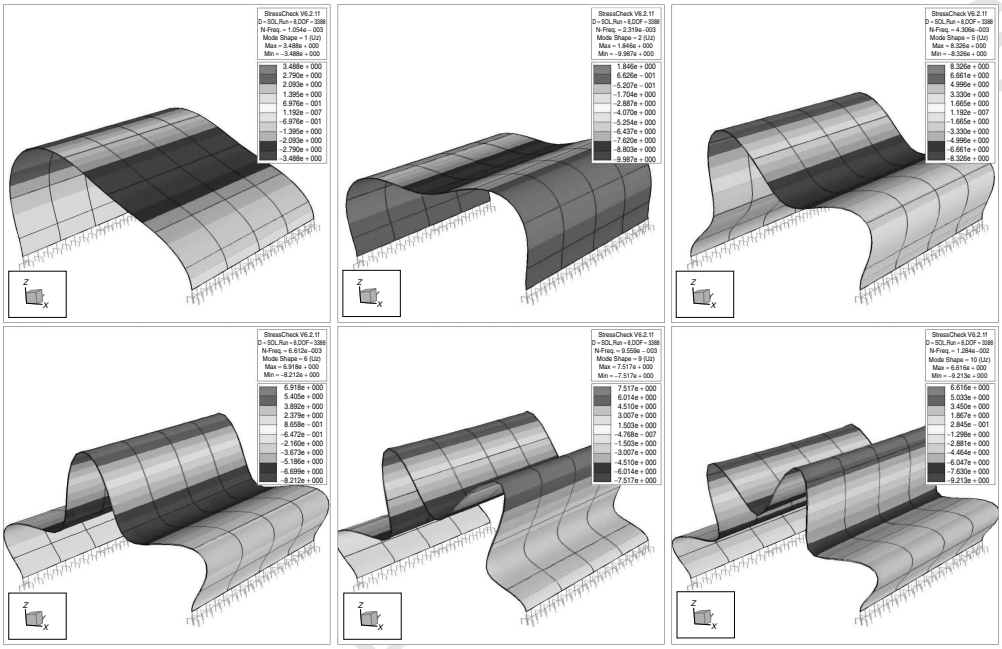

Figure 14. Model (c). Vertical components of modes 1, 2, 5, 6, 9 and 10 for $\varepsilon = 0.0025$. A color version of this image is available at http://www.mrw.interscience.wiley.com/ecm

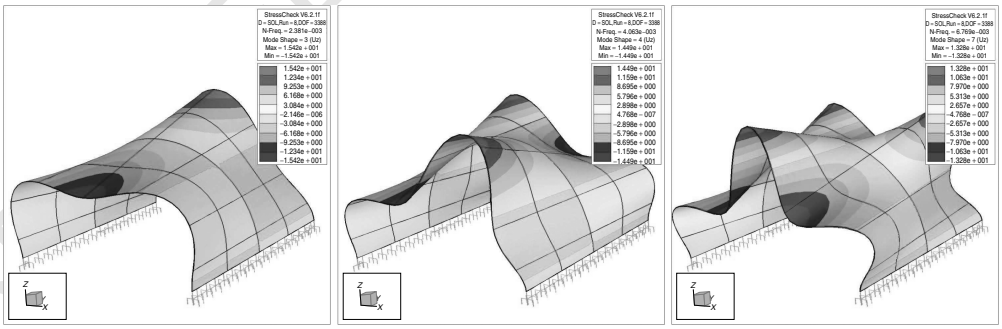

Figure 15. Model (c). Vertical components modes 3, 4 and 7 for $\varepsilon = 0.0025$. A color version of this image is available at http://www.mrw.interscience.wiley.com/ecm

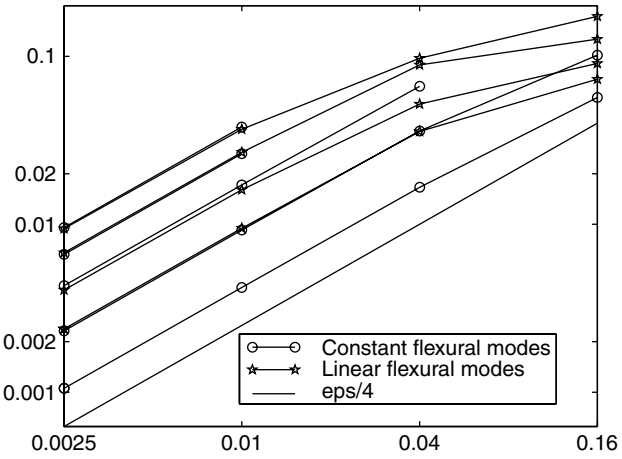

Figure 16. Model (c). Eigen-frequencies versus ε in log–log scale. A color version of this image is available at http://www.mrw.interscience.wiley.com/ecm

6.4.3 Thin element eigen-frequency computations

We present in Tables 2–4 the computation of the first eigen-frequency of the shell Ω^ε in families (a) and (b) for a moderate thickness ($\varepsilon = 0.02$) and a small thickness ($\varepsilon = 0.00125$) and for family (c) for a moderate thickness ($\varepsilon = 0.04$) and a small thickness ($\varepsilon = 0.0025$), respectively, for a moderate thickness ($\varepsilon = 0.04$) and a small thickness ($\varepsilon = 0.0025$). The degree q is the degree in the transverse direction (according to Section 6.1.3 there is *one layer of elements*). We notice that, for an accuracy of 0.01% and $\varepsilon = 0.02$, the quadratic kinematics is not sufficient, whereas it is for $\varepsilon = 0.00125$. No locking is visible there. In fact, the convergence of the q-models *to their own limits* is more rapid for $\varepsilon = 0.02$.

6.5 Conclusion

It is worthwhile to point out that the most serious difficulties we have encountered in computing all these models occurred for $\varepsilon = 0.00125$ and model (b) – the sensitive shell: Indeed, in that case, when $\varepsilon \to 0$, the first eigenmode is more and more oscillating, and the difficulties of approximation are those of a high-frequency analysis. It is also visible from Tables 3 and 4 that the computational effort is lower for the cylinder than for the sensitive shell, for an even better quality of approximation.

It seems that, considering the high performance of the p-version approximation in a smooth midsurface (for each fixed ε and fixed degree q we have an exponential convergence in p), the locking effects can be equilibrated by slightly increasing the degree p as ε decreases.

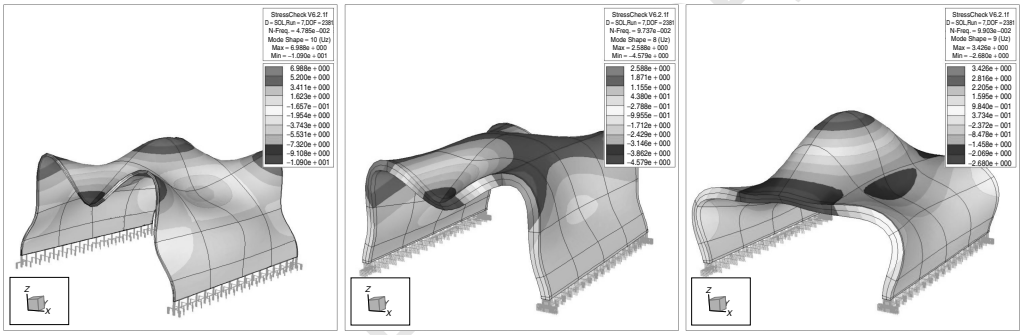

Figure 17. Model (c). First nonflexural modes for $\varepsilon = 0.01$ and $\varepsilon = 0.04$. A color version of this image is available at http://www.mrw.interscience.wiley.com/ecm

Table 2. Thin element computations for the first eigen-frequency of model (a).

p	$\varepsilon = 0.02$ and $q = 2$			$\varepsilon = 0.02$ and $q = 3$			$\varepsilon = 0.00125$ and $q = 2$		
	DOF	e-freq.	% err.	DOF	e-freq.	% err.	DOF	e-freq.	% err.
1	297	0.2271659	37.967	396	0.2264908	37.557	297	0.2055351	36.437
2	729	0.1694894	2.938	828	0.1694269	2.900	729	0.1560694	3.601
3	1209	0.1652870	0.386	1308	0.1652544	0.366	1209	0.1537315	2.049
4	2145	0.1648290	0.108	2244	0.1648001	0.090	2145	0.1517604	0.741
5	3321	0.1646992	0.029	3636	0.1646693	0.011	3321	0.1508741	0.152
6	4737	0.1646859	0.021	5268	0.1646555	0.002	4737	0.1506988	0.036
7	6393	0.1646849	0.020	7140	0.1646544	0.002	6393	0.1506544	0.007
8	8289	0.1646849	0.020	9252	0.1646543	0.002	8289	0.1506447	0.000

REVISED PROOFS

Table 3. Thin element computations for the first eigen-frequency of model (b).

p	$\varepsilon = 0.02$ and $q = 2$			$\varepsilon = 0.02$ and $q = 3$			$\varepsilon = 0.00125$ and $q = 2$		
	DOF	e-freq.	% err.	DOF	e-freq.	% err.	DOF	e-freq.	% err.
1	864	0.0597700	89.68	1152	0.0595287	88.91	864	0.0462144	932.2
2	2016	0.0326855	3.73	2304	0.0326036	3.46	2016	0.0129819	189.9
3	3168	0.0318094	0.95	3456	0.0317325	0.70	3168	0.0064504	44.06
4	5472	0.0316330	0.39	5760	0.0315684	0.18	5472	0.0047030	5.04
5	8352	0.0316071	0.30	9216	0.0315319	0.06	8352	0.0045085	0.69
6	11 808	0.0316011	0.28	13 248	0.0315223	0.03	11 808	0.0044800	0.06
7	15 840	0.0316000	0.28	17 856	0.0315200	0.03	15 840	0.0044780	0.01
8	20 448	0.0315998	0.28	23 040	0.0315195	0.03	20 448	0.0044779	0.01

Table 4. Thin element computations for the first eigen-frequency of model (c).

p	$\varepsilon = 0.04$ and $q = 2$			$\varepsilon = 0.04$ and $q = 3$			$\varepsilon = 0.0025$ and $q = 2$		
	DOF	e-freq.	% err.	DOF	e-freq.	% err.	DOF	e-freq.	% err.
1	567	0.0514951	210.2	756	0.0510683	208.7	567	0.0397025	3666.
2	1311	0.0207290	24.9	1500	0.0206911	24.7	1311	0.0079356	653.1
3	2055	0.0167879	1.2	2244	0.0167596	0.98	2055	0.0011505	9.188
4	3531	0.0166354	0.02	3720	0.0166091	0.08	3531	0.0010578	0.395
5	5367	0.0166293	0.02	5928	0.0166011	0.03	5367	0.0010548	0.108
6	7563	0.0166289	0.02	8496	0.0166004	0.02	7563	0.0010541	0.045
7	10 119	0.0166288	0.02	11 424	0.0166003	0.02	10 119	0.0010538	0.012
8	13 035	0.0166288	0.02	14 712	0.0166002	0.02	13 035	0.0010537	0.002

Of course, there exist many strategies to overcome locking in different situations: Let us quote here (Bathe and Brezzi, 1985; Brezzi, Bathe and Fortin, 1989; Arnold and Brezzi, 1997) as 'early references', on mixed methods, which result in a relaxation of the zero-membrane-energy constraint. These methods are addressed in other chapters of the Encyclopedia.

ACKNOWLEDGMENTS

The authors wish to thank Domique Chapelle (INRIA) for stimulating discussions, Martin Costabel and Yvon Lafranche (`fig4tex` macro package for drawing figures, see `http://perso.univ-rennes1.fr/yvon.lafranche/fig4tex/ReferenceGuide.html`) (University of Rennes) for their valuable technical support.

NOTES

[1] We have a similar situation with plates, where the solution $\mathbf{u}^{\varepsilon,\mathsf{KL}}$ of the Kirchhoff–Love model gives back the first generating terms on the asymptotics of $\mathbf{u}^{\varepsilon}$, cf. Theorem 2.

[2] The actual Kirchhoff–Love displacement (satisfying $e_{i3} = 0$) is slightly different, containing an extra quadratic surface term.

[3] The complementing operator $\mathbf{C}$ defined in (45) for plates satisfies $\mathbf{CU}^{1,1,0}_{\mathsf{KL}} = \mathbf{U}^{1,1,2}_{\mathsf{K}}$.

[4] These norms are those of the domains of the fractional powers A^s of the Sturm–Liouville operator $\mathsf{A}\colon \zeta \mapsto \partial_x((1-x^2)\partial_x\zeta)$ on the interval $(-1, 1)$. Such an approach is now a standard tool in the p-version analysis.

[5] Of course, different mesh designs are possible on thin domains. If one wants to capture boundary layer terms with an exponential rate of convergence, a h-p refinement should be implemented near the edges of Ω^{ε}, Dauge and Schwab (2002).

[6] Here, for ease of presentation, we use the numbering system for plate models displayed in Table 1, where we also provide the number d_j of fields in each direction for *bending models*, that is, for which the surface components are odd and the normal component even in x_3.

REFERENCES

Actis RL, Szabo BA and Schwab C. Hierarchic models for laminated plates and shells. *Comput. Methods Appl. Mech. Eng.* 1999; **172**(1–4):79–107.

REVISED PAGE PROOFS

Agmon S, Douglis A and Nirenberg L. Estimates near the boundary for solutions of elliptic partial differential equations satisfying general boundary conditions II. *Commun. Pure Appl. Math.* 1964; **17**:35–92.

Agratov II and Nazarov SA. Asymptotic analysis of problems in junctions of domains of different limit dimension. An elastic body pierced by thin rods. *J. Math. Sci. (New York)* 2000; **102**(5):4349–4387.

Akian JL and Sanchez-Palencia E. Approximation de coquesélastiques minces par facettes planes: Phénoméne de blocage membranaire. *C. R. Acad. Sci. Paris, Sér. I* 1992; **315**:363–369.

Andreoiu G and Faou E. Complete asymptotics for shallow shells. *Asymptot. Anal.* 2001; **25**(3–4):239–270.

Anicic S and Léger A. Formulation bidimensionnelle exacte du modèle de coque 3D de Kirchhoff-Love. *C. R. Acad. Sci. Paris, Sér. I Math.* 1999; **329**(8):741–746.

Arnold DN and Brezzi F. Locking-free finite element methods for shells. *Math. Comput.* 1997; **66**(217):1–14.

Arnold DN and Falk RS. The boundary layer for the Reissner-Mindlin plate model. *SIAM J. Math. Anal.* 1990b; **21**(2):281–312.

Arnold DN and Falk RS. Asymptotic analysis of the boundary layer for the Reissner-Mindlin plate model. *SIAM J. Math. Anal.* 1996; **27**(2):486–514.

Avalishvili M and Gordeziani D. Investigation of two-dimensional models of elastic prismatic shell. *Georgian Math. J.* 2003; **10**(1):17–36.

Babuška I and Li L. Hierarchic modeling of plates. *Comput. Struct.* 1991; **40**:419–430.

Babuška I and Li L. The h-p-version of the finite element method in the plate modelling problem. *Commun. Appl. Numer. Methods* 1992a; **8**:17–26.

Babuška I and Li L. The problem of plate modelling: Theoretical and computational results. *Comput. Methods Appl. Mech. Eng.* 1992b; **100**:249–273.

Babuška I and Pitkäranta J. The plate paradox for hard and soft simple support. *SIAM J. Math. Anal.* 1990; **21**:551–576.

Babuška I and Suri M. On locking and robustness in the finite element method. *SIAM J. Numer. Anal.* 1992; **29**:1261–1293.

Babuška I, d'Harcourt JM and Schwab C. *Optimal Shear Correction Factors in Hierarchic Plate Modelling*, Technical Note BN-1129. Institute for Physical Science and Technology, University of Maryland: College Park, 1991a.

Babuška I, Szabó BA and Actis RL. Hierarchic models for laminated composites. *Int. J. Numer. Methods Eng.* 1992; **33**(3):503–535.

Bathe KJ and Brezzi F. On the convergence of a four node plate bending element based on Mindlin-Reissner plate theory and a mixed interpolation. In *The Mathematics of Finite Elements and Applications*, vol. 5, Whiteman JR (ed.). Academic Press: London, 1985; 491–503.

Bernadou M and Ciarlet PG. Sur l'ellipticité du modèle linéaire de coques de W.T. Koiter. In *Computing Methods in Applied Sciences and Engineering*, Lecture Notes in Economics and Mathematical Systems, vol. 134, Glowinski R and Lions JL (eds). Springer-Verlag: Heidelberg, 1976; 89–136.

Bischoff M and Ramm E. On the physical significance of higher order kinematic and static variables in a three-dimensional shell formulation. *Int. J. Solids Struct.* 2000; **37**:6933–6960.

Brezzi F, Bathe K-J and Fortin M. Mixed-interpolated elements for Reissner-Mindlin plates. *Int. J. Numer. Methods Eng.* 1989; **28**(8):1787–1801.

Budiansky B and Sanders JL. On the "best" first-order linear shell theory. In *Progress in Applied Mechanics*, Anniversary Volume, Prager W (ed.). Macmillan: New York, 1967; 129–140.

Chapelle D and Bathe K-J. The mathematical shell model underlying general shell elements. *Int. J. Numer. Methods Eng.* 2000; **48**(2):289–313.

Chapelle D and Bathe KJ. *The Finite Element Analysis of Shells – Fundamentals. Computational Fluid and Solid Mechanics*. Springer: Berlin, 2003.

Chapelle D, Ferent A and Bathe K-J. 3D-shell elements and their underlying mathematical model. *Math. Models Methods Appl. Sci.* 2004; **14**(1):105–142.

Chapelle D, Ferent A and Le Tallec P. The treatment of "pinching locking" in 3D-shell elements. *M2AN Math. Modell. Numer. Anal.* 2003; **37**(1):143–158.

Ciarlet PG. *Mathematical Elasticity*, *Vol. I, Three-Dimensional Elasticity*. North Holland: Amsterdam, 1988.

Ciarlet PG. *Mathematical Elasticity*, *Vol. II, Theory of Plates*. North Holland: Amsterdam, 1997.

Ciarlet PG. *Mathematical Elasticity*, vol. III. North Holland: Amsterdam, 2000.

Ciarlet PG and Destuynder P. A justification of the two-dimensional plate model. *J. Méc.* 1979a; **18**:315–344.

Ciarlet PG and Kesavan S. Two-dimensional approximation of three-dimensional eigenvalue problems in plate theory. *Comput. Methods Appl. Mech. Eng.* 1981; **26**:149–172.

Ciarlet PG and Lods V. Asymptotic analysis of linearly elastic shells. I. Justification of membrane shell equations. *Arch. Ration. Mech. Anal.* 1996a; **136**:119–161.

Ciarlet PG and Lods V. Asymptotic analysis of linearly elastic shells. III. Justification of Koiter's shell equations. *Arch. Ration. Mech. Anal.* 1996b; **136**:191–200.

Ciarlet PG, Lods V and Miara B. Asymptotic analysis of linearly elastic shells. II. Justification of flexural shell equations. *Arch. Ration. Mech. Anal.* 1996; **136**:163–190.

Ciarlet PG and Paumier JC. A justification of the Marguerre-von-Kármán equations. *Comput. Mech.* 1986; **1**:177–202.

Dauge M and Faou E. *Koiter Estimate Revisited*. Research report, INRIA, 2004; to appear.

Dauge M and Gruais I. Asymptotics of arbitrary order for a thin elastic clamped plate. I: Optimal error estimates. *Asymptot. Anal.* 1996; **13**:167–197.

Dauge M and Gruais I. Asymptotics of arbitrary order for a thin elastic clamped plate. II: Analysis of the boundary layer terms. *Asymptot. Anal.* 1998a; **16**:99–124.

Dauge M and Schwab C. '*hp*-FEM for three-dimensional elastic plates. *M2AN Math. Model. Numer. Anal.* 2002; **36**(4):597–630.

Dauge M and Yosibash Z. Boundary Layer Realization in Thin Elastic 3-D Domains and 2-D Hierarchic Plate Models. *Int. J. Solids Struct.* 2000; **37**:2443–2471.

REVISED PAGE PROOFS

Dauge M and Yosibash Z. Eigen-frequencies in thin elastic 3-D domains and Reissner-Mindlin plate models. *Math. Methods Appl. Sci.* 2002; **25**(1):21–48.

Dauge M, Gruais I and Rössle A. The influence of lateral boundary conditions on the asymptotics in thin elastic plates. *SIAM J. Math. Anal.* 1999/2000; **31**(2):305–345.

Dauge M, Djurdjevic I, Faou E and Rössle A. Eigenmodes asymptotic in thin elastic plates. *J. Math. Pures Appl.* 1999; **78**:925–964.

Düster A, Bröker H and Rank E. The *p*-version of the finite element method for three-dimensional curved thin walled structures. *Int. J. Numer. Methods Eng.* 2001; **52**:673–703.

Faou E. Développements asymptotiques dans les coques elliptiques:équations tridimensionnelles linéarisées. *C. R. Acad. Sci. Paris, Sér. I Math.* 2001a; **333**(4):389–394.

Faou E. Développements asymptotiques dans les coques elliptiques: modèle de Koiter. *C. R. Acad. Sci. Paris, Sér. I Math.* 2001b; **333**(2):139–143.

Faou E. Elasticity on a thin shell: Formal series solution. *Asymptot. Anal.* 2002; **31**:317–361.

Faou E. *Multiscale Expansions for Linear Clamped Elliptic Shells*. Research Report RR-4956, INRIA; *Commun. Partial Diff. Equations*, 2004, to appear.

Friedrichs KO and Dressler RF. A boundary-layer theory for elastic plates. *Commun. Pure Appl. Math.* 1961; **14**:1–33.

Genevey K. A regularity result for a linear membrane shell problem. *RAIRO Modéll. Math. Anal. Numér.* 1996; **30**(4):467–488.

Gerdes K, Matache AM and Schwab C. Analysis of membrane locking in *hp* FEM for a cylindrical shell. *ZAMM Z. Angew. Math. Mech.* 1998; **78**(10):663–686.

Gol'denveizer AL. Derivation of an approximate theory of bending of a plate by the method of asymptotic integration of the equations of the theory of elasticity. *Prikl. Matem. Mekhan* 1962; **26**(4):668–686, English translation *J. Appl. Math. Mech.* 1964; 1000–1025.

Gregory RD and Wan FY. Decaying states of plane strain in a semi-infinite strip and boundary conditions for plate theory. *J. Elastic.* 1984; **14**:27–64.

Havu V and Pitkäranta J. Analysis of a bilinear finite element for shallow shells. I. Approximation of inextensional deformations. *Math. Comput.* 2002; **71**(239):923–943.

Havu V and Pitkäranta J. Analysis of a bilinear finite element for shallow shells. II. Consistency error. *Math. Comput.* 2003; **72**(244):1635–1653.

Il'in AM. *Matching of Asymptotic Expansions of Solutions of Boundary Value Problems*, vol. 102 of *Translations of Mathematical Monographs*. American Mathematical Society: Providence, 1992.

Irago H and Viaño JM. Error estimation in the Bernoulli-Navier model for elastic rods. *Asymptot. Anal.* 1999; **21**(1):71–87.

John F. Refined interior equations for thin elastic shells. *Commun. Pure Appl. Math.* 1971; **24**:583–615.

Koiter WT. A consistent first approximation in the general theory of thin elastic shells. In *Proceedings of IUTAM Symposium on the Theory on Thin Elastic Shells, August 1959*, Delft, 1960; 12–32.

Koiter WT. On the foundations of the linear theory of thin elastic shells: I. *Proc. Kon. Ned. Akad. Wetensch., Ser. B* 1970a; **73**:169–182.

Koiter WT. On the foundations of the linear theory of thin elastic shells: II. *Proc. Kon. Ned. Akad. Wetensch., Ser. B* 1970b; **73**:183–195.

Koiter WT and Simmonds JG. Foundations of shell theory. *Theoretical and Applied Mechanics*, Springer: Berlin, 1973; 150–176; *Proceedings of Thirteenth International Congress*, Moscow University, Moscow, 1972.

Kondrat'ev VA. Boundary-value problems for elliptic equations in domains with conical or angular points. *Trans. Moscow Math. Soc.* 1967; **16**:227–313.

Kozlov V, Maz'ya V and Movchan A. *Asymptotic Analysis of Fields in Multi-Structures*, Oxford Mathematical Monographs. The Clarendon Press Oxford University Press, Oxford Science Publications: New York, 1999.

Lods V and Mardare C. A justification of linear Koiter and Naghdi's models for totally clamped shell. *Asymptot. Anal.* 2002; **31**(3–4):189–210.

Love AEH. *A Treatise on the Mathematical Theory of Elasticity* (4th edn). Dover Publications: New York, 1944.

Mardare C. Asymptotic analysis of linearly elastic shells: error estimates in the membrane case. *Asymptot. Anal.* 1998a; **17**:31–51.

Maz'ya VG, Nazarov SA and Plamenevskii BA. *Asymptotische Theorie elliptischer Randwertaufgaben in singulär gestörten Gebieten II. Mathematische Monographien*, Band 83. Akademie Verlag: Berlin, 1991b.

Mindlin RD. Influence of rotatory inertia and shear on flexural motions of isotropic elastic plates. *J. Appl. Mech.* 1951; **18**:31–38.

Naghdi PM. Foundations of elastic shell theory. *Progress in Solid Mechanics*, vol. 4. North Holland: Amsterdam, 1963; 1–90.

Naghdi PM. The theory of shells and plates. In *Handbuch der Physik*, vol. VI a/2, Flügge S and Truesdell C (eds). Springer-Verlag: Berlin, 1972; 425–640.

Nazarov SA. Two-term asymptotics of solutions of spectral problems with singular perturbation. *Math. USSR Sbornik* 1991c; **69**(2):307–340.

Nazarov SA. Justification of the asymptotic theory of thin rods. Integral and pointwise estimates. *J. Math. Sci* 1999; **97**(4):4245–4279.

Nazarov SA. Asymptotic analysis of an arbitrarily anisotropic plate of variable thickness (a shallow shell). *Math. Sbornik* 2000a; **191**(7):129–159.

Nazarov SA. On the asymptotics of the spectrum of a problem in elasticity theory for a thin plate. *Sibirsk. Mat. Zh* 2000b; **41**(4):iii, 895–912.

Nazarov SA and Zorin IS. Edge effect in the bending of a thin three-dimensional plate. *Prikl. Matem. Mekhan* 1989; **53**(4):642–650. English translation *J. Appl. Math. Mech.* 1989; 500–507.

Novozhilov VV. *Thin Shell Theory*. Walters-Noordhoff Publishing: Groningen, 1959.

REVISED PAGE PROOFS

Oleinik OA, Shamaev AS and Yosifian GA. *Mathematical Problems in Elasticity and Homogenization. Studies in Mathematics and Its Applications*. North Holland: Amsterdam, 1992.

Paumier JC. Existence and convergence of the expansion in the asymptotic theory of elastic thin plates. *Math. Modell. Numer. Anal.* 1990; **25**(3):371–391.

Paumier J-C and Raoult A Asymptotic consistency of the polynomial approximation in the linearized plate theory. Application to the Reissner-Mindlin model. In *Élasticité, Viscoélasticité et Contrôle Optimal (Lyon, 1995)*, vol. 2 of ESAIM Proc., Society of Mathematical Applied Industry, Paris, 1997; 203–213.

Pitkaranta J. The problem of membrane locking in finite element analysis of cylindrical shells. *Numer. Math.* 1992; **61**:523–542.

Pitkäranta J and Sanchez-Palencia E. On the asymptotic behaviour of sensitive shells with small thickness. *C. R. Acad. Sci. Paris, Sér. II* 1997; **325**:127–134.

Pitkäranta J, Matache A-M and Schwab C. Fourier mode analysis of layers in shallow shell deformations. *Comput. Methods Appl. Mech. Eng.* 2001; **190**:2943–2975.

Rössle A, Bischoff M, Wendland W and Ramm E. On the mathematical foundation of the (1,1,2)-plate model. *Int. J. Solids Struct.* 1999; **36**(14):2143–2168.

Sanchez-Hubert J and Sanchez-Palencia E. *Coques élastiques minces. Propriétés asymptotiques, Recherches en mathématiques appliquées*. Masson: Paris, 1997.

Schwab C. A-posteriori modeling error estimation for hierarchic plate models. *Numer. Math.* 1996; **74**(2):221–259.

Schwab C and Suri M. The p and hp versions of the finite element method for problems with boundary layers. *Math. Comput.* 1996; **65**:1403–1429.

Schwab C and Wright S. Boundary layer approximation in hierarchical beam and plate models. *J. Elastic.* 1995; **38**:1–40.

Schwab C, Suri M and Xenophontos C. The hp finite element method for problems in mechanics with boundary layers. *Comput. Methods Appl. Mech. Eng.* 1998; **157**:311–333.

Scott LR and Vogelius M. Conforming finite element methods for incompressible and nearly incompressible continua. *Large-Scale Computations in Fluid Mechanics*, Part 2 (La Jolla, 1983), vol. 22 of *Lectures in Applied Mathematics*, American Mathematical Society: Providence, 1985; 221–244.

Stein E and Ohnimus S. Coupled model- and solution-adaptivity in the finite-element method. *Comput. Methods Appl. Mech. Engrg.* 1997; **150**(1–4):327–350.

Stoker JJ. *Differential Geometry. Pure and Applied Mathematics*, vol. XX. Interscience Publishers, John Wiley & Sons: New York-London-Sydney, 1969.

Suri M. The *p* and *hp* finite element method for problems on thin domains. *J. Comput. Appl. Math.* 2001; **128**(1–2):235–260.

Suri M, Babuška I and Schwab C. Locking effects in the finite element approximation of plate models. *Math. Comput.* 1995; **64**:461–482.

Szabó B and Babuška I. *Finite Element Analysis*. Willey: New York, 1991.

Szabó B and Sahrmann GJ. Hierarchic plate and shell models based on p-extension. *Int. J. Numer. Methods Eng.* 1988; **26**:1855–1881.

Vekua IN. On a method of computing prismatic shells. *Akad. Nauk Gruzin. SSR. Trudy Tbiliss. Mat. Inst. Razmadze* 1955; **21**:191–259.

Vekua IN. Theory of thin shallow shells of variable thickness. *Akad. Nauk Gruzin. SSR Trudy Tbiliss. Mat. Inst. Razmadze* 1965; **30**:3–103.

Vekua IN. *Shell Theory: General Methods of Construction. Monographs, Advanced Texts and Surveys in Pure and Applied Mathematics*, 25. Pitman (Advanced Publishing Program): Boston, 1985.

Vishik MI and Lyusternik LA. Regular degeneration and boundary layers for linear differential equations with small parameter. *Am. Math. Soc. Transl.* 1962; **2**(20):239–364.

Vogelius M and Babuška I. On a dimensional reduction method. III. A posteriori error estimation and an adaptive approach. *Math. Comput.* 1981a; **37**(156):361–384.

Vogelius M and Babuška I. On a dimensional reduction method. II. Some approximation-theoretic results. *Math. Comput.* 1981b; **37**(155):47–68.

Vogelius M and Babuška I. On a dimensional reduction method. I. The optimal selection of basis functions. *Math. Comput.* 1981c; **37**(155):31–46.

FURTHER READING

Agmon S, Douglis A and Nirenberg L. Estimates near the boundary for solutions of elliptic partial differential equations satisfying general boundary conditions I. *Commun. Pure Appl. Math.* 1959; **12**:623–727.

Aganovic C and Tutek Z. A justification of the one-dimensional model of an elastic beam. *Math. Methods Appl. Sci.* 1986; **8**:1–14.

Agranovich MS and Vishik MI. Elliptic problems with a parameter and parabolic problems of general type. *Russian Math. Surv.* 1964; **19**:53–157.

Alessandrini SM, Arnold DN, Falk RS and Madureira AL. Derivation and justification of plate models by variational methods. In *Proceeding of the Summer Seminar of the Canadian Mathematical Society on "Plates and Shells: From Mathematical Theory to Engineering Practice"*, CRM Proceeding and Lecture Notes, Quebec, 1996.

Andreoiu G. Comparaison entre modèles bidimensionnels de coques faiblement courbées. *C. R. Acad. Sci. Paris, Sér. I* 1999b; **329**:339–342.

Andreoiu G. *Analyse des coques faiblement courbées*. Thèse de doctorat, Université Pierre et Marie Curie, Paris, 1999a.

Andreoiu G, Dauge M and Faou E. Développements asymptotiques complets pour des coques faiblement courbées encastrées ou libres. *C. R. Acad. Sci. Paris, Sér. I Math.* 2000; **330**(6):523–528.

Argatov II and Nazarov SA. Asymptotic solution to the problem of an elastic body lying on several small supports. *J. Appl. Math. Mech.* 1994; **58**(2):303–311.

Arnold DN and Falk RS. Edge effects in the Reissner-Mindlin plate model. In *Analytical and Computational Models for Shells*,

REVISED PAGE PROOFS

Noor AK, Belytschko T and Simo J (eds). American Society of Mechanical Engineers: New York, 1990a; 71–90.

Guo B and Babuška I. Regularity of the solutions for elliptic problems on nonsmooth domains in $\mathbf{R}^3$. I. Countably normed spaces on polyhedral domains. *Proc. R. Soc. Edinburgh, Sect. A* 1997b; **127**(1):77–126.

Guo B and Babuška I. Regularity of the solutions for elliptic problems on nonsmooth domains in $\mathbf{R}^3$. II. Regularity in neighbourhoods of edges. *Proc. R. Soc. Edinburgh, Sect. A* 1997a; **127**(3):517–545.

Babuška I, d'Harcourt JM and Schwab C. Optimal shear correction factors in hierarchic plate modelling. *Math. Modell. Sci. Comput.* 1991b; **1**:1–30.

Babuška I and Prager M. Reissnerian algorithms in the theory of elasticity. *Bull. Acad. Polon. Sci. Sér. Sci. Math. Astr. Phys.* 1960; **8**:411–417.

Basar Y and Kräzig WB. A consistent shell theory for finite deformations. *Acta Mech.* 1988; **76**:73–87.

Bauer L and Reiss EL. Nonlinear buckling of rectangular plates. *SIAM J. Appl. Math.* 1965; **13**:603–626.

Berdichevskiĭ VL. *Variatsionnye printsipy mekhaniki sploshnoĭsredy (Variational Principles of Continuum Mechanics)*, Nauka, Moscow, 1983.

Berger MS. On the von Kármán equations and the buckling of a thin elastic plate. I. The clamped plate. *Commun. Pure Appl. Math.* 1967; **20**:687–719.

Berger MS and Fife PC. On the von Kármán equations and the buckling of a thin elastic plate. II. Plate with general edge conditions. *Commun. Pure Appl. Math.* 1968; **21**:227–241.

Bermudez A and Viaño JM. Une justification deséquations de la thermoélasticité des poutres à section variable par des méthodes asymptotiques. *RAIRO Anal. Numér.* 1984; **18**:347–376.

Bernadou M. Variational formulation and approximation of junctions between shells. In *Proceedings, Fifth International Symposium on Numerical Methods in Engineering*, *vol. 18 of Computational Mechanics Publications*, Gruber R, Périaux J and Shaw RP (eds). Springer-Verlag: Heidelberg, 1989; 407–414.

Bernadou M. *Méthodes d'Eléments Finis pour les Problèmes de Coques Minces*. Masson: Paris, 1994.

Bernadou M and Boisserie JM. *The Finite Element Metod in Thin Shell Theory: Application to Arch Dam Simulations*. Birkhäuser: Boston, 1982.

Bernadou M, Fayolle S and Léné F. Numerical Analysis of junctions between plates. *Comput. Math. Appl. Mech. Eng.* 1989; **74**:307–326.

Bernadou M and Lalanne B. Sur l'approximation des coques minces par des méthodes B-splines etéléments finis. In *Tendances Actuelles en Calcul des Structures*, Grellier JP and Campel GM (eds). Pluralis: Paris, 1985; 939–958.

Bernadou M and Oden JT. An existence theorem for a class of nonlinear shallow shell theories. *J. Math. Pures Appl.* 1981; **60**:285–308.

Bielski W and Telega JJ. On existence of solutions for geometrically nonlinear shells and plates. *Z. Angew. Math. Mech.* 1988; **68**:155–157.

Blouza A and Le Dret H. Sur le lemme du mouvement rigide. *C. R. Acad. Sci. Paris, Sér. I* 1994b; **319**:1015–1020.

Blouza A and Le Dret H. Existence et unicité pour le modèle de Koiter pour une coque peu régulière. *C. R. Acad. Sci. Paris, Sér. I* 1994a; **319**:1127–1132.

Bolley P, Camus J and Dauge M. Régularité Gevrey pour le problème de Dirichlet dans des domaines à singularités coniques. *Commun. Partial Diff. Equations* 1985; **10**(2):391–432.

Brezzi F and Fortin M. Numerical approximation of Mindlin-Reissner plates. *Math. Comput.* 1986; **47**:151–158.

Busse S, Ciarlet PG and Miara B. Justification d'un modele lineaire bi-dimensionnel de coques "faiblement courbees" en coordonnees curvilignes. *RAIRO Modéll. Math. Anal. Numer.* 1997; **31**(3):409–434.

Chen C. *Asymptotic Convergence Rates for the Kirchhoff Plate Model*. PhD thesis, Pennsylvania State University, 1995.

Ciarlet PG. *Elasticité tridimensionnelle. Recherches en mathématiques appliquées*. Masson: Paris, 1986.

Ciarlet PG. *Plates and Junctions in Elastic Multi-Structures: An Asymptotic Analysis. R.M.A*, vol. 14. Masson and Springer-Verlag: Paris and Heidelberg, 1990.

Ciarlet PG and Destuynder P. A justification of a nonlinear model in plate theory. *Comput. Methods Appl. Mech. Eng.* 1979b; **17–18**:227–258.

Ciarlet PG and Lods V. Ellipticité des équations membranaires d'une coque uniformément elliptique. *C. R. Acad. Sci. Paris, Sér. I* 1994c; **318**:195–200.

Ciarlet PG and Lods V. Analyse asymptotique des coques linéairement élastiques. I. Coques "membranaires". *C. R. Acad. Sci. Paris, Sér. I* 1994a; **318**:863–868.

Ciarlet PG, Lods V and Miara B. Analyse asymptotique des coques linéairementélastiques. II. Coques en "en flexion". *C. R. Acad. Sci. Paris, Sér. I* 1994; **319**:95–100.

Ciarlet PG and Lods V. Analyse asymptotique des coques linéairement élastiques. III. Une justification du modèle de W. T. Koiter. *C. R. Acad. Sci. Paris, Sér. I* 1994b; **319**:299–304.

Ciarlet PG and Miara B. Justification d'un modèle bi-dimensionnel de coque "peu profonde" enélasticité linéarisée. *C. R. Acad. Sci. Paris, Sér. I* 1990; **311**:571–574.

Ciarlet PG and Miara B. Une démonstration simple de l'ellipticité des modèles de coques de W. T. Koiter et de P. M. Naghdi. *C. R. Acad. Sci. Paris, Sér. I* 1991; **312**:411–415.

Ciarlet PG and Miara B. Justification of the two-dimensional equations of a linearly elastic shallow shell. *Commun. Pure Appl. Math.* 1992a; **45**(3):327–360.

Ciarlet PG and Miara B. On the ellipticity of linear shell models. *Z. Angew. Math. Phys.* 1992c; **43**:243–253.

Ciarlet PG and Miara B. Justification of the two-dimensional equations of a linearly elastic shallow shell. *Commun. Pure Appl. Math.* 1992b; **45**:327–360.

Ciarlet PG and Sanchez-Palencia E. Un théorème d'existence et d'unicité pour les équations de coques membranaires. *C. R. Acad. Sci. Paris, Sér. I* 1993; **317**:801–805.

Costabel M and Dauge M. General Edge Asymptotics of Solutions of Second Order Elliptic Boundary Value Problems I. *Proc. R. Soc. Edinburgh* 1993b; **123A**:109–155.

REVISED PAGE PROOFS

Costabel M and Dauge M. General Edge Asymptotics of Solutions of Second Order Elliptic Boundary Value Problems II. *Proc. R. Soc. Edinburgh* 1993c; **123A**:157–184.

Costabel M and Dauge M. Edge asymptotics on a skew cylinder: complex variable form. *Partial Differential Equations*, Banach Center Publications, vol. 27. Warszawa: Poland, 1992; 81–90.

Costabel M and Dauge M. Construction of corner singularities for Agmon-Douglis-Nirenberg elliptic systems. *Math. Nachr.* 1993a; **162**:209–237.

Costabel M and Dauge M. Stable asymptotics for elliptic systems on plane domains with corners. *Commun. Partial Diff. Equations* n° 1994; **9 & 10**:1677–1726.

Costabel M and Dauge M. Computation of corner singularities in linear elasticity. In *Boundary Value Problems and Integral Equations in Nonsmooth Domains*, Lecture Notes in Pure and Applied Mathematics, vol. 167, Costabel M, Dauge M and Nicaise S (eds). Marcel Dekker: New York, 1995; 59–68.

Coutris N. Théorème d'existence et d'unicité pour un problème de coque élastique dans le cas d'un modèle linéaire de Naghdi. *RAIRO Anal. Numér.* 1978; **12**:51–57.

Damlamian A and Vogelius M. Homogenization limits of the equations of elasticity in thin domains. *SIAM J. Math. Anal.* 1987; **18**(2):435–451.

Dauge M and Gruais I. *Complete Asymptotics and Optimal Error Estimates in the Kirchhoff-Love Problem*. Preprint 95-06, Université de Rennes 1, 1995a.

Dauge M and Gruais I. Edge layers in thin elastic plates. *Comput. Methods Appl. Mech. Eng.* 1998b; **157**:335–347.

Dauge M and Gruais I. Développement asymptotique d'ordre arbitraire pour une plaque élastique mince encastrée. *C. R. Acad. Sci. Paris, Sér. I* 1995b; **321**:375–380.

Dautray R and Lions J-L. *Analyse Mathématique et Calcul Numérique pour les Sciences et les Techniques*. Tome 1. Masson: Paris, 1984.

Dauge M. *Elliptic Boundary Value Problems in Corner Domains – Smoothness and Asymptotics of Solutions*, Lecture Notes in Mathematics, vol. 1341. Springer-Verlag: Berlin, 1988.

Dauge M, Djurdjevic I and Rössle A. Higher order bending and membrane responses of thin linearly elastic plates. *C. R. Acad. Sci. Paris, Sér. I* 1998b; **326**:519–524.

Dauge M, Djurdjevic I and Rössle A. Full Asymptotic Expansions for Thin Elastic Free Plates. *C. R. Acad. Sci. Paris, Sér. I* 1998a; **326**:1243–1248.

de Figueiredo I and Trabucho L. A Galerkin approximation for linear elastic shallow shells. *Comput. Mech.* 1992; **10**:107–119.

Delfour MC and Zolésio JP. Differential equations for linear shells: Comparison between intrinsic and classical models. *Adv. Math. Sci.* 1997; **11**:42–144.

Destuynder P. *Sur une Justification des Modèles de Plaques et de Coques par les Méthodes Asymptotiques*. Thèse d'Etat, Université Pierre et Marie Curie, Paris, 1980.

Destuynder P. Comparaison entre les modèles tridimensionnels et bidimensionnels de plaques enélasticité. *RAIRO Anal. Numér.* 1981; **15**:331–369.

Destuynder P. A classification of thin shell theories. *Acta Appl. Math.* 1985; **4**:15–63.

Destuynder P. *Une théorie asymptotique des plaques minces enélasticité linéaire*. Masson: Paris, 1986.

Destuynder P. *Modélisation des coques minces élastiques. Physique fondamentale et appliquée.* Masson: Paris, 1990.

Dickmen M. *Theory of Thin Elastic Shells*. Pitman: Boston, 1982.

Carmo MP. *Differential Geometry of Curves and Surfaces*. Prentice Hall, 1976.

Carmo MP. *Riemannian Geometry. Mathematics : Theory and Applications*. Birkhäuser: Boston, 1992.

Dunford N and Schwartz JT. *Linear Operators – Part II*. Interscience Publishers: New York, 1963.

Duvaut G and Lions J-L. *Les Inéquations en Mécanique et en Physique*. Dunod: Paris, 1972.

Duvaut G and Lions J-L. Problèmes unilatéraux dans la théorie de la flexion forte des plaques. *J. Méc.* 1974a; **13**:51–74.

Duvaut G and Lions J-L. Problèmes unilatéraux dans la théorie de la flexion forte des plaques. II: le cas d'évolution. *J. Méc.* 1974b; **13**:245–266.

Eckhaus W. Boundary layers in linear elliptic singular perturbations. *SIAM Rev.* 1972; **14**:225–270.

Eckhaus W. *Asymptotic Analysis of Singular Perturbations*. North Holland: Amsterdam, 1979.

Faou E. Élasticité linéarisée tridimensionnelle pour une coque mince: résolution en série formelle en puissances de l'épaisseur. *C. R. Acad. Sci. Paris, Sér. I Math.* 2000b; **330**(5):415–420.

Faou E. *Développements asymptotiques dans les coques linéairement élastiques*. Thèse, Université de Rennes 1, 2000a.

Feigin VI. Elliptic equations in domains with multidimensional singularities of the boundary. *Uspehi-Mat. Nauk.* 1972; **2**:183, 184.

Fichera G. Existence theorems in elasticity. In *Handbuch der Physik*, vol. VIa-2, Flügge S and Truesdell C (eds). Springer-Verlag: Berlin, 1972; 347–389.

Friedrichs KO and Stoker JJ. Buckling of a circular plate beyond the critical thrust. *J. Appl. Mech.* 1942; **9**:A7–A14.

Gol'denveizer AL. *Theory of Elastic Thin Shells*. Pergamon: New York, 1961.

Gol'denveizer AL. The construction of an approximate theory of shells by means of asymptotic integration of elasticity equations. *Prikl. Math. Mekh* 1963; **27**(4):593–608, English translation *J. Appl. Math. Mech.* 1963; 903–924.

Golenveizer AL. The principles of reducing three-dimensional problems of elasticity to two-dimensional problems of the theory of plates and shells. In *Proceedings of the 11th International Congress of Theoretical and Applied Mechanics*, Görtler H (ed.). Springer-Verlag: Berlin, 1964; 306–311.

Gordeziani DG. The solvability of certain boundary value problems for a variant of the theory of thin shells. *Dokl. Akad. Nauk SSSR* 1974b; **215**:1289–1292.

Gordeziani DG. The accuracy of a certain variant of the theory of thin shells. *Dokl. Akad. Nauk SSSR* 1974a; **216**:751–754.

Gruais I. Modélisation de la jonction entre une plaque et une poutre en élasticité linéarisée. *Modéll. Math. Anal. Numér.* 1993b; **27**:77–109.

REVISED PAGE PROOFS

Gruais I. Modeling of the junction between a plate and a rod in nonlinear elasticity. *Asymptot. Anal.* 1993a; **7**:179–194.

John F. Estimates for the derivatives of the stresses in a thin shell and interior shell equations. *Commun. Pure Appl. Math.* 1965; **18**:235–267.

John F. A priori estimates, geometric effects and asymptotic behaviour. *Commun. Pure Appl. Math.* 1975; **81**:1013–1023.

Kato T. *Perturbation Theory for Linear Operators*. Springer-Verlag: Berlin – Heidelberg – New York, 1976.

Kato T. Perturbation theory for nullity, deficiency and other quantities of linear operators. *J. Anal. Math.* 1958; **6**:261–322.

Keller HB, Keller JB and Reiss E. Buckled states of circular plates. *Q. J. Appl. Math.* 1962; **20**:5–65.

Kirchhoff G. Über das Gleichgewicht und die Bewegung einer elastischen Scheibe. *J. Reine Angew. Math.* 1850; **40**:51–58.

Kirchhoff G. *Vorlesungen über Mathematische Physik*. Mechanik: Leipzig, 1876.

Koiter WT. On the nonlinear theory of thin shells. *Proc. Kon. Ned. Akad. Wetensch., Ser. B* 1966; **69**:1–59.

Koiter WT. General theory of shell stability. Thin shell theory. *New Trends and Applications*, vol. 240 of *C. I. S. M. Courses and Lectures*. Springer-Verlag: New York, 1980; 65–87.

Kondrat'ev VA. On estimates of intermediate derivatives by means of moments of the highest derivative. *Proc. Steklov Inst. Math.* 1992; **2**:193–203.

Kondrat'ev VA and Oleinik OA. Boundary-value problems for partial differential equations in non-smooth domains. *Russian Math. Surv.* 1983; **38**:1–86.

Kondrat'ev VA and Oleinik OA. On Korn's Inequalities. *C. R. Acad. Sci. Paris, Sér. I* 1989; **308**:483–487.

Kozlov VA, Maz'ya VG and Movchan AB. Asymptotic analysis of a mixed boundary value problem in a multi-structure. *Asymptot. Anal.* 1994; **8**:105–143.

Kozlov VA, Maz'ya VG and Schwab C. On singularities of solutions of the displacement problem of linear elasticity near the vertex of a cone. *Arch. Ration. Mech. Anal.* 1992; **119**:197–227.

Leino Y and Pitkäranta J. On the membrane locking of *h-p* finite elements in a cylindrical shell problem. *Int. J. Numer. Methods Eng.* 1994; **37**(6):1053–1070.

Lions J-L and Magenes E. *Problèmes aux limites non homogènes et applications.* Dunod: Paris, 1968.

Lions J-L and Sanchez-Palencia E. Problèmes aux limites sensitifs. *C. R. Acad. Sci. Paris, Sér. I* 1994; **319**:1021–1026.

Lods V and Mardare C. Asymptotic justification of the Kirchhoff-Love assumptions for a linearly elastic clamped shell. *J. Elastic.* 2000; **58**(2):105–154.

Lods V and Mardare C. Error estimates between the linearized three-dimensional shell equations and Naghdi's model. *Asymptot. Anal.* 2001; **28**(1):1–30.

Lods V and Mardare C. Justification asymptotique des hypotheses de Kirchhoff-Love pour une coque encastree lineairement elastique. *C. R. Acad. Sci. Paris, Sér. I* 1998; **326**:909–912.

Mardare C. Estimations d'erreur dans l'analyse asymptotique des coques lineairement elastiques. *C. R. Acad. Sci. Paris, Sér. I* 1996; **322**:895–898.

Mardare C. Two-dimensional models of linearly elastic shells: error estimates between their solutions. *Math. Mech. Solids* 1998b; **3**:303–318.

Maz'ya VG, Nazarov SA and Plamenevskii BA. *Asymptotische Theorie elliptischer Randwertaufgaben in singulär gestörten Gebieten I. Mathematische Monographien*, Band 82. Akademie Verlag: Berlin, 1991a.

Miara B. Optimal spectral approximation in linearized plate theory. *Applicable Anal.* 1989; **31**:291–307.

Miara B. Justification of the asymptotic analysis of elastic plate. I: The linear case. *Asymptot. Anal.* 1994a; **9**:47–60.

Miara B. Justification of the asymptotic analysis of elastic plate. II: The nonlinear case. *Asymptot. Anal.* 1994b; **9**:119–134.

Miara B and Trabucho L. A Galerkin spectral approximation in linearized beam theory. *Modéll. Math. Anal. Numér.* 1992; **26**:425–446.

Mielke A. Normal hyperbolicity of center manifolds and Saint-Venant's principle. *Arch. Ration. Mech. Anal.* 1990; **110**:353–372.

Mielke A. Reduction of PDEs in domains with several unbounded directions: a step towards modulation equations. *Z. Angew. Math. Phys.* 1992; **43**(3):449–470.

Mielke A. On the justification of plate theories in linear elasticity theory using exponential decay estimates. *J. Elastic.* 1995; **38**:165–208.

Morgenstern D. Herleitung der Plattentheorie aus der dreidimensionalen Elastizitästheorie. *Arch. Ration. Mech. Anal.* 1959; **4**:145–152.

Narasimhan R. *Analysis on Real and Complex Manifolds. Advanced Studies in Pure Mathematics.* North Holland: Amsterdam, 1968.

Nazarov SA. Justification of asymptotic expansions of the eigenvalues of nonselfadjoint singularly perturbed elliptic boundary value problems. *Math. USSR Sbornik* 1987; **57**(2):317–349.

Nazarov SA. On three-dimensional effects near the vertex of a crack in a thin plate. *J. Appl. Math. Mech.* 1991a; **55**(4):407–415.

Nazarov SA. The spatial structure of the stress field in the neighbourhood of the corner point of a thin plate. *J. Appl. Math. Mech.* 1991b; **55**(4):523–530.

Nazarov SA and Plamenevskii BA. *Elliptic Problems in Domains with Piecewise Smooth Boundaries. De Gruyter Expositions in Mathematics.* Walter de Gruyter: Berlin, New York, 1994.

Necas J and Hlavacek I. *Mathematical Theory of Elastic and Elasto-Plastic Bodies: An Introduction.* Elsevier Scientific Publishing Company: Amsterdam, 1981.

Paumier JC and Rao B. Qualitative and quantitative analysis of buckling of shallow shells. *Eur. J. Mech. A., Solids* 1989; **8**:461–489.

Piila J and Pitkäranta J. Energy estimates relating different linear elastic models of a thin cylindrical shell I. The membrane-dominated case. *SIAM J. Math. Anal.* 1993; **24**(1):1–22.

Piila J and Pitkäranta J. Energy estimates relating different elastic linear models of a thin cylindrical shell II. The case of free boundary. *SIAM J. Math. Anal.* 1995; **26**(4):820–849.

REVISED PAGE PROOFS

Pitkäranta J, Leino Y, Ovaskainen O and Piila J. Shell deformation states and the finite element method: a benchmark study of cylindrical shells. *Comput. Methods Appl. Mech. Eng.* 1995; **128**(1–2):81–121.

Prager W and Synge JL. Approximations in elasticity based on the concept of the function space. *Q. Appl. Math.* 1947; **5**:241–269.

Raschewski PK. *Riemannsche Geometrie und Tensoranalysis.* VEB deutscher Verlag der Wissenschaften: Berlin, 1959.

Reissner E. On the theory of bending of elastic plates. *J. Math. Phys.* 1944; **23**:184–191.

Reissner E. The effect of transverse shear deformations on the bending of elastic plates. *J. Appl. Mech.* 1945; **12**:A69–A77.

Reissner E. On a variational theorem in elasticity. *J. Math. Phys.* 1950; **28**:90–95.

Reissner E. On the derivation of boundary conditions for plate theory. *Proc. R. Soc. Ser. A* 1963; **276**:178–186.

Reissner E. Reflections on the theory of elastic plates. *Appl. Mech. Rev.* 1985; **38**:453–464.

Reissner E. On small finite deflections of shear deformable elastic plates. *Comput. Methods Appl. Mech. Eng.* 1986; **59**:227–233.

Rodriguez JM and Viaño JM. Analyse asymptotique de l'équation de Poisson dans un domaine mince. Application à la théorie de torsion des poutresélastiques à profil mince.I. Domaine "sans jonctions". *C. R. Acad. Sci. Paris, Sér. I* 1993a; **317**:423–428.

Rössle A. *Asymptotische Entwicklungen für dünne Platten im Rahmen der linearen Elastostatik*. Doctoral Dissertation, Mathematisches Institut A, Universität Stuttgart, Germany, 1999.

Sanchez-Hubert J and Sanchez-Palencia E. *Vibration and Coupling of Continuous Systems; Asymptotic Methods.* Springer-Verlag: Heidelberg, 1989.

Sanchez-Palencia E. *Non-Homogeneous Media and Vibration Theory*, vol. 127 of *Lecture Notes in Physics*. Springer-Verlag: Heidelberg, 1980.

Sanchez-Palencia E. Forces appliquées à une petite région de surface d'un corps élastique. Applications aux jonctions. *C. R. Acad. Sci. Paris, Sér. II* 1988; **307**:689–694.

Sanchez-Palencia E. Statique et Dynamique des Coques minces. I. Cas de flexion pure non inhibée. *C. R. Acad. Sci. Paris, Sér. I* 1989a; **309**:411–417.

Sanchez-Palencia E. Statique et Dynamique des Coques minces. II. Cas de flexion pure inhibée. Approximation Membranaire. *C. R. Acad. Sci. Paris, Sér. I* 1989b; **309**:531–537.

Sanchez-Palencia E. Passage à la limite de l'élasticité tridimensionnelle à la théorie asymptotique des coques minces. *C. R. Acad. Sci. Paris, Sér. II* 1990b; **311**:909–916.

Sanchez-Palencia E and Suquet P. Friction and Homogenization of a Boundary. In *Free Boundary Problems: Theory and Applications*, Fasano A and Primicerio M (eds). Pitman: London, 1983; 561–571.

Sanders JL. *An Improved First-Approximation Theory for Thin Shells*. Report 24, NASA, 1959.

Sändig AM, Richter U and Sändig R. The regularity of boundary value problems for the Lamé equations in a polygonal domain. *Rostock. Math. Kolloq* 1989; **36**:21–50.

Schwab C. *The Dimension Reduction Method*. PhD thesis, University of Maryland, College Park, 1989.

Schwab C. Boundary layer resolution in hierarchical models of laminated composites. *Math. Modell. Numer. Anal.* 1994; **28**(5):517–537.

Schwab Ch. Theory and applications in solid and fluid mechanics. *p- and hp-Finite Element Methods*. The Clarendon Press Oxford University Press: New York, 1998.

(1996) *Stress Check User's Manual*, Release 2.0. ESRD, St. Louis.

Shoikhet BA. On asymptotically exact equations of thin plates of complex structures. *Prikl. Matem. Mekhan* 1973; **37**(5):914–924. English translation *J. Appl. Math. Mech.* 1973; 867–877.

Shoikhet BA. On existence theorems in linear shell theory. *Prikl. Matem. Mekhan* 1974; **38**(3):567–571.English translation *J. Appl. Math. Mech.* 1974; 527–531.

Shoikhet BA. An energy identity in physically nonlinear elasticity and error estimates of the plate equations. *Prikl. Matem. Mekhan* 1976; **40**(2):317–326.English translation *J. Appl. Math. Mech.* 1976; 291–301.

Slicaru SL. Sur l'ellipticité de la surface moyenne d'une coque. *C. R. Acad. Sci. Paris, Sér. I* 1996; **322**:97–100.

Slicaru SL. *Quelques Résultats dans la Théorie des Coques Linéairement Elastiques à Surface Moyenne Uniformément Elliptiques ou Compacte sans bord*. Thèse de doctorat, Université Pierre et Marie Curie, Paris, 1998.

Timosheno S and Woinovsky-Krieger W. *Theory of Plates and Shells*. McGraw-Hill: New York, 1959.

Trabucho L and Viaõ JM. A derivation of generalized Saint-Venant's torsion theory from three-dimensional elasticity by asymptotic expansion methods. *Appl. Anal.* 1988; **31**:129–148.

Trabucho L and Viaõ JM. Existence and characterization of higher order terms in an asymptotic expansion method for linearized elastic beams. *Asymptot. Anal.* 1989; **2**:223–255.

Trabucho L and Viaño JM. Mathematical modeling of rods. In *Handbook of Numerical Analysis*, vol. 4, Ciarlet PG and Lions J-L (eds). North Holland: Amsterdam, 1994.

Triebel H. *Interpolation Theory. Function Spaces. Differential Operators*. North Holland Mathematical Library, North Holland: Amsterdam, 1978.

Vishik MI and Lyusternik LA. Asymptotic behaviour of solutions of linear differential equations with large or quickly changing coefficients and boundary condition. *Russian Math. Surv.* 1960; **4**:23–92.

REVISED PAGE PROOFS

Abstract: Concerning thin structures, such as plates and shells, the idea of reducing the equations of elasticity to two-dimensional models defined on the midsurface seems relevant. Such a reduction was first performed thanks to kinematical hypotheses about the transformation of normal lines to the midsurface. As nowadays, the asymptotic expansion of the displacement solution of the three-dimensional linear model is fully known at least for plates and clamped elliptic shells, we start from a description of these expansions in order to introduce the two-dimensional models known as hierarchical models: These models extend the classical models, and presuppose the displacement to be polynomial in the thickness variable, transverse to the midsurface. Because of the singularly perturbed character of the elasticity problem as the thickness approaches zero, boundary, or internal layers may appear in the displacements and stresses, and so may numerical locking effects. The use of hierarchical models, discretized by higher degree polynomials (p-version of finite elements) may help overcome these severe difficulties.

Keywords: shells, plates, hierarchical models, asymptotic expansion, modal analysis, eigen-frequencies, finite elements

REVISED PAGE PROOFS